

Republic of Iraq
Ministry of Higher Education
and Scientific Research



*NONLINEAR ANALYSIS AND ULTIMATE STRENGTH
INVESTIGATION OF HORIZONTALLY CURVED
CELLULAR DECK STRUCTURES*

A Thesis

Submitted to the College of Engineering
of the University of Babylon in Partial
Requirements of the Fulfillment
for the Degree of Master
of Science in Civil
Engineering

By

SADJAD AMIR HEMZAH

Supervised by

**PROF. DR. HUSAIN M. HUSAIN
ASST. PROF. DR. HAITHAM AL-DAAMI**

Thu-Alhejjah ١٤٢٣

February ٢٠٠٣

جمهورية العراق
وزارة التعليم العالي والبحث العلمي



التحليل الأخطي وتقصي المقاومة القصوى للمنشآت السطحية المحلوية المنحنية أفقياً

مرسالة

مقدمة إلى كلية الهندسة في جامعة بابل
كجزء من متطلبات نيل درجة الماجستير
في علوم الهندسة المدنية

من قبل

سجاد عامر حمزة

أشرف

الأستاذ الدكتور حسين محمد حيسن
الدكتور هيثم الداعي

ذو الحجة ١٤٢٣

شباط ٢٠٠٣

بِسْمِ اللَّهِ الرَّحْمَنِ الرَّحِيمِ

وفوق كل ذي علم عليم

صدق الله العلي العظيم

المنحنية يشيد من لوحتين علوية و سفلية مفصولتين بحواجز طولية منحنية و عرضية مستقيمة. أن كفاءة هذا النوع من المنشآت تأتي من مقاومتها العالية وخفة وزنها. مثل هذه المنشآت تستعمل بكثرة في أرضيات الجسور , أجنحة الطائرات , قيعان السفن و الحالات الأخرى التي تكون فيها المقاومة العالية و خفة الوزن من العوامل التصميمية المهمة.

تم تطوير طريقة تشابه المشبكات المبسطة لتكون قادرة على التنبؤ بالسلوكية اللاخطية وحسب المقاومة القصوى لهذا النوع من المنشآت الخلوية. يتم تسليط الأحمال بصورة متزايدة للتعامل خطوة بخطوة مع كلا نوعي الاستجابة اللاخطية (اللاخطية الهندسية و اللاخطية المادية).

اللاخطية الهندسية تحصل نتيجة السلوكية ما بعد الانبعاج للشفة المنضغطة أو الحواجز أو كليهما. تم اعتماد مبدأ (فون كارمن) للعرض المؤثر لمتابعة سلوكية الشفة المنضغطة عند حدوث الانبعاج , بينما استخدمت طريقة (رو كي) بعد إدخال بعض التعديلات عليها لتكون ملائمة لتتبع التحمل الأقصى للحواجز الطولية و العرضية غير المتوازية والسلوكية ما بعد الانبعاج.

تم تبني مبدأ المفصل اللدن لتمثيل اللاخطية المادية التي تحصل نتيجة وصول الاجهادات في الألواح إلى إجهاد الخضوع لمادة المنشأ اعتماداً على الطريقة المقترحة تم كتابة برنامج خاص (NLCRVGA) تطبيقه على عدة أمثلة , حيث ظهر توافق جيد عند مقارنة نتائج الهطول الشاقولي و المقاومة القصوى مع تلك المستحصلة من استخدام عناصر لوحيه / قشرية والمتوفرة في مجموعة ناستران (NASTRAN). اكبر فرق بالنتائج في الحالة القصوى كان (١٥,٧%) بالهطول و(١٤,٠٦ %) بالحمل للأمثلة المستخدمة.



ABSTRACT

A
horizontally

curved cellular plate structure with curved webs is constructed of top and bottom flange plates separated by longitudinal curved and transverse straight webs. The efficiency of such form of construction arises from its high strength to weight ratio. It is widely used in bridge decks, aircraft wings, ship bottoms and other situations where strength and reduction of self-weight are important design objectives.

The simplified grillage approach is extended to investigate the nonlinear post-buckling behavior and ultimate strength of such structures. An incremental loading procedure is adopted to follow step by step both types of nonlinear responses (geometric and material nonlinearities).

The geometric nonlinearity is due to the post-buckling behavior of the compression flange and/or panels. *Von Karman's* effective width concept is utilized to follow the post-buckling behavior of the compression flange panel. *Rockey's* approach for the ultimate load determination is used with some modifications to predict the post-buckling and ultimate strength of the curved web panel.

A plastic hinge approach is adopted to investigate the material nonlinearity which arises due to the occurrence of local yielding in the component plates.

Based on the suggested simplified method, A computer program (*NLCRVGA*) is written and applied to several examples. Results of vertical deflections and ultimate loads predicted by the proposed grillage method are found to be in good agreement when compared with those obtained by the plate/shell element in the package program (*NASTRAN*). The maximum differences at ultimate state are (10.7%) in deflection and (14.6%) in ultimate load in the examples considered herein.

ACKNOWLEDGEMENT

❁ *In The Name of Allah the Most Gracious, The Merciful* ❁

*Before every thing and after every thing, praise to be to my generous God (**Allah**) for providing me the willingness and strength to accomplish this work.*

I would like to express my sincere appreciation and deepest gratitude to Prof. Dr. Husain M. Husain and Dr. Haitham H. Muteb, who I had the honor of working under their supervision, for their guidance, valuable suggestions and continuous encouragement through all stages of this research.

I would like to express my sincere thanks with deepest respect to Dr. Namir A. Alwash the head of the civil engineering department. I wish also to express my deepest thanks to all the staff of the civil engineering department.

*Appreciation and thanks to my friends, especially **Mohammed H. Younis, Haider K. Ammash and Ali H. Kadum.***

Finally, the author extends his sincere gratitude to his parents and family for their patience endurance.

Sadiq A. H. Al-Janary

APPEDEX B Sample of data file for Plated Structure Fixed at All Edges

Fixed at ξ Edges		

Angle per Mem./ Tf,Tw,D/ Inc,Fy/ NCR,NCT,NDR,NDT,Ls,R		
10		
10	10	1000
000	240	
xi	xi	1 1 2000 10000
No. of Riest. D.O.F / No. of Loaded Node		
74		9
Node No./ D.O.F./D.O.Ries.		
1	1	.
1	2	.
1	3	.
1	xi	.
2	1	.
2	2	.
2	3	.
2	xi	.
.	.	.
.	.	.
.	.	.
20	1	.
20	2	.
20	3	.
20	xi	.
Loaded Node/D.O.F/ Load Value		
7	3	-10000
8	3	-10000
9	3	-10000
.	.	.
.	.	.
.	.	.
.	.	.
Modulus of Elasticity/ Poisson Ratio		
200000		.3

Where:

Inc = No. of Increment

Fy = Yield Stress of Steel

NCR = No. of Cell in Radial Direction

NCT = No. of Cell in Thaita Direction

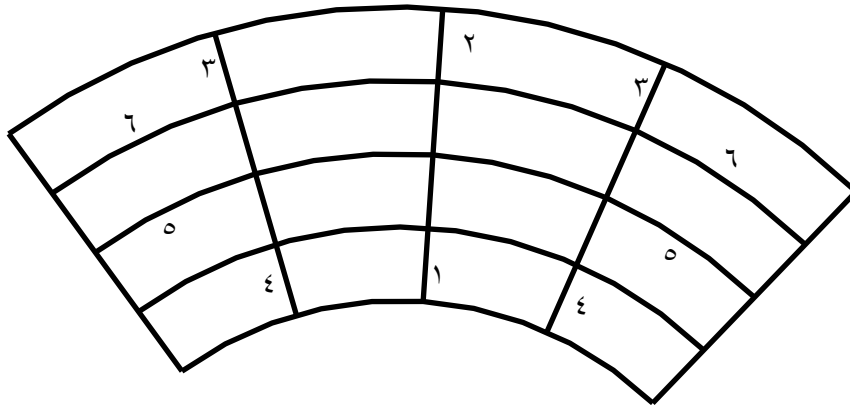
NDR = No. of Division Per Cell in Radial Direction

NDT = No. of Division Per Cell in Thaita Direction

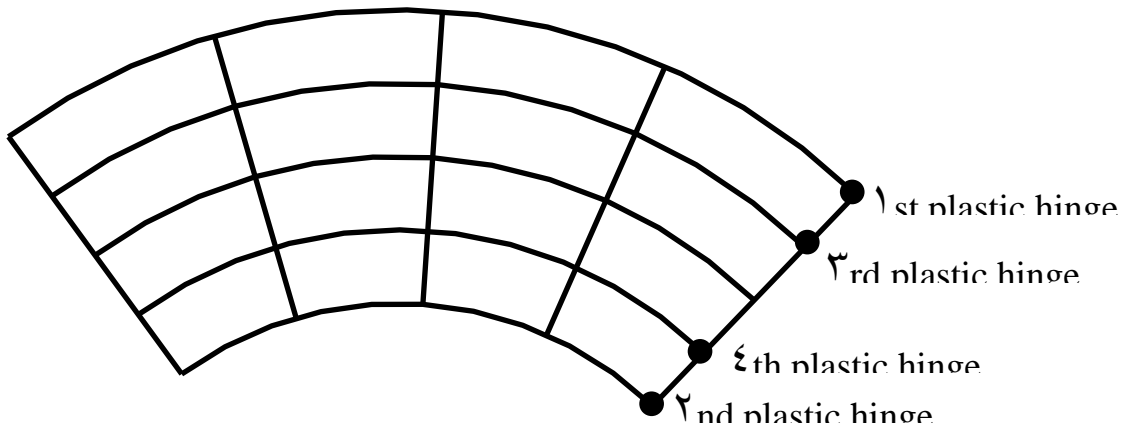
Ls = Length of Straight Member

R = Inner Radius of The Structure

Appendix C



*Sequence of failing member for example no. 1
(Fixed at all edges)*



*Sequence of plastic hinges for example no. 2
(Cantilever structure)*



Certification

We certify that this thesis titled **“Nonlinear Analysis And Ultimate Strength Investigation of Horizontally Curved Deck Structure”**, was prepared by **“Sadjad Amir Hemzah ”** under our supervision at Babylon University in fulfillment of partial requirements for the degree of Master of Science in Civil Engineering.

Signature:

Name: Prof. Dr. Husain M. Husain

Date: / / ٢٠٠٣

Signature:

Name: Dr. Haithem H. Muteb

Date: / / ٢٠٠٣

CERTIFICATION

We certify that we have read this thesis, titled (**Nonlinear Analysis and ultimate strength investigation of horizontally curved deck structures**), and as examining committee examined the student **Sadjad Amir Hemzah** in its contents and in what is connected with it, and that in our opinion it meets the standard of thesis for the Degree of Master of Science in Civil Engineering (**Structure**).

Signature:	Signature:
Name: Ass. Prof. Dr. Bayan S. Al-Nu'man	Name: Ass. Prof. Dr. Ammar Y. Ali
(Member)	(Member)
Date: / / ٢٠٠٣	Date: / / ٢٠٠٣

Signature:
Name: Ass. Prof. Dr. Ing. Ali M. Al-Athary
(Chairman)
Date: / / ٢٠٠٣

Signature:	Signature:
Name: Prof. Dr. Husain M. Husain	Name: Ass. Prof. Dr. Haitham H. Al-Daami
(Supervisor)	(Supervisor)
Date: / / ٢٠٠٣	Date: / / ٢٠٠٣

Approval of the Civil Engineering Department
Head of the Civil Engineering Department

Signature
Name: **Asst. Prof. Dr. Nameer A. Alwash**
Date: / / ٢٠٠٣

Approval of the Deanery of the College of Engineering
Dean of the College of Engineering

Signature
Name: **Ass. Prof. Dr. Haroun A. K. Shahad**
Dean of the College of Engineering
University of Babylon
Date: / / ٢٠٠٣

CHAPTER 1

INTRODUCTION

1.1 *Thin Walled Structures*

Thin-walled structures are made from thin plates joined along their edge^(c). The thickness of plate is small compared with other dimensions and with the overall length of the member. Thin-walled structures can be designed to exhibit great flexural and torsional rigidity such as box girders or any other member having a closed section. But they may have a little torsional rigidity as in the case of plate girders or any member having an open section. However, the common property of these structures is that they are very light compared with alternative structures, therefore they are used in long span bridges and other structures where weight and cost are prime considerations. More advantageous are the thin-walled cellular plates where materials are concentrated at concentration of the stresses. The top and bottom flanges take predominantly the flexural stresses while webs take the transverse shearing stresses.

1.2 *Exposition*

The multi-cellular steel plate structures represent an efficient form of construction. They are suitable in bridge decks, aircraft wings, ship bottoms and any situations needing high strength to weight ratio.

A steel cellular plate structure curved in plans consists of double metal plates having circularly curved shape, and separated by webs and diaphragms in two directions. The longitudinal webs are curved and the transverse webs are usually placed radially. This type of structure is more practical and economical than solid-section structures due to its lightweight and high strength.

1.4 Characteristic Feature of Thin-Walled Section

One of the most important features of thin-walled sections is their response to the torsional loading. In solid and thick-walled sections, out-of-plane warping is usually small for any secondary stresses arising from warping restraint, therefore these stresses can be neglected. Therefore the applied torsion is resisted entirely by a system of pure Saint-Venant shear stress. In thin-walled sections, out-of-plane warping displacement resulting from torsional loading are generally much larger. Open sections are more susceptible than closed sections in this regard. If these relatively much larger warping displacements are restrained, a system of longitudinal normal stresses (producing bimoment) are set up. These may not be necessarily local in effect and may extend for a considerable distance from the point of restraint. Complementary warping stresses are also created which have the effect of modifying the transverse distribution of shear stress due to pure shear Fig. (1-1).

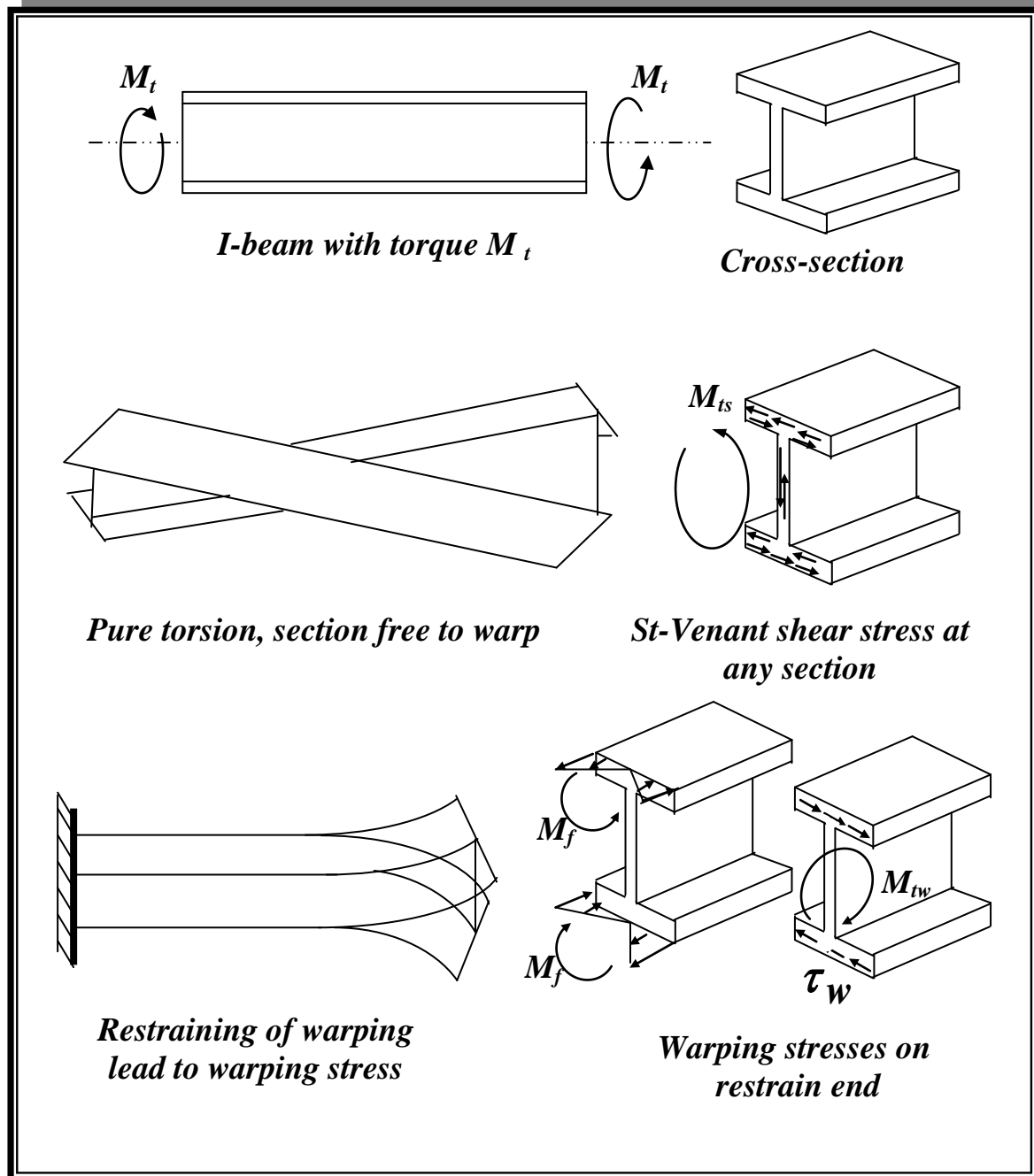
1.5 Construction

Methods of construction of cellular plate structures depend on various factors such as the type and size of the structure and the plate thickness. Generally, flanges and webs are composed of several connected pieces of

plate. Webs may be made of flat plates with double angle section at top and bottom or may have bent edges to become like wide channels or Z-sections or framed sections such as I-sections to facilitate the construction with

flanges.

In a



construction procedure, webs in the two directions are connected together and fixed to one flange. The other flange is connected to the web piece by peripheral

Figure 1.1) Torsional Behavior of Thin-Walled Members

welding or by riveting to the protruding plates at top of webs. The flange plates are assumed rigidly fixed to the webs plate for full interaction. No slip or any other form of partial interaction is assumed to occur.

1.7 The Need For Simplified Analysis For Cellular Plate Structure

Because of the development of finite element method and the availability of large capacity digital computers, it is now possible to analyze plate structures of arbitrary geometry and boundary conditions and subjected to several loading conditions. Moreover, effects and modifying factors (such as shear lag, biaxial effect and composite actions) can be included in the analysis.

The theory used in the derivation of the characteristic properties of the cellular plate structure based on the shell elements. The shell theory is more complicated than those used for beam element, moreover the number of elements is generally very largewhen using shell element. Therefore the three dimensional shell element program data preparatons may need large computer capacity and considerable computer time and effort preparation (specially for collapse problem). Certainly, at initial design stages when the designer is trying to optimize the proportion of the structure by repeated analysis, the cost involved in using the finite elements may become unfavorable.

There is a real need for a simplified computer method as an alternative to the finite element methods for use at the preliminary design stages and for quick and inexpensive analysis of plate structures. Ideally, once the designer has established a reasonably efficient structure by repeated analysis using a simplified method, a final check by a sophisticated finite element method may be carried out.

1.8 Objectives of the Present Study

The present study deals with the static (linear and non-linear) analysis of steel cellular plates curved in plan. For linear static grillage analysis of cellular plate structures, the more accurate torsional properties of straight and curved thin-walled multi-cell members are obtained by including the effect of warping restraints. The effect of torsional warping can be significant in the behavior of structures made of thin-walled members.

Timoshenko's concept of torsional warping is utilized for studying the torsional behavior of straight and curve thin-walled members with open and closed cross sections and with different boundary conditions. Various torsional stiffness expressions are derived. Results of solution to straight and curved members are presented and comparison is made available results from other studies.

The widely known grillage method has a simplified discretization approach for the linear analysis of plate structures. This method is extended to investigate the non-linear analysis and ultimate load of cellular plate structures. The grillage simulation is used to deal with the post-buckling and elastic-plastic analysis of cellular plate structures.

The cellular plate structures are assumed to fail under the action of high bending stresses, high shearing stresses or due to interaction between the two types of stress. The analysis of ultimate load behavior of cellular plate structures must deal with the effects of non-linearity arising from both material and geometric non-linearity. To control the effect of material non-linearity in the proposed method of grillage analogy, the plastic hinge approach is adopted.

The geometric non-linearity effects (arising from the problem of buckling of compression flange) are taken into account by implementing *Von-Karman's* approach (effective width concept). Different assumptions regarding the effective width of compression flange are reviewed.

An incremental loading procedure is adopted and the results are presented to indicate the rate of convergence of the solution. Two computer

programs have been written to perform static linear and non-linear analysis of the problem. A numerical method is presented to evaluate the required sectional properties of closed sections, which are the main part of the problem. The results given by the proposed simplified grillage method are compared with those obtained from more accurate and sophisticated-3D shell elements using the computer program (*MSC/NASTRAN*)⁽¹⁾.

1.1 Thesis Layout

The thesis consists of seven chapters.

Chapter one is the present introduction.

Chapter two presents a review of literature on the use of different methods for analyzing the cellular plate structure.

Chapter three covers the evaluation of the elastic section properties required to analyze cellular plate structure as a two dimensional grillage.

Chapter four provides guidelines on the application of the grillage analogy in the nonlinear behavior of steel cellular plate structure.

Chapter five presents the nonlinear behavior and collapse load investigation of a steel cellular plate structure curved in plan and /or with nonparallel diaphragms due to instability of the compression flange panels and/or the web panels and also due to the occurrence of local yielding in the highly stressed component plates.

Chapter six includes some examples models, which are analyzed using the suggested grillage method. The results obtained by this method are checked with those obtained from the nonlinear finite element analysis using the package program (*NASTRAN*).

Chapter seven gives conclusions and suggests recommendations for future research related to this subject.

CHAPTER 2

REVIEW OF LITERATURE

2.1 Introduction

As mentioned in the previous chapter, the use of thin-walled sections has been increasing rapidly in many types of engineering structures. This is due to the continuous development of modern structures, requiring greater span with reduced self-weight. These factors have encouraged the wider application of thin-walled beam section in design. Accordingly, many simplified and sophisticated methods of analysis have been developed to be applied to cellular plate structures. In the search of previous work on grillage analogy for linear and non-linear analysis of curved cellular plate structures, no analytical or numerical work has been met on the behavior of a cellular plate structure curved in plane the non-linear range and at ultimate load. In this chapter, the application of the grillage analogy for linear and non-linear analysis to general plate structures is reviewed.

2.2 Application of Grillage Analogy to Linear Analysis of Cellular Plate Structures

The application of grillage analogy to cellular plate structure is well supported by published literatures. The work by *Husain* (1974)⁽²²⁾ was the first to idealize a cellular plate structure (aircraft cantilever cellular wing) as a grillage of orthogonally connected beams. The grillage structure

consisted of beams with both flexural and torsional rigidities. The flexural rigidity of a grillage member was derived from the partitioning web together with attached top and bottom cover plates (as an I- section), while the torsional rigidity was derived from the torsional rigidities of the adjacent cells (as closed rectangular section). The deflections by the grillage analogy compared favorably with the experimental and with plane stress finite element results.

Sawko and *Willcock* (1974)⁽¹⁴⁾ extended *Husain's* method to the analysis of cellular plate structure having variable section depth in the longitudinal (or main span) direction. They also considered the transverse shearing rigidities of the grillage members to account for cell distortion. By comparing the grillage analogy with model test results, they concluded that cellular plate structures with several transverse webs could be analyzed by the grillage analogy with due account for transverse shear distortions of cells.

Smyth and *Srinivasan* (1971)⁽¹⁵⁾ applied the grillage analogy to the analysis of a cellular bridge deck, which was trapezoidal in cross section and made of prestressed concrete. By comparing the grillage analogy results with model test and the equivalent space frame results, the grillage gave quite good results for the longitudinal action but required supplementary information for the transverse action (due to neglecting cell distortion).

Hambly and *Pennels* (1970)⁽¹⁶⁾ used the grillage analogy in the analysis of concrete cellular bridge decks having skew plan geometry and rectangular or trapezoidal cross sections. They discussed in details the effect of cell distortion in cellular bridge decks. A method for calculating the torsional rigidity of the grillage members was proposed by considering the effect of shear flows in the top and bottom slabs and side webs only as in one cell by neglecting the rather small shear flows in intermediate webs.

They had been the first to consider the effect of shear lag in calculating the flexural (or bending) rigidity of the grillage beams by adopting the principle of effective flange width. The result of the analysis compared favorably with the result by the folded plate theory.

Evans and **Shanmugam** (1979)⁽³⁰⁾ applied the grillage analogy in the analysis of steel cellular plate structures. In case where the spacing of webs in one direction is more than twice the spacing of webs in the other direction they proposed the use of intermediate (or fictitious) members between the main members to increase the accuracy of the grillage structure in idealizing the cellular plate structure to avoid the incorrect assessment of effective widths of flanges. The intermediate fictitious members consisted of top and bottom flanges only (without web). In calculating the torsional constant of the grillage members, they proposed the same method by **Husain**⁽³¹⁾. Like other investigators, they also neglected the effect of Poisson's ratio in calculating the flexural (or bending) rigidities of the grillage members, which may be considerable in steel cellular structures when compared with concrete cellular structures.

Jaeger and **Bakht** (1982)⁽³²⁾ provided guidance on idealization of various types of bridge decks. In cellular structures, they suggested to neglect the interior webs or diaphragms and treat the whole cross section as a single cell for calculating the torsional constant. The value of the torsional constant for this single cell section is then distributed to the main grillage members in the section (almost the same suggestion by **Hambly** and **Pennels** (1979)⁽³³⁾

Mohammed (1994)⁽³⁴⁾ used various types of grillage methods for analyzing steel cellular plate structures with parallel webs and diaphragms. He suggested to use effective modulus of elasticity $E/(1-\nu^2)$ in the flexural rigidities of the beams of the substitute grillage. Thus, more rigidity (or stiffness) was given to the grillage. The results obtained by the grillage

meshes compared favorably with the orthotropic plate method, the three-dimensional flat shell finite element method and with available experimental results.

Al-Sherrawi (1990)⁽¹¹⁾ extended *Mohammed's* (1989)⁽¹⁰⁾ work to analyze steel cellular plate structures with non-parallel webs and diaphragms, which are usually used in aircraft wings and some bridge decks and approaches. He also used three alternatives of grillage meshes to represent the cellular plate structure. Grillage analysis results were compared with the orthotropic plate method and with the finite element method.

Fairooz (1990)⁽¹²⁾ used the grillage analogy for linear analysis of cellular steel bridge decks curved in plan. The cellular decks contained circumferential curved webs and radial straight webs (or diaphragms). The substitute grillage consisted of orthogonally connected curved and straight beams. Warping restraint effects were not included. The results show a good agreement compared with the results by the three-dimensional shell elements.

Hasan (1991)⁽¹³⁾ presented a simplified space grillage analogy for the analysis of spherical cellular domes consisting of top and bottom plates with a grid of orthogonally connected arch webs. A Method for calculating the rigidities of the closed sections under restrained warping was suggested. Also, a method of interpretation of the results from the grillage output is presented.

Husain, Al-Ausi and *Al-Azawi* (1999)⁽¹⁴⁾ presented a simplified grillage analogy for the linear analysis of cellular plate structures curved in plan including implicitly the effect of warping restraints. A more accurate torsional stiffness of the straight and curved thin walled members was obtained by including the effect of warping restraints. *Timoshenko's* concept (1959)⁽¹⁵⁾ of torsional warping is utilized for studying the torsional behavior of straight and curved thin-walled members. Various torsional

stiffness expressions were derived. Results of solutions to straight and curved members were presented and compared with results from other studies and available results⁽¹⁵⁾.

2.2 Application of Grillage Analogy To Nonlinear Analysis of Cellular Plate Structures

As mentioned earlier, there is little available information regarding the behavior of cellular plate structures in the non-linear range and at collapse.

Fujita and Yoshida (1977)⁽¹⁶⁾ investigated the collapse due to buckling of arbitrarily shaped stiffened plate structures (such as cellular plate structures) used in ship design. An analytical method was formulated using an incremental finite element method with inclusion of elastic-plastic and large deflection non-linearities. In addition to the use of the triangular plate elements for plates and beam elements for stiffeners, beam elements were also used for components where girder behavior predominated, thereby reducing the number of degrees of freedom.

Shanmugam and Evans (1981)⁽¹⁷⁾ suggested an extension to the grillage analogy approach, used in linear analysis of steel cellular plate structures, for analysis in the non-linear range and at collapse. The structures were assumed to have failed under the action of high bending stress only. Regarding buckling of compression flange panels, these panels were assumed to be simply supported under uniaxial or biaxial compression and their post buckling behavior was controlled by implementing the effective width approach. An incremental loading procedure is adopted during which there would be continuous updating of the stiffness matrix.

Evans, et al. (1982)⁽¹⁸⁾ suggested a development to the application of finite element method to the analysis of large deflection elastic –plastic

behavior of plate structures (such as cellular plate structures). The analysis was applicable to structures with thin plates, which would operate in the post-buckling range. Therefore, the method took into account the effect of geometrical non-linearity arising from the plate buckling and the effect of material non-linearity due to the spread of yield during the approach to collapse. A four-noded rectangular element with five degrees of freedom per node was adopted for the solution. These degrees of freedom are three translational displacements plus two rotations around the two perpendicular axes in the plane of the plate. The drilling rotation (normal to the plane of the plate) was ignored.

Harding (1990)⁽³⁹⁾ summarized the work undertaken by him and his colleagues, on the behavior of steel plate structures (like cellular plate structures) relating to bridges and offshore platforms. His work demonstrated the power of the non-linear finite element packages in examining the non-linear behavior of the structural components and how the results of organized parametric studies can be used to formulate design guidance. The study showed the effects of using longitudinal and/or transverse stiffeners in the flanges or in the webs. It has clearly shown that these stiffeners affected considerably the local buckling of the component plates as well as the failure load.

Mashal (1991)⁽⁴⁰⁾ used the grillage analogy to analyze rectangular steel cellular plate structures in their non-linear range and at collapse. The effective width approach was used to represent the post-buckling behavior of the compression flange panel. The method proposed by **Rocky et al**⁽⁴¹⁾ (for the ultimate analysis of stiffened plate structures) was applied to represent the non-linear behavior of the web panels of the cellular plate structure.

Aldaami (2000)⁽⁴²⁾ used the grillage analogy in the analysis of cellular domes having a spherical shape. The dome was represented by an

assemblage of meridian and hoop curved beams. These curved beams were connected rigidly and orthogonally intersected to form a spherical grid (mesh) of curved beams. The flexibility and stiffness matrices of the thin walled curved beams were given, warping restraint effect was taken into consideration. The results were compared with the results obtained from the finite flat shell elements using the *MSC/NASTRAN* program. The results were satisfactory.

Al-Azawi (2007)⁽⁶⁾ used the grillage method for both linear and nonlinear analysis of cellular plate structures curved in plan. Regarding the linear analysis, restrained warping effects were included. While in the nonlinear analysis, he extended *Mashal's* work to analyze cellular plate structure curved in plan. Also, the elastic buckling stresses in curved compression flange panels were evaluated by including the effect of the geometric curvature and by using the finite difference method in polar coordinates. Comparison of the results given by the proposed grillage method with the finite element method using the (*NASTRAN*) package program verified the accuracy of the proposed method.

Younis (2007)⁽⁷⁾ applied the grillage analogy to steel cellular plate structures with non-parallel webs and diaphragms in the nonlinear range. Both types of nonlinear response (material and geometrical nonlinearities) were considered. The post-buckling behavior of the compression flange panels was traced by depending on the effective width concept presented by *Von Karman*.⁽⁸⁾ The results of the vertical deflection and collapse load by the proposed simplified method showed good agreement when compared with those obtained from the finite element method using the flat shell element in *MSC/NASTRAN* program

In the present study the stiffness matrix of straight and curved members are derived by including the effect of restraint warping deformations. Restraint warping effects were included in both types of

analysis (linear and nonlinear). A plastic hinge is considered to occur when both top and bottom flange reach yeild stress, then the stiffness matrix of the member will be modified by using the plastic modulus of elsticity suggested by *Lagerqvist*⁽¹⁷⁾.

CHAPTER 3

EVALUATION OF SECTION PROPERTIES

۳.۱ *Introduction*

Grillage analogy is used in the present study for analyzing cellular plate structures curved in plan. The method involves the conversion of a curved cellular decks into a grid of longitudinal curved members (or beams) intersecting at right angle with radial straight members. The accuracy of this method can be achieved within acceptable limits and depends largely on the proper evaluation of the section rigidities of the grillage members. Furthermore, the grillage analogy gives the designer a good appreciation and feeling of how the actual structure behaves.

This chapter presents the techniques of grillage idealization of curved cellular plate structures. The most important features of the idealization include the proper planning of the grillage members. Guide-lines on the application of the grillage analogy to linear and non-linear analysis and ultimate load investigation of steel cellular plate structures curved in plan are discussed herein.

۳.۲ *Evaluation of elastic Rigidities*

It is necessary to evaluate the appropriate elastic section properties of the grillage members from the actual multi-cell structure. These are needed in

the grillage analogy for the linear and nonlinear analysis of the cellular plate structure.

3.2.1 Flexural Rigidities

In representing a cellular plate structure by an equivalent plane grillage, many investigations (31, 32, and 33) considered the cross section of the grillage member as an I-section in calculating the moment of inertia (or second moment of area).

Generally two more factors must be considered in calculating the flexural rigidities of the grillage members. These are the shear lag and Poisson's ratio. A brief review of literature pertaining to the evaluation of flexural rigidities is presented herein.

Basu and Dawson (34) proposed the following equations for calculating the values of D_x and D_y for rectangular cellular plate structures having top and bottom flanges of equal thickness, longitudinal webs with equal thickness and without transverse diaphragms

$$D_x = \frac{Et_x \cdot v_{xy} \cdot d^2}{2(1 - v_{xy} \cdot v_{yx})} \quad (3-1)$$

$$D_y = \frac{Et_x d^2}{2(1 - v_{xy} \cdot v_{yx})} \quad (3-2)$$

where: -

$$\left. \begin{aligned} v_{xy} &= 1 - \frac{1}{6} \frac{t_x}{t_{fc}} \frac{d}{B_x} \\ v_{yx} &= v \end{aligned} \right\} \quad (3-3)$$

all relevant notations are shown in Fig.(3-1)

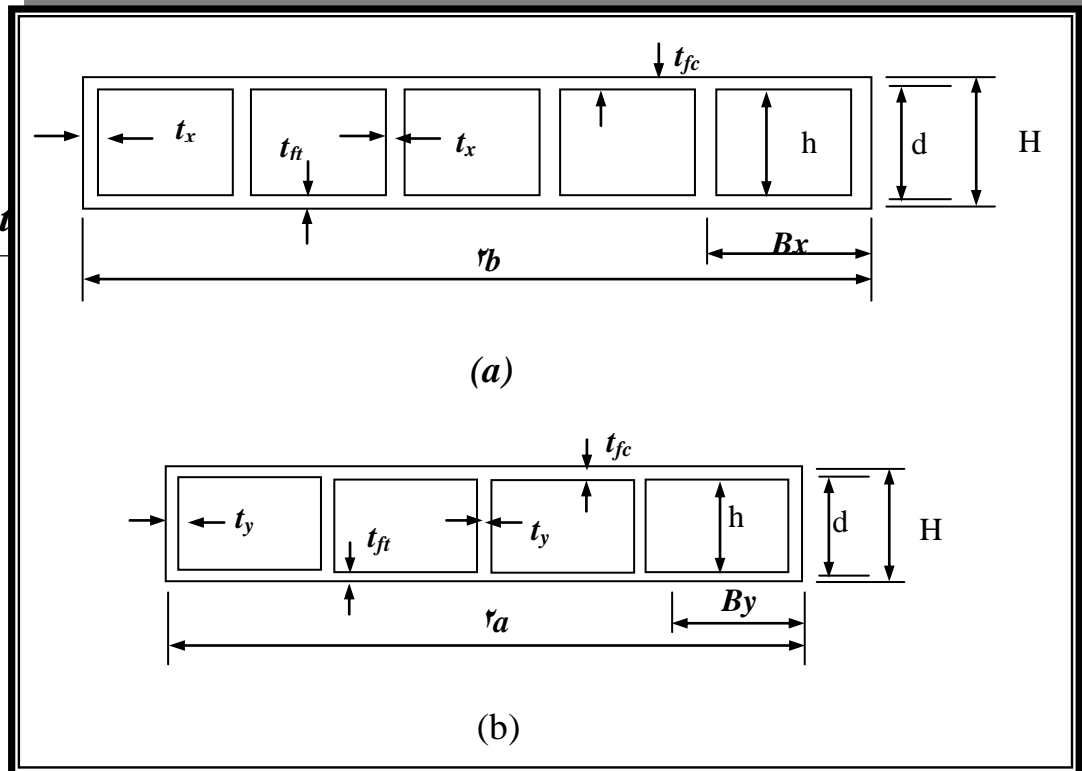
Crisfield and Twemlow (35) proposed the following equations for values of D_x and D_y for a rectangular cellular plate structure having

flanges of equal thickness ($t_{fc} = t_{ft}$), web thickness (t_x) and diaphragms thickness (t_y):

$$D_x = \frac{E}{(1-\nu^2)} \frac{t_{fc} \cdot d^2}{2} + \frac{E \cdot t_x \cdot d^3}{12B_x}$$

(3-1)

$$D_y = \frac{E}{(1-\nu^2)}$$



(3-2)

Cusens and
Pama
(1970) (3-3)

suggested the following

Figure (3-1) Details of cellular plate structure
(a) Longitudinal section (b) Transverse section

formula for calculating the flexural rigidity for a cellular plate structure having two unequal flange thickness (t_{fc} and t_{ft}) and web thicknesses

($t_x = t_y$):

$$D_x = \frac{E t_{ft}^3}{12} - \frac{E^* t_x^3}{6B_x} \left(e_{x1} - \frac{t_{ft}}{2} \right)^2 \left(e_{x2} - \frac{t_{ft}}{2} \right) + \frac{E^* t_x^3}{6B_x} \left(h + \frac{t_{ft}}{2} - e_{x1} \right)^2 + E^* t \left(h + \frac{t_{ft}}{2} - e_{x2} \right) + \left(h + \frac{1}{2} (t_{ft} + t_{fc}) \right) + \frac{E^* t_{fc}^2}{2} \left(h + \frac{t_{ft}}{2} - \frac{2t_{fc}}{3} \right)$$

(3-6)

$$E' = \frac{E}{1 - \nu^2} \quad (3-7)$$

$$E^* = \frac{E}{\left(1 - \nu^2 \frac{t_x t_y}{B_x B_y}\right)} \quad (3-8)$$

where e_{x2} is the distance from the neutral axis of the cellular deck to the centerline of the upper flange in x-direction and other notations are shown in Fig.(3-1).

As discussed by *Cusens* and *Pama* ⁽³⁰⁾ formula (3-6) is unwisely (or clumsy) for practical use and only becomes of value if the vertical webs are particularly thick and closely spaced. *Jaeger* and *Bakth* (1947) ⁽³¹⁾ suggested to neglect the effect of Poisson's ratio and the effect of the webs in calculating D_x and D_y and proposed the following formula:

$$D_x = D_y = E(t_{fc} \cdot e_{x1}^2 + t_{ft} \cdot e_{x2}^2) \quad (3-9)$$

where e_{x1} and e_{x2} , the distances from the neutral axis of the section to the centerlines of the lower and upper flanges respectively.

Mohammed (1994) ⁽³²⁾ derived the following formula for calculating D_x and D_y for a rectangular plate structure having two equal thicknesses ($t_{fc} = t_{ft}$) web thickness (t_x) and diaphragm thickness (t_y): -

$$D_x = \frac{E' t_{fc} d^2}{2} + \frac{E t_x d^3}{12 B_x} \quad (3-10)$$

(3-10)

$$D_y = \frac{E' t_{ft} d^2}{2} + \frac{E t_y d^3}{12 B_y} \tag{3-11}$$

11)

These formulas are simple and satisfactorily accurate. The grillage idealization in the present study consists of a grid having circularly curved members intersecting at right angles with radial straight members. Each radial member is idealized as a number of stepped prismatic elements as shown in fig (3-12).

For a curved grillage member, the second moment of area in two directions (x and y) may be

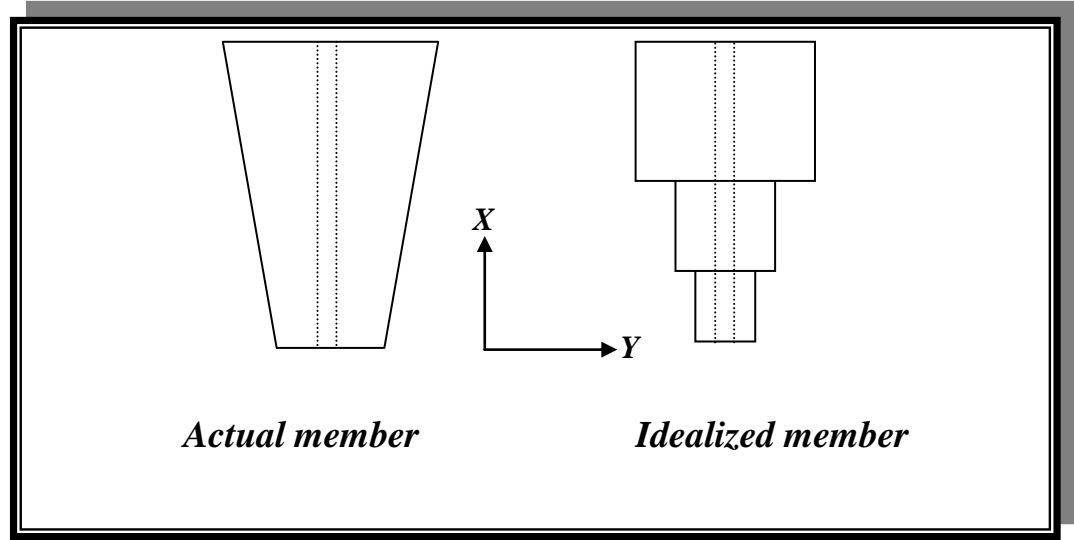


Fig. (3-12) actual and idealized radial straight member

calculated by using the following formulas (71, 92, 26, 08, 20): -

$$I_x = \int_A \frac{R}{R+y} y^2 dA \tag{3-12}$$

$$I_y = \int_A \frac{R}{R+y} x^2 dA \tag{3-13}$$

$$I_{xy} = \int_A \frac{R}{R+y} xy dA \tag{3-14}$$

where R is the radius of curvature to the centroid. A detailed study by Waldron (1979) (19) on curved box girders has shown that the second

moment of area are not significantly influenced by the degree of curvature, this concept is considered in the present study when $R \rightarrow \infty$ the above formulas will be for straight beams. Also, the effect of Poisson’s ratio is considered by using the concept of separating (or dividing) the moment of inertia (I) of a grillage member into two parts as follows:

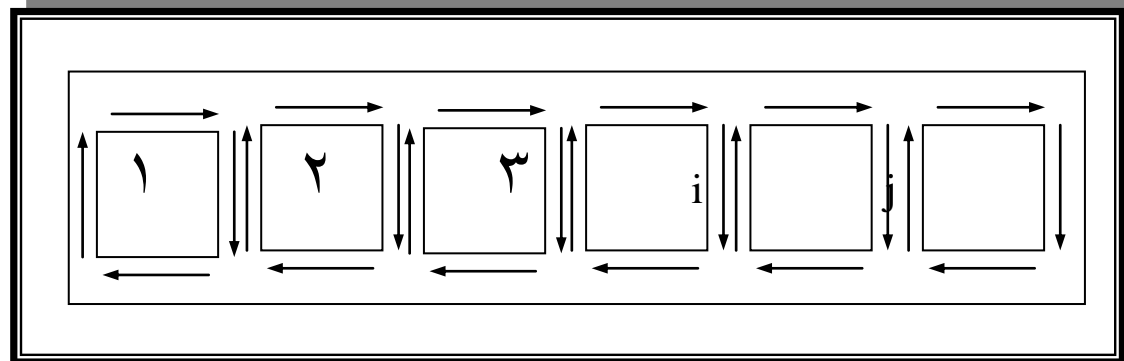
$$I = \frac{I_f}{1 - \nu^2} + I_w$$

where I_f is the moment of inertia of the flanges about the section neutral axis and I_w is the moment of inertia of the web.

3.2.2 Torsional Rigidities

When a cellular plate structure is twisted a network of shear stress develops round the flanges and webs as shown in Fig. (3-3)

Timoshenko
and Goodier
(1901) (16)



gave a
procedure for
the

Fig. (3-3) shear flow in cellular plate structure

calculation the torsional constant (J) of a cellular section under pure torsion and free to warp. The basic assumption used for establishing the torsional constant for a multi-cell is by considering the shear flow in the walls, as shown in Fig.(3-3) and employing the elastic theory. The distribution of

the shear flows in n-cell section is shown in Fig.(3-3). The n-independent shear flows are taken as unknowns.

For three typical cells i, j and k , the angle of twist per unit length θ (rate of twist) of the intermediate cell (j) is:

$$\theta_j = \frac{1}{2GA_j} \left[-q_i \int_w \frac{ds}{t} + q_j \int_c \frac{ds}{t} - q_k \int_w \frac{ds}{t} \right] \quad (3-14)$$

where:

where:

$\int_w \frac{ds}{t}$ = the integral along the common webs of cells (i & j) and (j & k)

$\int_c \frac{ds}{t}$ = the contour integral around the cell (j)

A_j = the enclosed area of the cell (j)

The authors assumed that each cell rotates at the same rate of twist as for the whole section (θ), therefore:

$$\theta_i = \theta_j = \theta_k = \dots = \theta_l = \theta_m = \dots = \theta_n = \theta \quad (3-15)$$

According to the elastic theory, the twisting moment (M_t) in a cell is equal to twice the shear flow (q) in the wall of the cell times the area (A) enclosed by the median line of the cell:

$$M_t = 2.q.A \quad (3-16)$$

Also, noting that:

$$M_t = G.J.\theta \quad (3-17)$$

Then:

$$J = \frac{2.q.A}{G.\theta} \quad (3-18)$$

Husain (1974)⁽²²⁾ proposed that the cellular plate structure is assumed to act as a series of independent closed tubes running in both longitudinal and transverse directions. The torsional constant for each cell is calculated from *Bredt's* formula:

$$J_i = \frac{4.A_i^2}{\oint \frac{ds}{t}} \quad (3-22)$$

(22)

Therefore, the torsional constant of the whole section (in any direction) is the summation of the torsional constants of the independent cells in that direction, as follows:

$$J = \sum_{i=1}^n J_i \quad (3-23)$$

Crisfield and *Twemlow* (1971)⁽²³⁾ and *Hambly* and *Pannells* (1970)⁽²⁴⁾ calculated the torsional constant (per unit width) for a structure having unequal flange thickness ($t_{fc} \neq t_{ft}$) by using equation (3-22) and neglecting the contribution of the interior webs and dividing the result by two (as the torque acts in two dimensions in a cellular plate while it acts in one dimension in a grillage):

$$J = \frac{2.t_{fc}.t_{ft}.d^2}{t_{fc} + t_{ft}} \quad (3-24)$$

(24)

A number of investigators (1,2,3,4,5,6,7,8,9,10,11,12,13,14,15,16,17,18,19,20,21,22,23,24,25,26,27,28,29,30,31,32,33,34,35,36,37,38,39,40,41,42,43,44,45,46,47,48,49,50,51,52,53,54,55,56,57,58,59,60,61,62,63,64,65,66,67,68,69,70,71,72,73,74,75,76,77,78,79,80,81,82,83,84,85,86,87,88,89,90,91,92,93,94,95,96,97,98,99,100) suggested that the torsional rigidity of the full cellular section may be approximated by considering the whole inclosed section as a single box and the torsional rigidity may be obtained from *Bredt's* formula for a single closed section using equation

(3.11). This approximation is justified by the fact that for a multi-cell structure the net shear flow through the interior webs is negligible and only the shear flow around the outer webs and top and bottom flanges is of prime significance.

Mohammed (1994)⁽⁹⁾ suggested the following formulas to express the torsional constant for exterior and interior cells of a multi-cell section having equal flange thickness ($t_{fc} = t_{ft}$):

For exterior cells:

$$J_n = \frac{4.A_n^2}{\frac{2B}{t_{fc}} + \frac{d}{t_x} + \frac{d}{\beta t'}} \quad (3-25)$$

20)

For interior cells: -

$$J_n = \frac{2.A_n^2}{\frac{B}{t_{fc}} + \frac{d}{\beta t'}} \quad (3-26)$$

where

$$\beta = \left(\frac{2b}{d} \right) \left(\frac{t'}{t_{fc}} \right) \cdot 10 \quad (3-27)$$

27)

B = width of cell (center to center)

t' = Thickness of the web in X or Y directions.

The factor (β) is suggested such that the calculated torsional constant will be identical to the value by the exact torsion theory of cellular sections shown by *Timoshenko* and *Goodier*. *Al-Sherrawi (1990)*⁽⁹⁾ benefited from equation (3-21) to transform equation (3-17) into the following form:

$$4.A_j^2 = -J_i \frac{A_j}{A_i} \int_w \frac{ds}{t} + J_j \oint \frac{ds}{t} - J_k \frac{A_j}{A_k} \int_w \frac{ds}{t} \quad (3-23)$$

23)

Each of the n-cells can provide one equation in term of the torsional constant of the cell and its adjacent cells and the solution of the resulting n independent linear equations gives the values of the torsional constant ($J_1, J_2, J_3, \dots, J_n$). Then the torsional constant for the whole section (J) is calculated from equation (3-23).

Mashal (1994)⁽²⁰⁾ modified the formulas presented by Mohammed (1994)⁽²¹⁾ to be suitable for a cellular section with unequal flange thickness ($t_{fc} \neq t_{ft}$) as follows:

For exterior cells:

$$J_n = \frac{4.A_n^2}{\frac{B(t_{fc} + t_{ft})}{2.t_{fc}.t_{ft}} + \frac{d}{t_{xt}} + \frac{d}{\beta t'}} \quad (3-24)$$

24)

For interior cells:

$$J_n = \frac{2.A_n^2}{\frac{B(t_{fc} + t_{ft})}{2.t_{fc}.t_{ft}} + \frac{d}{\beta t'}} \quad (3-25)$$

where

$$\beta = \left(\frac{2b}{d} \right) \left(\frac{t'}{\sqrt{t_{fc} \cdot t_{ft}}} \right) \cdot 10 \quad (3-10)$$

3.1)

In the present study the torsional constant for a single cell cross-section can be evaluated by Eq. (3-10). For a multi-cell cross-section (with n cells) which is undergoing Saint-Venant torsion the rate of twist (θ) for each cell is the same, so a set of simultaneous equations in the shear flow constants ($q_{sv1}, q_{sv2}, q_{sv3}, q_{sv4}, \dots$) can be obtained. Therefore for the i th cell (recalling Eq. (3-10) with new arrangement) the following expression may be written:

$$2A_i = \left(-\psi_{i-1} \int_w \frac{ds}{t} + \psi_i \int_i \frac{ds}{t} - \psi_{i+1} \int_w \frac{ds}{t} \right)$$

where

$$\psi_i = \frac{q_{svi}}{G\theta'}$$
 for the cell i

$$\psi_{i-1} = \frac{q_{svi}}{G\theta'}$$
 for the left cell

$$\psi_{i+1} = \frac{q_{svi}}{G\theta'}$$
 for the right cell

For a cellular section, the torsional constant (J_i) to each cell is:

$$J_i = 2 \cdot A_i \cdot \psi_i$$

and the torsional constant for the whole section is:

$$J_t = \sum_{i=1}^n J_i$$

3.2.3 Shearing Rigidity

In a cellular plate structure having few or no transverse diaphragms, the vertical (or transverse) shearing forces developed across a cell causes the flanges and the webs to flex independently out of plane. This pattern of deformation is referred to as distortion and this may become pronounced in cellular sections with relatively thin webs. The shearing rigidity is (GA_v) , where A_v is taken to be the full area of the web. The effect of shearing rigidity on deformation is usually very small.

3.2.3.1 Shear correction factor

The shear shape factor $1/C^r$ is defined as the ratio of the exact shear strain energy to that calculated by average (or constant) shear stress.

The always positive C^r is called shear correction factor. The study done by Day (1980)⁽²⁴⁾ on curved members with rectangular cross sections indicated that C^r -value for a curved member is almost the same as that for straight member ($C^r = 6/7$ when $R \rightarrow \infty$). For a thin walled cross section the shear correction factor was found to be close to unity⁽⁷⁾.

3.2.4 Warping Moment of Inertia

Warping moment of inertia is a geometric property of a thin-walled section and may be defined for straight member as^(43, 60, 66, 67, 9):

$$I\omega = \int_w \omega^2 dA \quad (3-32)$$

where dA is the infinitesimal area of the cross section of the wall and ω is the sectorial area or (warping function). For a curved member $I\omega$ is defined as ^(A9):

$$I\omega = \int_a \frac{R+y}{R_s} \cdot \omega^2 \cdot dA \quad (3-33)$$

where R and R_s are the radii of curvature of the centroidal and shear axis. The evaluation of $I\omega$ requires the evaluation of warping function ω .

3.2.4.1 Straight Members

The warping displacement u of any portion of the wall relative to the origin of the wall peripheral s -coordinate is given by ^(A9):

$$\bar{u} = u - u_o = \frac{1}{G} \int \frac{q_{sv}}{t} ds - \theta \int r_s ds \quad (3-34)$$

where r_s normal radius from the shear center to the tangent at the point considered and q_{sv} is the shear flow and θ is the twist per unit length by assuming that the origin of the peripheral coordinates coincides with a point of zero warping, then u_o vanishes and equation (3-34) becomes :

$$u = \frac{1}{G} \int \frac{q_{sv}}{t} ds - \theta \int r_s ds \quad (3-35)$$

In agreement with *Vlasov's* original analysis, it is here assumed that the transverse distribution of warping displacement u is fully described by the warping function or (sectional area). Since the degree of warping is directly proportional to the rate of twist θ , warping displacement at any point may be conveniently defined in the following way: -

$$u = -\omega\theta \quad (3-36)$$

36)

by introducing Eq. (3-36) into Eq. (3-35) the following expression is obtained for the warping:-

$$\omega = \int r_s ds - \frac{1}{G\theta} \int \frac{q_{sv}}{t} ds \quad (3-37)$$

This Eq. may be written as: -

$$\omega = \int \left(r_s - \frac{\psi}{t} \right) ds \quad (3-38)$$

3.2.4. Curved Members

The warping function ω for a curved cellular member with closed section can be derived by following the same procedure as for the straight cellular member.

The shear flow q_{svc} in a curved bar is related to the shear flow q_{sv} in a straight member by ^(92, 00, 47).

$$q_{svc} = \frac{R_s^2}{(R+y)^2} q_{sv} \quad (3-39)$$

39)

where R_s the radius of curvature of the shear axis and R is the radius of curvature of the centroidal axis. Then the warping function ω for a curved member with closed section can be given as ^(92, 00)

$$\omega = \int \frac{R_s^2}{(R+y)^2} r ds - \frac{1}{G\theta} \int \frac{R_s^3}{(R+y)^3} \frac{q_{sv}}{t} ds \quad (3-40)$$

Waldron (1979) ⁽⁸⁹⁾ showed that the warping moment of inertia (or warping constant) is not significantly influenced by the degree of curvature.

This concept will be used in the present study, and also the warping function for sections of both straight and curved members is calculated by Eq. (3-38)

3-3 Programming of Section Properties

A computer program (*SECPRO*) is coded in *FORTRAN* language to evaluate the section properties of any cellular section having n cells and with different dimensions. The tables from (3-1) to (3-30) are obtained by using this program. These tables contain the constants of (J, ω and I_w) for a cellular section up to 10 cells and aspect ratio $(B/d) \alpha = (0.5, 0.6$ and $0.7)$ with equal flanges and web thicknesses. The values in each table are in terms of the width of the cell and its thickness, that they should not be used directly. The following equations must be applied first:

$$J_i = \bar{J} \cdot b^3 \cdot t \quad (3-42)$$

$$\omega = \bar{\omega} \cdot b \cdot t \quad (3-43)$$

$$I_w = \bar{I}_w \cdot b^5 \cdot t \quad (3-44)$$

where:

b = width of cell

t = thickness of wall of section

\bar{J} = the constant value from tables (3-1) to (3-10)

$\bar{\omega}$ = the constant value from tables (3-11) to (3-20)

\bar{I}_w = the constant value from tables (3-21) to (3-30)

Table (r- 1) Torsional Constant (\bar{J}) For Cell No.(1)

No. of Cells	$\alpha = 0.7$	$\alpha = 0.0$	$\alpha = 0.9$
1	0.45000000	0.33333333	0.22805140
2	0.00388472	0.40000000	0.27777777
3	0.07478999	0.41176470	0.27234040
4	0.07889450	0.41379310	0.27317080
5	0.07979444	0.41414141	0.27329190
6	0.07980010	0.41420120	0.27330960
7	0.07980840	0.41421140	0.27331220
8	0.07981173	0.41421320	0.27331250
9	0.07981170	0.41421300	0.27331260
10	0.07981177	0.41421300	0.27331260

Table (r- 2) Torsional Constant (\bar{J}) For Cell No.(2)

No. of Cells	$\alpha = 0.7$	$\alpha = 0.0$	$\alpha = 0.9$
2	0.00388472	0.40000000	0.27777777
3	0.76004730	0.47088820	0.37383000
4	0.78743720	0.48270870	0.31219020
5	0.79170310	0.48484880	0.31343360
6	0.79203340	0.48520710	0.31316730
7	0.79279010	0.48527870	0.31318040
8	0.79272700	0.48527920	0.31318800
9	0.79273270	0.48528100	0.31318840
10	0.79273380	0.48528130	0.31318840

Table (r- 3) Torsional Constant (\bar{J}) For Cell No.(3)

No. of Cells	$\alpha = 0.7$	$\alpha = 0.0$	$\alpha = 0.9$
3	0.07478999	0.41176470	0.27234040
4	0.78743720	0.48270870	0.31219020
5	0.70938887	0.49494990	0.31801200
6	0.71377170	0.49704140	0.31887120
7	0.71449320	0.49740030	0.31890010
8	0.71470490	0.49747190	0.31898010
9	0.71478700	0.49747200	0.31900310
10	0.71479060	0.49747430	0.31900710

Table (r- 4) Torsional Constant (\bar{J}) For Cell No.(4)

No. of Cells	$\alpha = 0.7$	$\alpha = 0.0$	$\alpha = 0.9$
5	0.05788946.	0.4137931.	0.27317.7.
0	0.7917.31.	0.48484880.	0.313.430.
7	0.7137777.	0.497.414.	0.3188712.
7	0.717930..	0.4991334.	0.31971.0..
8	0.7187777.	0.4994924.	0.3198339.
9	0.7189280.	0.4990039.	0.3198019.
10	0.7189099.	0.4990740.	0.3198047.

Table (r-0) Torsional Constant (\bar{J}) For Cell No.(0)

No. of Cells	$\alpha = 0.7$	$\alpha = 0.0$	$\alpha = 0.9$
0	0.0797944.		0.2732919.
7	0.7920334.		0.3131773.
7	0.7144932.		0.3189801.
8	0.7187777.		0.3198338.
9	0.7190982.		0.3199077.
10	0.71977.0..		0.3199708.

Table (r-1) Torsional Constant (\bar{J}) For Cell No.(1)

No. of Cells	$\alpha = 0.7$	$\alpha = 0.0$	$\alpha = 0.9$
7	0.07980.1.	0.4142.11.	0.2733.97.
7	0.7927901.	0.4802787.	0.3131803.
8	0.714700..	0.4974719.	0.319.031.
9	0.7189284.	0.4990039.	0.3198019.
10	0.7197099.	0.4999129.	0.3199708.

Table (r-2) Torsional Constant (\bar{J}) For Cell No.(2)

No. of Cells	$\alpha = 0.7$	$\alpha = 0.0$	$\alpha = 0.9$
7	0.07988.4.	0.4142114.	0.2733122.
8	0.7927760.	0.4802792.	0.3131879.
9	0.7147870.	0.4974720.	0.319.008.
10	0.7189099.	0.4990740.	0.3198047.

Table (r-3) Torsional Constant (\bar{J}) For Cell No.(3)

No. of Cells	$\alpha = 0.7$	$\alpha = 0.0$	$\alpha = 0.9$
8	0.0798873.	0.4142132.	0.2733127.
9	0.7927327.	0.480281.0.	0.3131883.
10	0.7147927.	0.4974743.	0.319.071.

Table (r-4) Torsional Constant (\bar{J}) For Cell No.(4)

No. of Cells	$\alpha = 0.7$	$\alpha = 0.0$	$\alpha = 0.3$
9	0.07988874	0.1142130	0.2733127
10	0.7927339	0.1142130	0.3131884

Table (r-10) Torsional Constant (\bar{J}) For Cell No.(10)

No. of Cells	$\alpha = 0.7$	$\alpha = 0.0$	$\alpha = 0.3$
10	0.07988876	0.1142130	0.2733127

Table (r-11) Sectorial Area ($\bar{\omega}$) For Cell No.(1)

No. of Cells	$\alpha = 0.7$		$A = 0.0$		$\alpha = 0.3$	
	ω_L	ω_R	ω_L	ω_R	ω_L	ω_R
1	0.370000	-	0.1177777	-0.1177777	0.4280714	-
		0.3749999				0.4280717
2	0.1710380	0.0000000	0.1000000	0.0000000	0.1333333	0.0000000
3	0.3073200	0.1273110	0.2720880	0.1102941	0.2319149	0.09148937
4	0.4002764	0.2728743	0.3960017	0.2325087	0.3317073	0.9024390
5	0.7000764	0.4219978	0.5214747	0.3073232	0.4317177	0.2900721
6	0.7000764	0.5718291	0.7474497	0.4822480	0.5317177	0.3900307
7	0.9000300	0.7219973	0.7714472	0.7073080	0.7317177	0.4900318
8	1.0000280	0.8717899	0.8974477	0.7322330	0.7317179	0.5900312
9	1.2000280	1.0217890	1.0214470	0.8072332	0.8317179	0.7900311
10	1.3000280	1.1717880	1.1474470	0.9822331	0.9317179	0.7900311

Table (r-12) Sectorial Area ($\bar{\omega}$) For Cell No.(2)

No. of Cells	$\alpha = 0.7$		$A = 0.0$		$\alpha = 0.3$	
	ω_L	ω_R	ω_L	ω_R	ω_L	ω_R
2	0.0000000	-0.1710384	0.0000000	-0.1000000	0.0000000	-
						0.1333333
3	0.1273110	-0.1273109	0.1102941	-0.1102941	0.09148937	-
						0.09148937
4	0.2728743	0.0000000	0.2325087	0.0000000	0.9024390	0.0000000
5	0.4219978	0.1400787	0.3073232	0.1224747	0.2900721	0.09880777
6	0.5718291	0.2947179	0.4022480	0.2470414	0.3900307	0.1980777
7	0.7219973	0.4440004	0.7073080	0.3719711	0.4900318	0.2980001
8	0.8717899	0.5940179	0.7322330	0.4979043	0.5900312	0.3980472
9	1.0217890	0.7440110	0.8072332	0.7219022	0.7900311	0.4980407
10	1.1717880	0.8940103	0.9822331	0.7479018	0.7900311	0.5980407

Table (r-1r) Sectorial Area ($\bar{\omega}$) For Cell No.(r)

No. of Cells	$A = \cdot 7$		$A = \cdot 0$		$a = \cdot 4$	
	ω_L	ω_R	ω_L	ω_R	ω_L	ω_R
3	-0.1273109	-	-0.1102941	-0.2720088	-0.09148937	-
		0.3073020				0.23191490
4	0.0000000	-	0.0000000	-0.2327087	0.0000000	-
		0.2728742				0.19024400
0	0.1400787	-	0.1224747	-0.1224748	0.09870777	-
		0.1400787				0.09870793
7	0.2947179	0.0000000	0.2470414	0.0000000	0.19807770	0.0000000
7	0.4440004	0.1491394	0.3719771	0.1240778	0.29800010	0.098188770
8	0.0940179	0.2989972	0.4979043	0.2494924	0.39804720	0.19999230
9	0.7440110	0.4489394	0.7219022	0.3744797	0.49084070	0.299988440
10	0.8940103	0.0989332	0.7479018	0.4994774	0.09804070	0.399988990

Table (r-1s) Sectorial Area ($\bar{\omega}$) For Cell No.(s)

No. of Cells	$A = \cdot 7$		$a = \cdot 0$		$a = \cdot 4$	
	ω_L	ω_R	ω_L	ω_R	ω_L	ω_R
4	-0.2728742	-0.4002773	-0.2327087	-0.3970017	-0.19024400	-0.33170740
0	-0.1400787	-0.4219978	-0.1224748	-0.3073233	-0.09870793	-0.29007230
7	0.0000000	-0.2947180	0.0000000	-0.2470414	0.0000000	-0.19807770
7	0.1491394	-0.1491397	0.1240778	-0.1240777	0.098188770	-0.098188770
8	0.2989972	0.0000000	0.2494924	0.0000000	0.19999230	0.0000000
9	0.4489394	0.1498324	0.3744797	0.1249207	0.299988440	0.099973040
10	0.0989332	0.2998000	0.4994774	0.2499129	0.399988990	0.199976970

Table (r-1o) Sectorial Area ($\bar{\omega}$) For Cell No.(o)

No. of Cells	$A = \cdot 7$		$a = \cdot 0$		$a = \cdot 4$	
	ω_L	ω_R	ω_L	ω_R	ω_L	ω_R
0	-0.4219978	-0.7000774	-0.3073233	-0.0214747	-0.29007230	-0.43177720
7	-0.2947180	-0.0518291	-0.2470414	-0.4822480	-0.19807770	-0.39003070
7	-0.1491397	-0.4440007	-0.1240777	-0.3719770	-0.098188770	-0.29800010
8	0.0000000	-0.2989972	0.0000000	-0.2494923	0.0000000	-0.19999230
9	0.1498324	-0.1498327	0.1249207	-0.1249207	0.099973040	-0.099973070
10	0.2998000	0.0000000	0.2499129	0.0000000	0.199976970	0.0000000

Table (r-1t) Sectorial Area ($\bar{\omega}$) For Cell No.(t)

No. of Cells	$a = \cdot 7$		$a = \cdot 0$		$a = \cdot 4$	
	ω_L	ω_R	ω_L	ω_R	ω_L	ω_R
7	0.2947179	0.0000000	-0.4822480	-0.7474497	-0.39003070	-0.031777270
7	0.4440004	0.1491394	-0.3719770	-0.7072307	-0.29800010	-0.49003170
8	0.0940179	0.2989972	-0.2494923	-0.4979043	-0.19999230	-0.39804720

9	.7440110	.4489394	-.1249207	-.3744497	-.09997307	-.2997880
10	.8940103	.0989332	0.0000000	-.2499129	0.0000000	-.1999797

Table (r-17) Sectorial Area ($\bar{\omega}$) For Cell No.(7)

No. of Cells	$\alpha = 0.7$		$\alpha = 0.0$		$\alpha = 0.4$	
	ω_L	ω_R	ω_L	ω_R	ω_L	ω_R
7	-.7217977	-.900302	-.7072307	-.7714470	-.4900317	-
						.7317718
8	-.0940179	-.8717899	-.4979043	-.7322330	-.3980472	-
						.7900311
9	-.4489397	-.7440117	-.3744497	-.7219021	-.2997880	-
						.4980407
10	-.2997999	-.0989331	-.2499129	-.4994774	-.1997879	-
						.3997879

Table (r-18) Sectorial Area ($\bar{\omega}$) For Cell No.(8)

No. of Cells	$\alpha = 0.7$		$\alpha = 0.0$		$\alpha = 0.4$	
	ω_L	ω_R	ω_L	ω_R	ω_L	ω_R
8	-.8717899	-1.000280	-.7322330	-.7714470	-.0900311	-
						.7317718
9	-.7440117	-1.217890	-.7219021	-.8072331	-.4980407	-
						.7900311
10	-.0989331	-.8940101	-.4994774	-.7479017	-.3997879	-
						.0980407

Table (r-19) Sectorial Area ($\bar{\omega}$) For Cell No.(9)

No. of Cells	$\alpha = 0.7$		$\alpha = 0.0$		$\alpha = 0.4$	
	ω_L	ω_R	ω_L	ω_R	ω_L	ω_R
9	-1.217890	-1.20028	-.8072331	-1.214470	-	-.8317718
					.7900311	
10	-.8940101	-1.171788	-.7479017	-.9822329	-	-.7900311
					.0980407	

Table (r-20) Sectorial Area ($\bar{\omega}$) For Cell No.(10)

No. of Cells	$\alpha = 0.7$		$\alpha = 0.0$		$\alpha = 0.4$	
	ω_L	ω_R	ω_L	ω_R	ω_L	ω_R
10	-1.1717880	-1.300280	-.9822329	-1.1474470	-	-
					.7900311	.9317719

Table (r-21) Warping Constant ($\bar{I}\omega$) For Cell No.(1)

No. of Cells	$\alpha = 0.7$	$\alpha = 0.0$	$\alpha = 0.4$
1	0.0112000	0.01302083	0.01280714

2	0.2102811	0.1781200	0.1348148
3	0.1328345	0.17814117	0.05284550
4	0.2720322	0.19744010	0.13105050
5	0.4071880	0.3829880	0.24845031
6	0.9173726	0.73770390	0.47774100
7	1.4127400	0.97998130	0.71248790
8	2.0374070	1.38474800	0.87005780
9	2.7989000	1.88780300	1.17004700
10	3.7109300	2.48010200	1.02888800

Table (3-22) Warping Constant ($\bar{\omega}$) For Cell No.(2)

No. of Cells	$\alpha = 0.7$	$\alpha = 0.0$	$\alpha = 0.4$
2	0.2102811	0.1781200	0.1348148
3	0.1824221	0.1374073	0.09373822
4	0.8471902	0.0994211	0.3889476
5	0.2303073	0.1078311	0.9911479
6	0.4767648	0.3193477	0.19711890
7	0.8421111	0.0071100	0.33080980
8	1.3480630	0.8797971	0.02431830
9	2.1062200	1.3020920	0.77748910
10	2.8730310	1.8347170	1.07137100

Table (3-23) Warping Constant ($\bar{\omega}$) For Cell No.(3)

No. of Cells	$\alpha = 0.7$	$\alpha = 0.0$	$\alpha = 0.4$
3	0.1328345	0.17814117	0.05284550
4	0.2027042	0.1798102	0.1173321
5	0.1093070	0.7940439	0.4370998
6	0.2082024	0.1730344	0.1079004
7	0.0174011	0.3421774	0.2071728
8	0.8989902	0.0870007	0.3000070
9	1.4229760	0.9197140	0.0430478
10	2.1097240	1.3020140	0.7907391

Table (3-24) Warping Constant ($\bar{\omega}$) For Cell No.(4)

No. of Cells	$\alpha = 0.7$	$\alpha = 0.0$	$\alpha = 0.4$
4	0.2720322	0.19744010	0.13105050
5	0.2802801	0.1947704	0.12427450
6	0.10774070	0.7290710	0.4033817
7	0.27994210	0.1790248	0.10949190
8	0.0300490	0.3094800	0.2108998
9	0.92314090	0.0989273	0.30000410
10	1.4040890	0.9301770	0.04940190

Table (3-25) Warping Constant ($\bar{\omega}$) For Cell No.(5)

No. of Cells	$\alpha = 0.7$	$\alpha = 0.0$	$\alpha = 0.3$
0	0.05071880	0.38209880	0.248450310
7	0.029738457	0.020328111	0.01281094
7	0.11123780	0.07471830	0.04709448
8	0.270576470	0.18238000	0.11077990
9	0.05301790	0.30005020	0.21207940
10	0.93472930	0.70442400	0.30777010

Table (r- 27) Warping Constant (\bar{I}_ω) For Cell No.(7)

No. of Cells	$\alpha = 0.7$	$\alpha = 0.0$	$\alpha = 0.3$
7	0.91737260	0.73770390	0.40777410
7	0.03020944	0.02009710	0.01291007
8	0.11271700	0.07034070	0.04732937
9	0.27812460	0.18342940	0.11107340
10	0.05701040	0.30707470	0.21311930

Table (r- 27) Warping Constant (\bar{I}_ω) For Cell No.(7)

No. of Cells	$\alpha = 0.7$	$\alpha = 0.0$	$\alpha = 0.3$
7	1.41274000	0.97998130	0.71248790
8	0.03003201	0.02074719	0.01297233
9	0.11330870	0.07070210	0.04744071
10	0.27927330	0.18392400	0.11123790

Table (r- 28) Warping Constant (\bar{I}_ω) For Cell No.(8)

No. of Cells	$\alpha = 0.7$	$\alpha = 0.0$	$\alpha = 0.3$
8	2.037450700	1.38474800	0.87007840
9	0.030744437	0.02079271	0.01298777
10	0.11307920	0.07077032	0.04747009

Table (r- 29) Warping Constant (\bar{I}_ω) For Cell No.(9)

No. of Cells	$\alpha = 0.7$	$\alpha = 0.0$	$\alpha = 0.3$
9	2.79890000	1.88780300	1.17004700
10	0.03070701	0.02081837	0.01299097

Table (r- 30) Warping Constant (\bar{I}_ω) For Cell No.(10)

No. of Cells	$\alpha = 0.7$	$\alpha = 0.0$	$\alpha = 0.3$
--------------	----------------	----------------	----------------

1.	3.7109300	2.48010200	1.02888800

CHAPTER 4

GRILLAGE ANALOGIES

4-1 Introduction

The use of structural members of thin-walled section has been increasing rapidly in many types of engineering structures. This is due to the continuous development of modern structure requiring greater spans with reduced self-weight. These factors (large spans and reduced weight) have encouraged the wider application of thin-walled beam section in design (77, 89). In thin-walled beams, in which warping deformations are usually relatively large, the effects of warping restraint may become significant and should be fully considered in the analysis. Free warping due to pure St.-Venent's torsion is identical at every cross-section along the beam, Fig. (1.1), and proportional to the rate of twist of the beam. It is caused by the development of circulatory shear flows around the perimeter. However, if this warping is in any way restrained, Fig. (1.1), or if the distribution of warping deformation along the beam is varied, then additional axial direct (or normal) stresses and complementary shearing stresses will be created. These axial stresses differ from the more familiar stress resultants, such as axial forces and bending moments, in that they cannot be determined from equilibrium conditions alone.

The main aim of this chapter is to provide guidelines on the applicability of the grillage analogy to elastic analysis of thin-walled plate structures

curved in plan including both implicitly and explicitly the effects of warping restraints.

4.2 Inclusion of Warping Implicitly with Torsional Stiffness

In the mathematical derivation that follows, various expressions are derived for the angle of twist and its rate of change, by applying *Timoshenko's* concept of torsional warping for straight members with open and closed section and various boundary conditions⁽¹⁾. Using the following expression for the total torque:

$$T = T_{sv} + T_w \quad (4-1)$$

where

T = the total torque

T_{sv} = the Saint-Venant torque ($GJ\theta$)

T_w = the warping torsional moment ($EI_w\theta''$)

Substituting these expressions into Eq.(4-1) the following differential equation of torsion with warping restraint will be obtained:

$$\frac{T}{GJ} = \theta - a^2 \frac{d^2\theta}{dx^2} \quad (4-2)$$

where

θ = is the rate of twist, and x is the longitudinal axis and $a^2 = EI_w / GJ$.

This is a non-homogeneous second-order ordinary differential equation (*Timoshenko's* differential equation for non-uniform torsion). The general solution of Eq. (4-2) is⁽³⁾:

$$\theta = A.e^{\frac{x}{a}} + B.e^{-\frac{x}{a}} + \frac{T}{GJ} \quad (4-3)$$

The constants A and B are to be found from the boundary conditions. The general boundary conditions for torque and bimoment are shown in table (ξ-1)

Table (ξ-1) Boundary conditions for thin-walled beam

Boundary	Deformation	Force
Fixed end	$\phi = \phi' = 0$	$T_{sv} = \cdot$
Free end	-----	$T_{bm} = \cdot$
Hinge	$\phi = 0$	$T_{bm} = \cdot$

ξ.2.1 Member with One End Restrained

By applying the following boundary conditions; when $X=0$ (the fixed end), the axial displacement $u=0$, consequently, the rate of twist $\theta=0$. Also at $X=L$ (the free end) the axial (or normal) stress $\sigma_x=0$ or, according to expression that $\sigma = E\omega \cdot (d\theta/dX)$ (¹), then the constants are:

$$A = \frac{T}{GJ} \left(\frac{-e^{-\frac{L}{a}}}{\frac{L}{a} - \frac{-L}{a}} \right) \quad (\xi-4)$$

$$B = \frac{T}{GJ} \left(\frac{-e^{-\frac{L}{a}}}{\frac{L}{a} + \frac{-L}{a}} \right) \quad (\xi-5)$$

Thus,

$$\theta = \frac{T}{GJ} \left(1 - \frac{\cosh \frac{L-x}{a}}{\cosh \frac{L}{a}} \right) \quad (\xi-6)$$

The maximum angular displacement at $x=L$, thus:

$$\phi_{x=L} = \int_0^L \theta \cdot dx = \frac{T \cdot L}{GJ} \left(1 - \frac{a}{L} \cdot \tanh \frac{L}{a} \right) \quad (\xi-7)$$

whereas in pure torsion (with no warping restraint):

$$\phi = \frac{T.L}{GJ} \quad (\xi-8)$$

Comparing Eq. ($\xi-8$) with Eq. ($\xi-7$), hence with warping restraint being included implicitly, the modified torsional constant is:

$$\bar{J} = \frac{J}{\left(1 - \frac{a}{L} \cdot \tanh \frac{L}{a}\right)} \quad (\xi-9)$$

It will be noticed $\bar{J} > J$ (indicating an increase in torsional stiffness due to warping restraint). Moreover, as the length (L) increase, $\bar{J} \rightarrow J$.

$\xi.2.2$ Member with Two Ends Restrained

By applying the following boundary conditions; when $X=0$ and $X=L$, the axial displacement $u=0$. Consequently, the rate of twist $\theta=0$, this follows from formula ($\xi-36$). Then, the constants are:

$$A = \frac{T}{GJ} \left(\frac{-e^{-\frac{L}{2a}}}{e^{\frac{L}{2a}} + e^{-\frac{L}{2a}}} \right) \quad (\xi-10)$$

$$B = \frac{T}{GJ} \left(\frac{-e^{-\frac{L}{2a}}}{e^{\frac{L}{2a}} + e^{-\frac{L}{2a}}} \right) \quad (\xi-11)$$

Then,

$$\theta = \frac{T}{GJ} \left(1 - \frac{\cosh \frac{L-x}{2a}}{\cosh \frac{L}{2a}} \right)$$

($\xi-12$)

$$\phi_{x=L} = \int_0^L \theta \cdot dx = \frac{T.L}{GJ} \left(1 - \frac{2a}{L} \cdot \tanh \frac{L}{2a} \right) \quad (\xi-13)$$

Comparing Eq. (4-8) with Eq (4-12), hence with warping restraint being included implicitly, the modified torsional constant is

$$\bar{J} = \frac{J}{\left(1 - \frac{2a}{L} \cdot \tanh \frac{L}{2a}\right)} \quad (4-13)$$

Also, here $\bar{J} > J$ and $\bar{J} \rightarrow J$ as L increases.

4-7 Grillage Analysis of Cellular Plate Structure

A curved cellular plate structure can be represented by a grillage composite of curved members representing the longitudinal curved ribs intersecting at right angles with straight radial members representing the transverse diaphragms. The curve may be represented by a series (or finite number) of straight segments. Nevertheless, such an approach will be an approximation, it will increase the size of the problem, the number of unknowns and the computing time by many times since the accuracy of this approach depends on the number of segments. *Sawko* (1967) showed that the approximation of the curved member by a series of straight members could lead to a serious misinterpretation of computer output. Therefore, the development of the stiffness matrix for a grillage curved member is needed for more useful analysis.

The sign convention used here and the sign of moments and shearing forces are as shown in Fig. (4-1).

There is no need in this analysis to transform the stiffness matrix from the local to the global coordinate systems since the straight members intersect the curved members at right angles.

4-7-1 Stiffness Matrix For Straight Member

The total strain energy of a deformed beam can be written in the form:

$$U = U_b + U_t + U_w \quad (4-14)$$

where U_b is the contribution by the bending to the element strain energy,

and U_t and U_w are the contributions to the element strain energy by torsion and bimoment, respectively (ξ, ξ^r) .

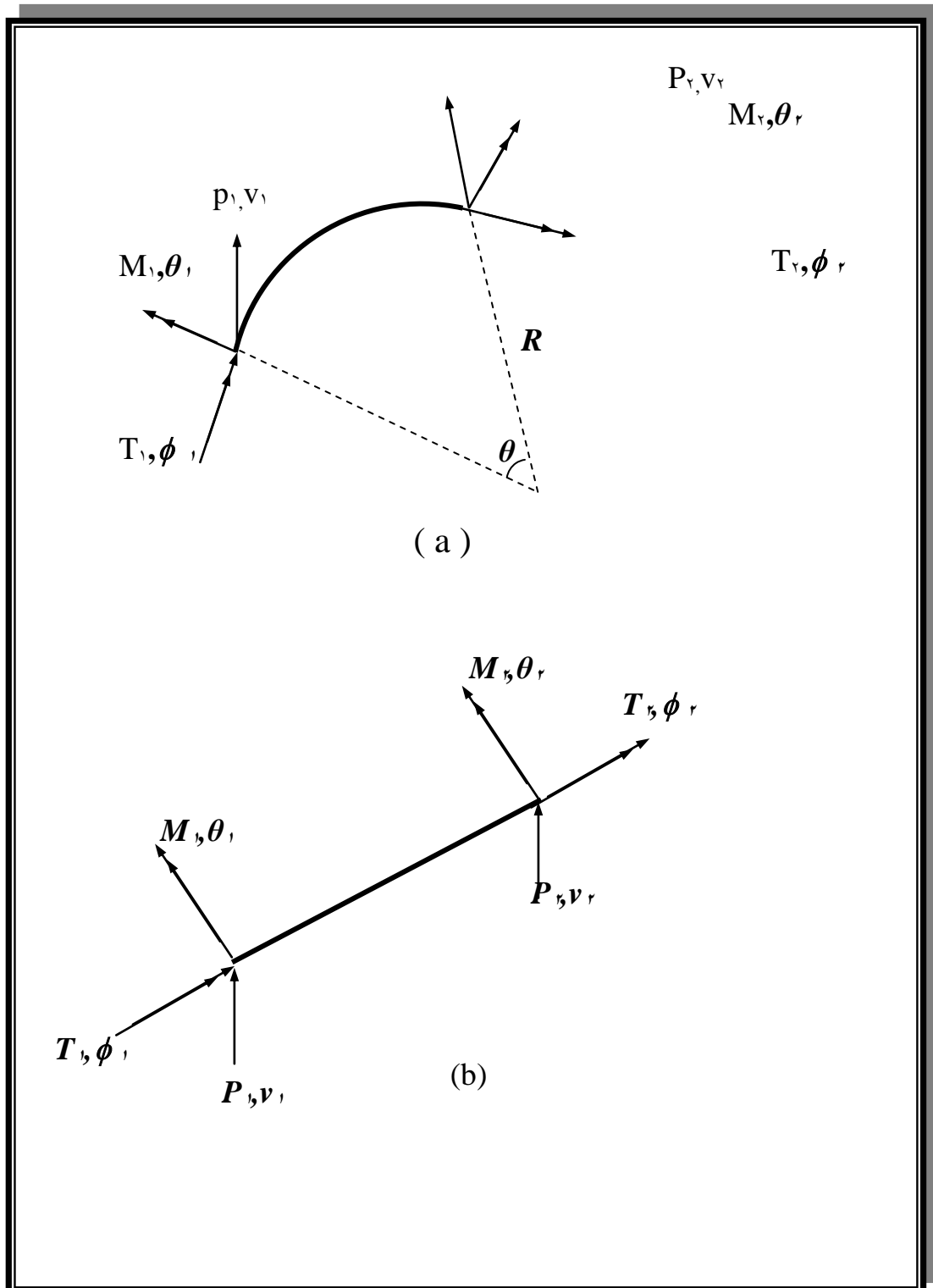


Figure (4-1) Sign convention of grillage members
 (a) Curved member
 (b) Straight member

The total strain energy can be expressed by:

$$U = \frac{EI}{2} \int_0^L (v'')^2 dx + \frac{GJ}{2} \int_0^L (\phi')^2 dx + \frac{EI_w}{2} \int_0^L (\phi'')^2 dx \quad (\xi-16)$$

The assumed displacement fields $v(x)$ and $\phi(x)$ corresponding to the translation and torsional degrees of freedom are :

$$v = a_1 + a_2 x + a_3 x^2 + a_4 x^3 \quad (\xi-17)$$

$$\phi = b_1 + b_2 x + b_3 x^2 + b_4 x^3 \quad (\xi-18)$$

The degree of freedoms considered at both ends of the element are:

$$\left\{ \phi_1, \left(\frac{dv_1}{dx} \right), v_1, \left(\frac{d\phi_1}{dx} \right), \phi_2, \left(\frac{dv_2}{dx} \right), v_2, \left(\frac{d\phi_2}{dx} \right) \right\}$$

Then, by solving Eqs.($\xi-17$) and ($\xi-18$) for the ends degrees of freedom the following results can be obtained:

$$v = (1 - 3x^2 + 2x^3) v_1 + (x - 2x^2 + x^3) L \left(\frac{dv_1}{dx} \right) + (3x^2 - 2x^3) v_2 + (-x^2 + x^3) L \left(\frac{dv_2}{dx} \right) \quad (\xi-19)$$

and

$$\phi = (1 - 3x^2 + 2x^3) \phi_1 + (x - 2x^2 + x^3) L \left(\frac{d\phi_1}{dx} \right) + (3x^2 - 2x^3) \phi_2 + (-x^2 + x^3) L \left(\frac{d\phi_2}{dx} \right) \quad (\xi-20)$$

By making use of the Eqs.($\xi-19$) and ($\xi-20$) and carrying out the integration of Eq.($\xi-16$), then the total strain energy may be written in matrix form as:

$$U = \frac{1}{2} \{\Delta\}^T \cdot [K_B] \cdot \{\Delta\} + \frac{1}{2} \{\Delta\}^T \cdot [K_T] \cdot \{\Delta\} + \frac{1}{2} \{\Delta\}^T \cdot [K_W] \cdot \{\Delta\} \quad (\xi-21)$$

where:

$$U = \frac{EI}{2} \int_0^L \left(v'' - \frac{\phi}{R} \right)^2 dx + \frac{GJ}{2} \int_0^L \left(\phi' + \frac{v'}{R} \right)^2 dx + \frac{EI_w}{2} \int_0^L \left(\phi'' + \frac{v''}{R} \right)^2 dx \quad (\xi-20)$$

By the same way used in the derivation of stiffness matrix of straight member, the stiffness of the curved member will be obtained. Therefore, by solving the displacement fields (v and ϕ) for the end degrees of freedom of the curved member the following equation will be obtained:

$$v = \left(1 - 3x^2 + 2x^3 \right) v_1 + \left(x - 2x^2 + x^3 \right) L \left(\frac{dv_1}{dx} \right) + \left(3x^2 - 2x^3 \right) v_2 + \left(-x^2 + x^3 \right) L \left(\frac{dv_2}{dx} \right) \quad (\xi-26)$$

and

$$\phi = \left(1 - 3x^2 + 2x^3 \right) \phi_1 + \left(x - 2x^2 + x^3 \right) L \left(\frac{d\phi_1}{dx} \right) + \left(3x^2 - 2x^3 \right) \phi_2 + \left(-x^2 + x^3 \right) L \left(\frac{d\phi_2}{dx} \right) \quad (\xi-27)$$

Then, by using the Eqs. (ξ-26) and (ξ-27) and carrying out the integration of Eq. (ξ-20) to get the strain energy, then the total strain energy may be written as:

$$U = \frac{1}{2} \{\Delta\}^T \cdot [K_B] \cdot \{\Delta\} + \frac{1}{2} \{\Delta\}^T \cdot [K_T] \cdot \{\Delta\} + \frac{1}{2} \{\Delta\}^T \cdot [K_W] \cdot \{\Delta\} \quad (\xi-28)$$

where:

$$\left\{ \phi_1, \left(\frac{dv_1}{dx} \right), v_1, \left(\frac{d\phi_1}{dx} \right), \phi_2, \left(\frac{dv_2}{dx} \right), v_2, \left(\frac{d\phi_2}{dx} \right) \right\}$$

$[K_B]$ = the contribution of bending to the stiffness matrix.

$[K_T]$ = the contribution of St. Venant torsion to the stiffness matrix.

$[K_W]$ = the contribution of bimoment to the stiffness matrix.

Also, Eq. (ξ-28) may be written as:

$$U = \frac{1}{2} \{\Delta\}^T \cdot [K] \cdot \{\Delta\} \quad (\xi-29)$$

where

$$[K] = [K_B] + [K_T] + [K_W] \quad (\xi-30)$$

which represent the required stiffness matrices for curved member. The elements of lower triangle of these matrices are shown in Table ($\xi-31$).

Table ($\xi-31$) Elements of Stiffness Matrix of Curved Beam

Index		Elements of Bending Stiffness Matrix
Row (I)	Column (j)	$EI_y \cdot K_c (I, J)$
1	1	$\frac{13L}{35R^2}$
2	1	$\frac{11}{10R} - \frac{11L^2}{10R^3}$
2	2	$\frac{4}{L} - \frac{4L}{15R^3} + \frac{L^3}{105R^4}$
3	1	$\frac{-6}{5RL}$
3	2	$\frac{6}{L^2} - \frac{1}{10R^2}$
3	3	$\frac{12}{L^3}$
4	1	$\frac{11L^2}{210R^3}$
4	2	$\frac{2L}{15R} - \frac{L^3}{105R^3}$
4	3	$\frac{-1}{10R}$

ε	ε	$\frac{L^3}{105R^2}$
ο	ι	$\frac{9L}{70R^2}$
ο	ϒ	$\frac{-1}{10R} - \frac{13L^2}{420R^3}$
ο	ϓ	$\frac{6}{5RL}$
ο	ε	$\frac{13L^2}{420R^2}$
ο	ο	$\frac{13L^2}{35R^2}$
ϒ	ι	$\frac{1}{10R} + \frac{13L^2}{420R^3}$
ϒ	ϒ	$\frac{2}{L} + \frac{L}{15R^2} - \frac{L^3}{140R^4}$
ϒ	ϓ	$\frac{6}{L^2} - \frac{1}{10R^2}$
ϒ	ε	$\frac{-L}{30R} + \frac{L^3}{140R^3}$
ϒ	ο	$\frac{-11}{10R} + \frac{11L^2}{210R^3}$
ϒ	ϒ	$\frac{4}{L} - \frac{4L}{15R^3} + \frac{L^3}{105R^4}$
ϒ	ι	$\frac{6}{5RL}$
ϒ	ϒ	$-\frac{6}{L^2} + \frac{1}{10R^2}$
ϒ	ϓ	$\frac{-12}{L^3}$
ϒ	ε	$\frac{1}{10R}$
ϒ	ο	$\frac{-6}{5RL}$
ϒ	ϒ	$-\frac{6}{L^2} + \frac{1}{10R^2}$

ν	ν	$\frac{12}{L^3}$
λ	ρ	$\frac{-13L^2}{420R^2}$
λ	τ	$\frac{-L}{30R} + \frac{L^3}{140R^3}$
λ	σ	$\frac{-1}{10R}$
λ	ϵ	$\frac{-L^3}{140R^2}$
λ	ϕ	$\frac{-11L^2}{210R^2}$
λ	ζ	$\frac{12L}{15R} - \frac{L^3}{105R^3}$
λ	ν	$\frac{1}{10R}$
λ	λ	$\frac{L^3}{105R^3}$

<i>Index</i>		<i>Elements of Twisting Stiffness Matrix</i>
<i>Row (I)</i>	<i>Column (j)</i>	<i>GJ. Kt (I , J)</i>
1	1	$\frac{6}{5L}$
2	1	.
2	2	.
3	1	$\frac{-6}{5RL}$
3	2	.
3	3	$\frac{6}{5RL^2}$
4	1	$\frac{1}{10}$
4	2	.

ε	ν	$\frac{-1}{10R}$
ε	ε	$\frac{2L}{15}$
σ	ν	$\frac{-6}{5L}$
σ	ν	.
σ	ν	$\frac{6}{5RL}$
σ	ε	$\frac{-1}{10R}$
σ	σ	$\frac{6}{5L}$
τ	ν	.
τ	ν	.
τ	ν	.
τ	ε	.
τ	σ	.
τ	τ	.
ν	ν	$\frac{6}{5RL}$
ν	ν	.
ν	ν	$\frac{-6}{5R^2L}$
ν	ε	$\frac{1}{10R}$
ν	σ	$\frac{-6}{5RL}$
ν	τ	.
ν	ν	$\frac{6}{5R^2L}$

1	1	$\frac{1}{10}$
1	2	.
1	3	$-\frac{1}{10R}$
1	4	$-\frac{L}{30}$
1	5	$-\frac{1}{10}$
1	6	.
1	7	$\frac{1}{10R}$
1	8	$\frac{2L}{15}$

Index		Elements of Warping Stiffness Matrix
Row (I)	Column (j)	$EI_{\omega}K_w(I, J)$
1	1	$\frac{12}{L^3}$
2	1	.
2	2	.
3	1	$-\frac{12}{RL^3}$
3	2	.
3	3	$-\frac{12}{R^2L^3}$
4	1	$\frac{6}{L^2}$
4	2	.
4	3	$-\frac{6}{RL^2}$
4	4	$\frac{4}{L}$

o	1	$\frac{-12}{L^3}$
o	2	.
o	3	$\frac{12}{RL^3}$
o	4	$\frac{-6}{L^2}$
o	o	$\frac{12}{L^3}$
γ	1	.
γ	2	.
γ	3	.
γ	4	.
γ	o	.
γ	γ	.
γ	1	$\frac{12}{RL^3}$
γ	2	.
γ	3	$\frac{-12}{R^2L^3}$
γ	4	$\frac{6}{RL^2}$
γ	o	$\frac{-12}{RL^3}$
γ	γ	.
γ	γ	$\frac{12}{R^2L^2}$
λ	1	$\frac{6}{L^2}$
λ	2	.

λ	μ	$-\frac{6}{RL^2}$
λ	ξ	$\frac{2}{L}$
λ	σ	$-\frac{6}{L^2}$
λ	τ	.
λ	ν	$\frac{6}{RL^2}$
λ	λ	$\frac{4}{L}$

4.2 Application Examples

In order to verify the validity and accuracy of the stiffness matrix of the straight and curved member, including implicitly and explicitly the effect of warping restraint as presented herein, two computer programs are constructed to perform the grillage analysis. Three examples are analyzed using these programs and also using *MSC/NASTRAN and STAAD III*. The results agreed closely with these two programs.

4.2.1 Example 1

A thin walled box beam subjected to a twisting moment is considered. Fig.(4-2) shows the thin wall box beam ($L=1000 \text{ mm}$, $b=100 \text{ mm}$, $h=100 \text{ mm}$, $t=1 \text{ mm}$, $E=200 \text{ GPa}$, $G=76.9 \text{ GPa}$) with one end fixed and other end free. The box beam is loaded by a twisting moment of magnitude ($T=100 \text{ N.m}$) at one end. The analysis is performed by the present computer programs and *MSC/NASTRAN (flat shell element) and STAAD III* packages. The magnitude of the tip rotation gives good agreement with those obtained by the two packages, Tab.(4-2).

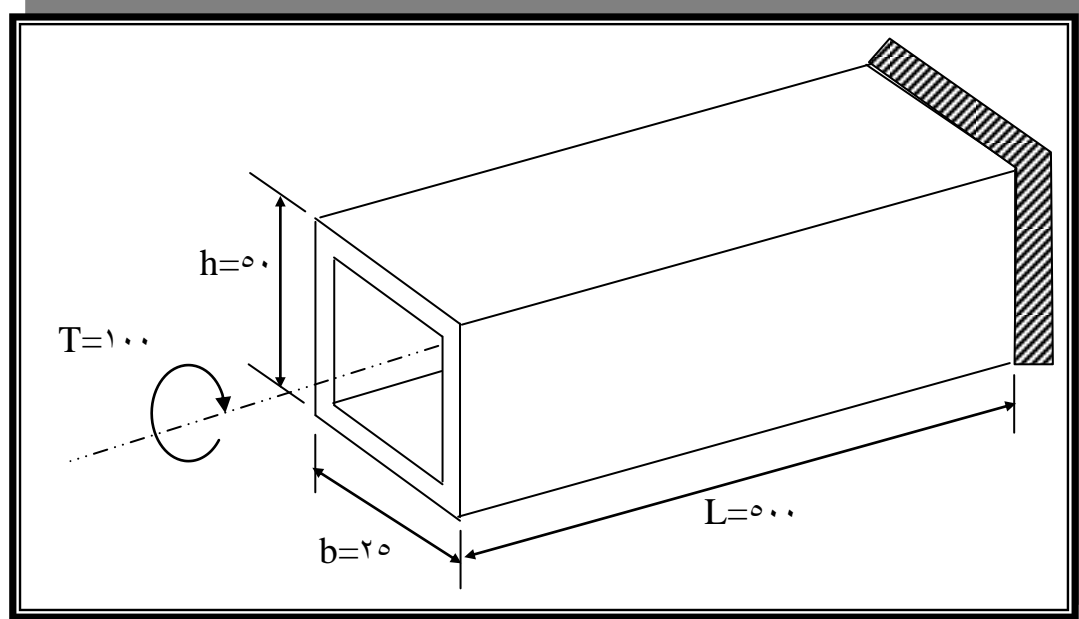


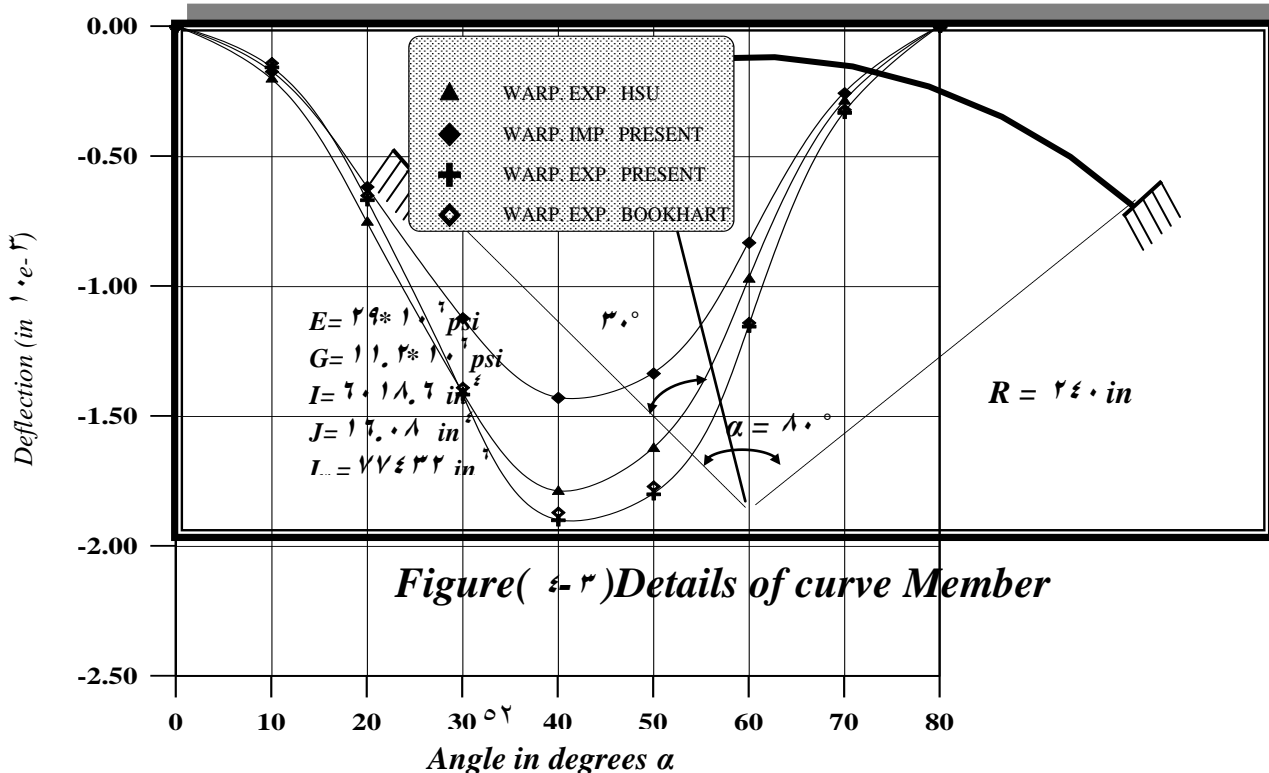
Figure.(4-7) Details of straight box beam member under torque

Table(4-2) Box beam subjected to a twisting moment

PROGRAM	No. of Element	Tip Rotation	%Error
(NASTRAN)	2600	1.004×10^{-2}	0.00
STAAD III Beam Column Element	2	1.06×10^{-2}	0.386
Grillage (4 DOF)	2	1.400×10^{-2}	6.370
Grillage (7 DOF) with imp. warping	2	1.401×10^{-2}	6.628
Grillage (7 DOF) Without warping	2	1.06×10^{-2}	0.386

4-2 Example Two

An example of a curved girder, Fig.(4-3),previously analyzed using a closed form solution by Brookhart, is analyzed by using the present mathematical expression and also by MSC/NASTRAN Package. The results of deflections and twisting angles obtained by the present computer programs give good agreement with those obtained by NASTRAN package and also by Brookhart, Fig.[(4-4)and(4-5)]. The percentages differences are about 0.20% and 11% for deflections and twisting angles



Figure(4-3)Details of curve Member

Figure(4-4) Deflection curve of example 2

4-2-3 Example Three

A cellular plate cantilever curved in plan Fig.(4-6) is analyzed by the present derivations and also by *MSC/NASTRAN* package program using flat shell elements. This is specially chosen to assess the efficiency of the present formulation for cellular plate structures having high twisting and bending moments. Two loading conditions are applied in this example. The first and the second loading conditions are a point load of 10 kn. over the outer corner and at the middle of the free edge respectively. The results of deflections and twisting angles obtained by the present study agreed with those obtained by *MSC/NASTRAN*. The percentage differences are about 1.1% **and** 1.4% for deflections and twisting angles respectively.

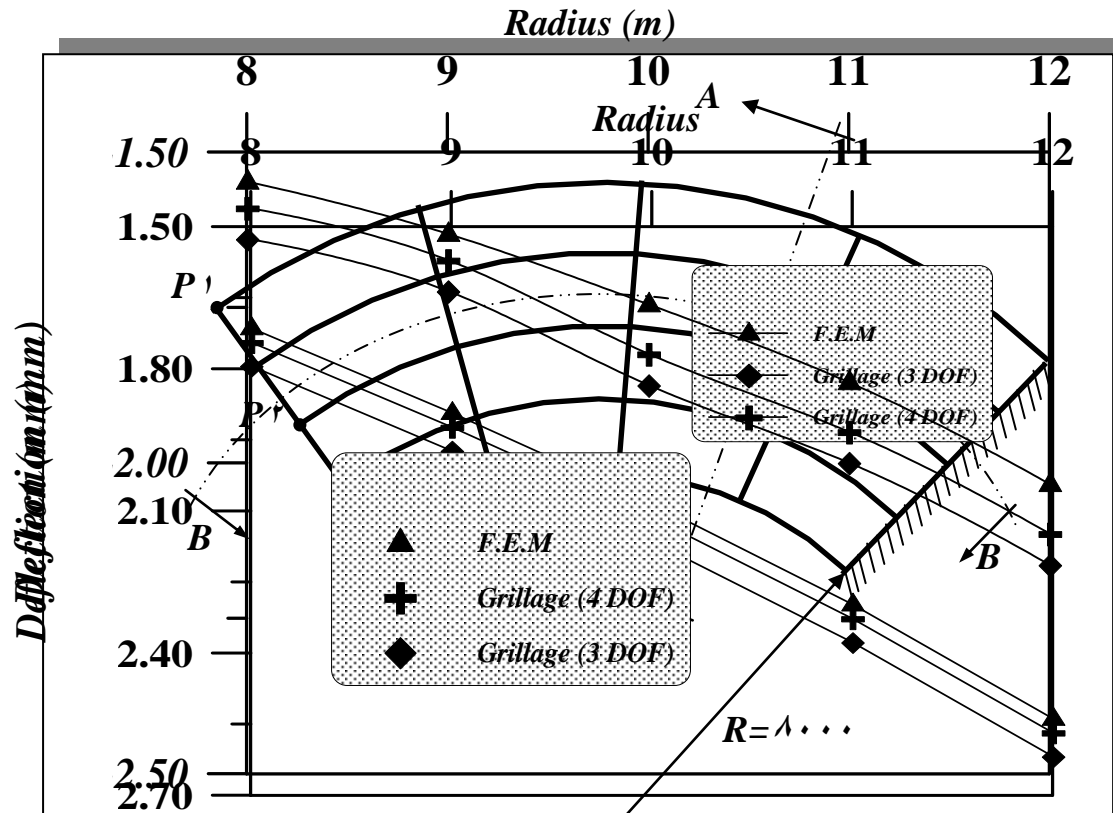


Figure (4-9) Vertical deflection along the free edge under 2nd loading condition
 Figure (4-10) Vertical deflection along the free edge under 1st loading condition

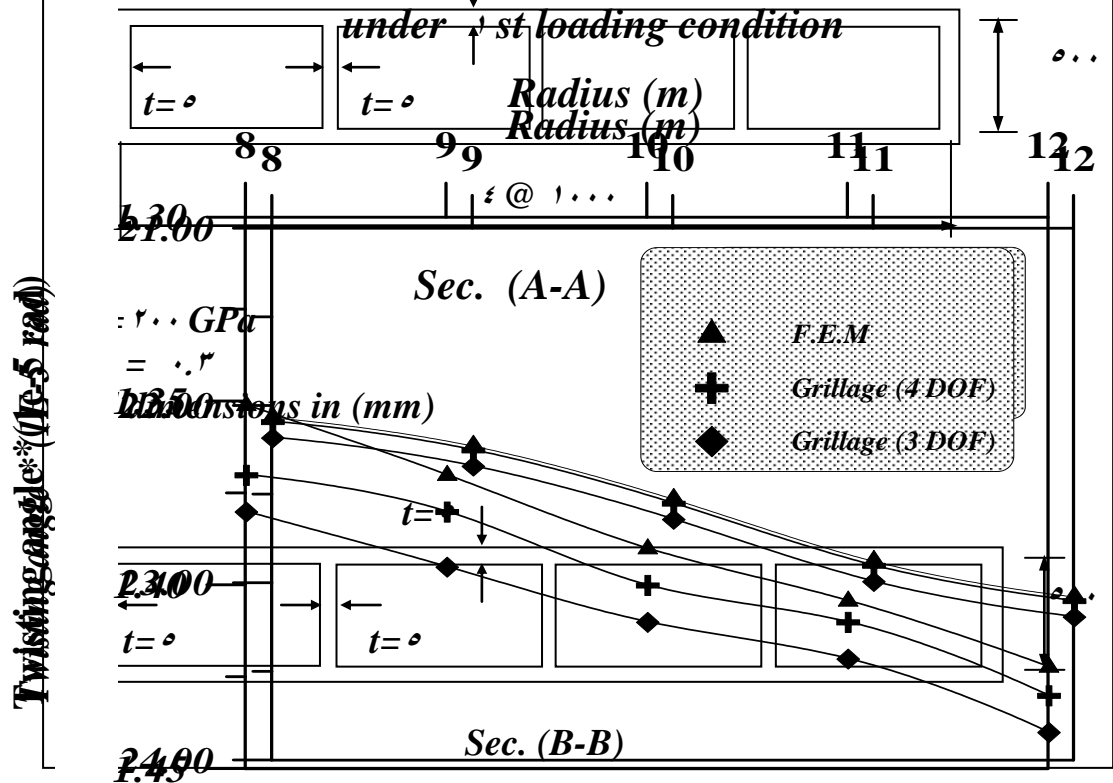


Figure (4-11) Twisting angle along the free edge under 2nd loading condition
 Figure (4-12) Twisting angle along the free edge under 1st loading condition
 Figure (4-13) Details of loading condition structure of example 4

CHAPTER 5

NONLINEAR BEHAVIOR OF CELLULAR PLATE STRUCTURES

5.1 Introduction

The objective of this chapter is to provide a theoretical basis for the nonlinear analysis and ultimate load investigation of cellular plate structures curved in plan and with or without diaphragms. A simple analysis method is presented, which is capable to predict the collapse load of cellular plate structures with a good degree of accuracy. This method consists of the extension of the grillage approach into the nonlinear range and at the collapse of the multi-cell structure.

As mentioned previously, steel or aluminium cellular plate structures are fabricated as an assemblage of individual plates forming the top and bottom cover plates and the longitudinal and transverse partitioning webs. This construction allows the structures to have high strength to weight ratio. So, this type of structure will be well suited to bridge decks, aircraft wings, ship bottoms and other situations where strength and reduction of self-weight are important design objectives. To maximize the saving in self-weight, the component plates are designed to be of thin proportions. Accordingly, they will have a low elastic critical (or buckling) stress and will normally operate in the post-buckling range. Thus, advantage must be taken of their post-buckling reserve of strength. Concerning the nonlinear

analysis, the present study takes into account the effects of two basic type of nonlinearity (material and geometric nonlinearities) to represent the nonlinear behavior of the component plates used in the construction of cellular plate structures.

5.1.1 Material Nonlinearity

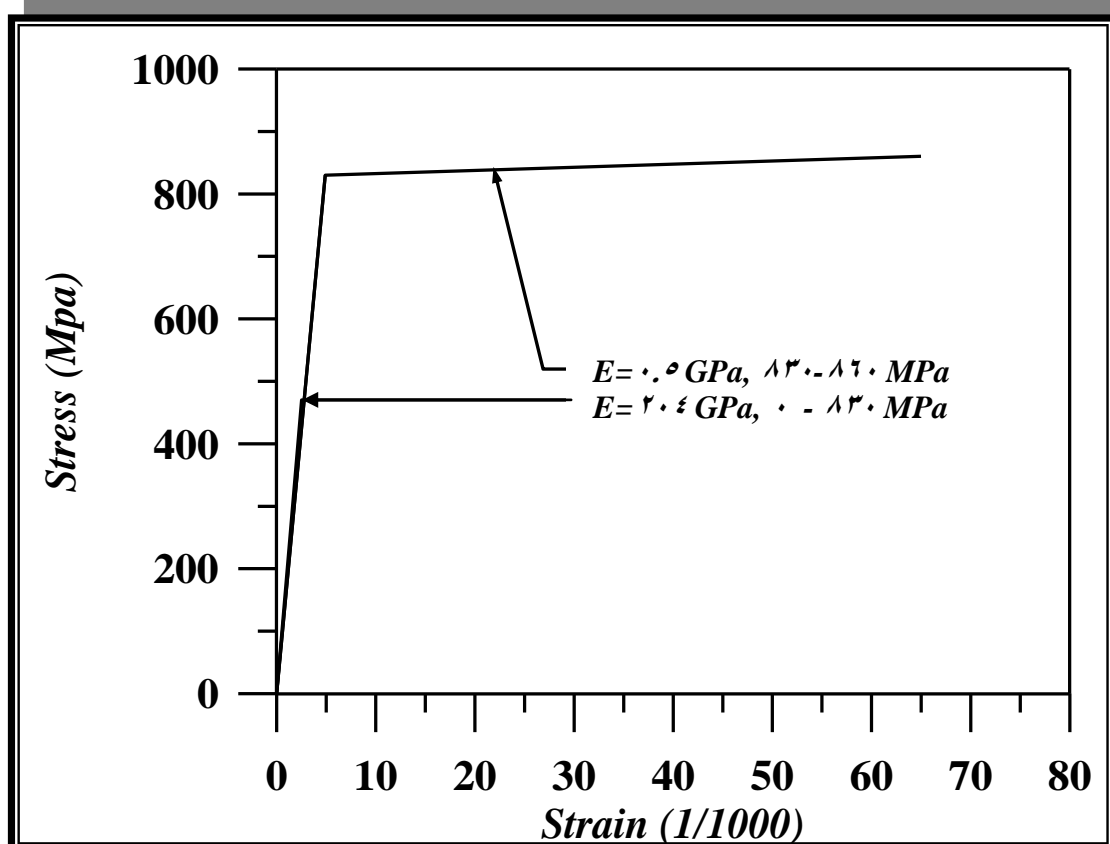
The effect of material nonlinearity is incorporated in the nonlinear analysis when the material properties vary with the growth of stress in the material; i.e. the constitutive laws are functions of the current stresses in the material. This variation is a consequence of the occurrence and spread of local yielding in component plates of the cellular plate structure.

In the present study, as the material yields (reaching the yield stress), a hypothetical hinge (plastic hinge) concept is adopted in which the structural model softens under increasing loads due to increasing spread of plasticity for the whole structure. The experimental study made by *Lagerqvist*⁽¹²⁾ on steel girders with modulus of elasticity $E = 2.0 \text{ GPa}$ showed that the modulus in the plastic stage becomes $E = 0.6 \text{ GPa}$ as shown in Fig.(5-1). This value is used in the present study.

5.1.2 Geometric Nonlinearity

This type of nonlinearity is introduced when deflections in the individual thin plates become large enough to activate membrane forces in the plane of the plate panels. When the membrane compressive stresses (acting upon the compression flange) reach the critical limit, the flange will buckle. Also, the webs (which are assumed to sustain constant shearing stresses in any cross section the analysis of cellular plate structures) will buckle when the shearing stress reaches the critical limit. So, while dealing with the nonlinear behavior and ultimate load investigation of the thin –

walled structures (like the cellular plate structure), it becomes important to consider the post-buckling behavior of the compression flange as well as



the web **Figure 4.1) Bi-linear stress-strain relation used for transforming measured strains to stresses⁽¹⁷⁾**

4.1.3 Necessary Assumptions

Regarding the present work, the following assumptions will be made to deal with the grillage simulation of the post-buckling and elastic-plastic behavior of steel cellular plate structures curved in plan:

- 1-The material of the plate is homogeneous and isotropic (the effect of strain hardening is neglected).
- 2-Concerning the critical stress evaluation of the nonprismatic compression flange (linearly varying in width), the following assumptions will be considered:

- a- The curved trapezoidal plan of the compression flange plate between radial webs is approximated to a rectangle with a width (b_{av}) equal to the average widths of the trapezoid (b_1 and b_2), as follows:

$$b_{av} = \frac{b_1 + b_2}{2} \quad (5-1)$$

- b- Since each grillage member represents the state of stress in one direction only, thus for simplicity, the critical stress (in each direction of the grillage structure) will be calculated as if the compression flange is under uniform uniaxial stress acting at that direction.
- c- The boundary edges for the compression flange panels are assumed to be simply supported (as the flexural rigidity of the thin flange plate is very small).
- Ⓝ- Regarding the evaluation of the shear buckling coefficients of the web panels, for straight members, the boundary edges of these panels are assumed to be partially restrained according to the parametric study presented by *Lee and Yoo* (1991)⁽⁵²⁾, and for curved members the proposed formula of *Batdorf, Stein and Shilderout*⁽⁵³⁾, is used. Also, the web panels are assumed to be under constant shearing stresses.
- Ⓞ- The effects of residual stresses due to welding and fabrication are neglected
- Ⓟ- All plate panels are assumed to be flat (without geometrical imperfections).

5.2 Post-Buckling Behavior of Compression Flange Panel

5.2.1 Introduction

Membrane (or in-plane) forces may be acting on a thin plate in this case. The middle surface of the plate is subjected to in plane stresses. When the plate deflects (by any means), these forces will have components in the

transverse (or lateral) direction and will cause moments on the section of the plate. The deflection will decrease or increase according to the tensile or compressive type of the membrane forces.

The theoretical treatment of local buckling of thin flat plates under the action of membrane forces (in the plane of the middle surface of the plate) is based on the governing differential equation of the buckled plate, which is given as follows:

$$\nabla^4 w = \frac{1}{D} \left[N_x \frac{\partial^2 w}{\partial x^2} + 2N_{xy} \frac{\partial^2 w}{\partial x \partial y} + N_y \frac{\partial^2 w}{\partial y^2} \right] \quad (5.2)$$

where:

$$\nabla^4 w = \left[\frac{\partial^4 w}{\partial x^4} + 2 \frac{\partial^4 w}{\partial x^2 \partial y^2} + \frac{\partial^4 w}{\partial y^4} \right] \quad (5.3)$$

w = the deflection of a point in the middle surface in the direction z , perpendicular to the xy -plane.

N_x, N_y = the membrane (or in plane) normal forces (per unit width) in the x and y directions, respectively.

N_{xy} = the membrane shearing force (per unit width).

$$D = \frac{Et^3}{12(1-\nu^2)}$$

t = thickness of the plate.

The plate remains flat until the compressive stress, which is assumed to be uniformly distributed over the width of the plate, exceeds the elastic critical stress, then the plate may buckle causing geometric nonlinearity.

5.2.2 Evaluation of Elastic Critical Stress

Based on the assumption (b) in section (5.1.3), the differential equation defining equilibrium of a buckled flat plate under uniform uniaxial

compressive stress is expressed by substituting ($\mathbf{N}_x = -\sigma_x \cdot t$) into Eq. (5.2) as follows ⁽⁵⁾:

$$\frac{\partial^4 w}{\partial x^4} + 2 \frac{\partial^4 w}{\partial x^2 \partial y^2} + \frac{\partial^4 w}{\partial y^4} = \frac{\sigma_x \cdot t}{D} \cdot \frac{\partial^2 w}{\partial x^2} \quad (5.4)$$

where:

σ_x = the uniform compressive stress in the x-direction (Fig(5.2)).

In order to evaluate the elastic critical stress utilizing the second assumption cited in Section (5.1.3), a simply supported flat rectangular plate subjected to uniform uniaxial compressive stress is considered, as shown in Fig(5.2). Accordingly, the deflected surface $w(x, y)$ of the buckled plate is expressed in double Fourier half-range sine series ⁽⁶⁾;

$$w(x, y) = \sum_{m=1}^{\infty} \sum_{n=1}^{\infty} A_{mn} \cdot \sin\left(\frac{m\pi x}{a}\right) \cdot \cos\left(\frac{n\pi y}{b_{av}}\right) \quad (5.5)$$

where:

A_{mn} = the amplitude of the deflection.

m, n = the number of half-waves in the x and y direction, respectively.

By substituting into Eq.(5.4) and equating the coefficients of identical terms, then the critical values of (σ_x) are:

$$\sigma_x = \frac{D\pi^2}{t \cdot a^2} \left(m + \frac{n^2 \cdot a}{m \cdot b_{av}^2} \right)^2 \quad (5.6)$$

From which:

$$\sigma_x = \frac{D\pi^2}{t \cdot b_{av}^2} \left(\frac{m \cdot b_{av}}{a} + \frac{n^2 \cdot a}{m \cdot b_{av}} \right)^2 \quad (5.7)$$

According to Eq.(5.7), it is obvious that the smallest value of (σ_x) will be obtained by taking (n) equal to (1). The physical meaning of this, is that the plate buckles in such a way that there can be several half-waves in the x-direction (the direction of compression) and only one half-wave along the

perpendicular
y-direction.
Thus, the
expression for
the critical
value of the
compressive
stress
becomes ^(9.8);

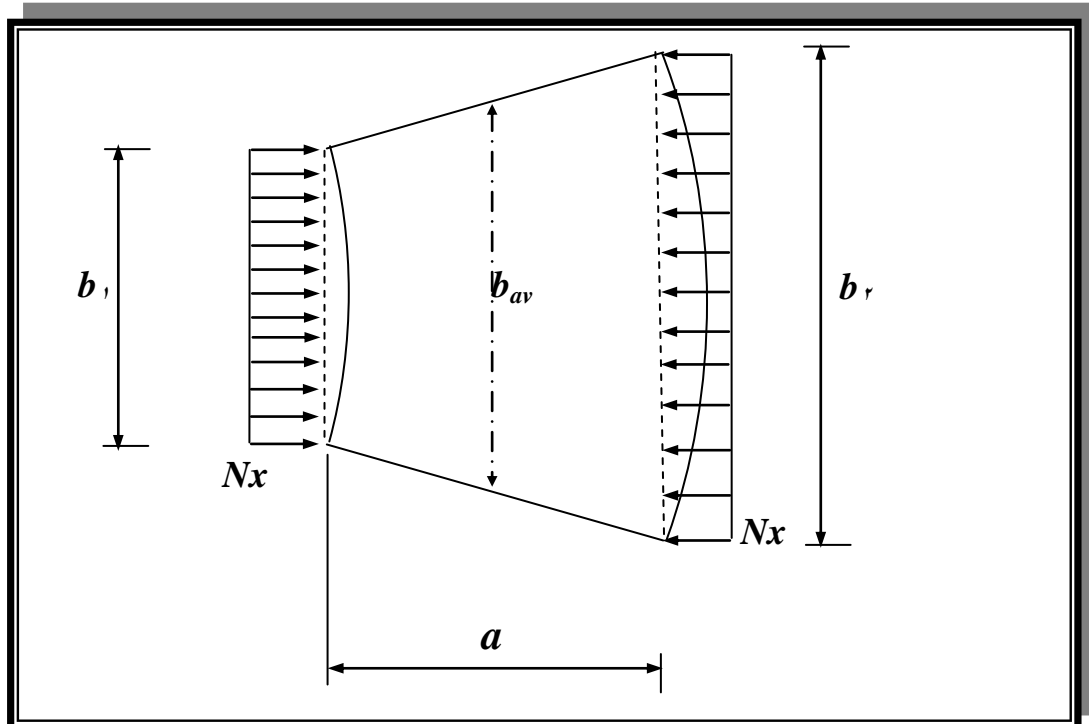


Figure (9.8) A plate panel under uniform uniaxial stress

$$\sigma_{x(cr)} = \frac{D\pi^2}{t.b_{av}^2} \left(\frac{m.b_{av}}{a} + \frac{a}{m.b_{av}} \right)^2 \tag{9.8}$$

then:

$$\sigma_{x(cr)} = K \cdot \frac{D.\pi^2}{t.b_{av}^2} \tag{9.9}$$

where the buckling coefficient(**K**) is expressed as follows:

$$K = \left(\frac{m.b_{av}}{a} + \frac{a}{m.b_{av}} \right)^2 \tag{9.10}$$

Along the x-direction, the number of half-waves (**m**) that yields the minimum value of ($\sigma_{x(cr)}$) is found by taking the first derivative of ($\sigma_{x(cr)}$) in Eq.(9.8) with respect to (**m**) and putting this derivative equal to zero, as follows:

$$\frac{d\sigma_{x(cr)}}{dm} = \frac{2D\pi^2}{t.b_{av}^2} \left(\frac{m.b_{av}}{a} + \frac{a}{m.b_{av}} \right) \left(\frac{b_{av}}{a} - \frac{a}{m^2.b_{av}} \right) = 0$$

Form which a real value of (m) is:

$$m = \frac{a}{b_{av}^2}$$

So, the minimum value of the buckling coefficient (K_{min}) is calculated by substituting ($m = a / b_{av}^2$) into Eq.(5.8); then:

$$\sigma_{x(cr)} = \frac{4D\pi^2}{t.b_{av}} \quad (5.11)$$

Equation (5.11) is valid if (a / b_{av}) is an integer, while for non-integer values, Eq.(5.8) is used (for $m = 1, 2, 3, \dots$).

In order to evaluate the stability of single plates with simply supported boundary conditions and subjected to uniform uniaxial compressive stress, *Timoshenko and Gere (1971)*⁽⁵⁷⁾ presented the following buckling curves that show the relationship between the buckling coefficient (K) and aspect ratio (a/b) with various values of (m). Regarding the present study, the buckling coefficient (K) for various aspect ratios is calculated from Fig.(5-7) depending on Eq. (5.10). This equation gives a good approximation for the buckling stress of curved plates having normal curvature. Fig.(5-8) shows a curved plate having radius $R=1000 \text{ mm}$ and width $B=1000 \text{ mm}$ and thickness $t=10 \text{ mm}$. The buckling stress of this plate is evaluated by using Eq.(5.10), the same plate is reanalyzed by adopting a more accurate method (three – dimensional flat shell finite elements) using the package program *NASTRAN*. From the comparisons of the results obtained by these two methods it is found that the buckling stress from Eq.(5.10) is (53.977 MPa) while the buckling stress from *NASTRAN*. Package program is (57.177 MPa), so a good approximation could be obtained from Eq.(5.10)

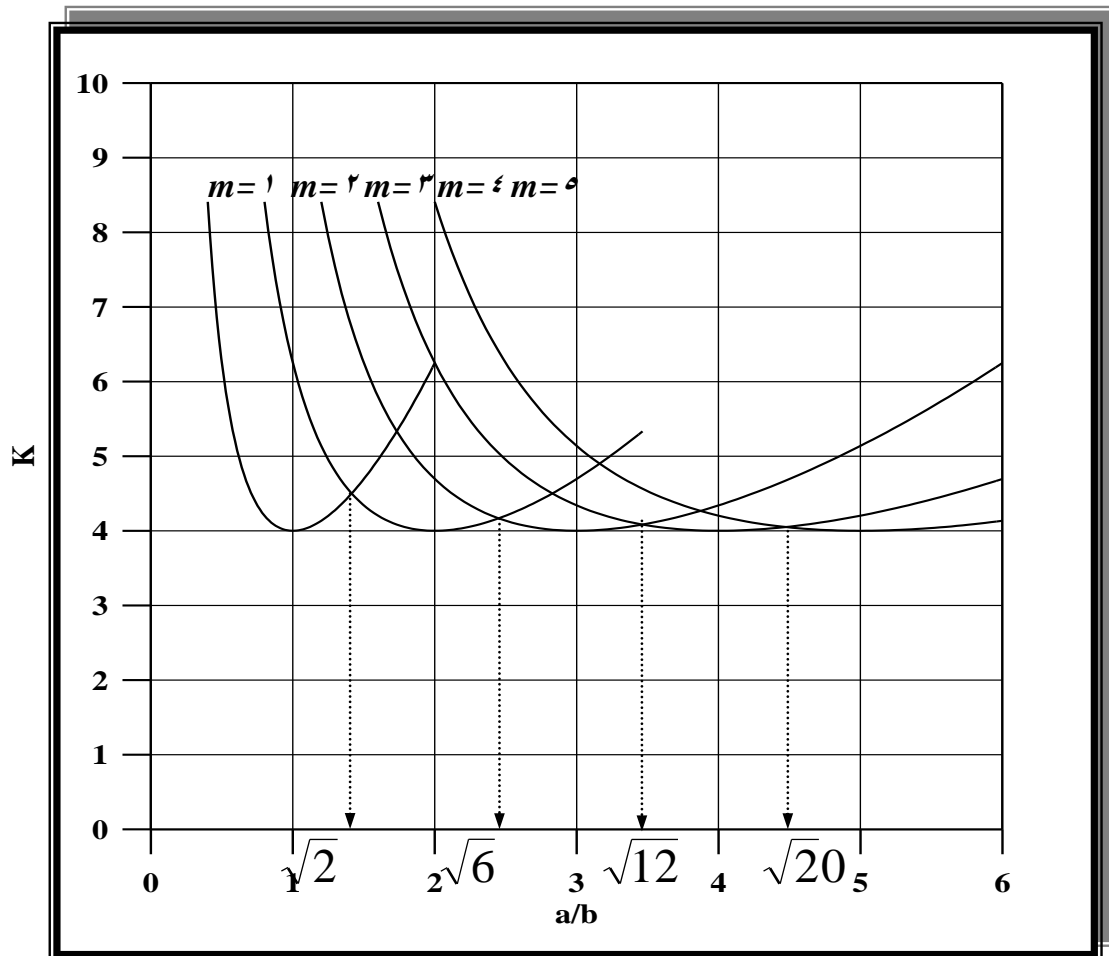


Figure 5.7 Stability of single plate with simply supported edges ^(5.7)

Beyond the critical stress, the compression flange enters into the nonlinear range due to post-buckling during which the distribution of the normal stress across the width of the flange will be nonuniform.

Von Karman et al. (1932) ^(5.8) argued that; when buckling occurs in a rectangular plate, the central portion of the plate deflects, and tends to shed away some of the compressive stress while, in contrast, the portion of the plate nearer the edges accepts higher stress and remain almost straight.

Accordingly, the distribution of the longitudinal compressive stress across the flange plate becomes nonuniform. Based on this, *Von Karman et al.* ^(5.9) made their bold assumption that the central strip of the plate can be thought to be completely ineffective, and the nonlinear post-buckling longitudinal stress in the plate is approximated by a uniform stress (equal to

the edge stress (σ_e) over two strips at the edges, each strip has width (b_e/r), as shown in Fig. (5-5); where (b_e) is the effective width of the plate. Thus, the in-plane load

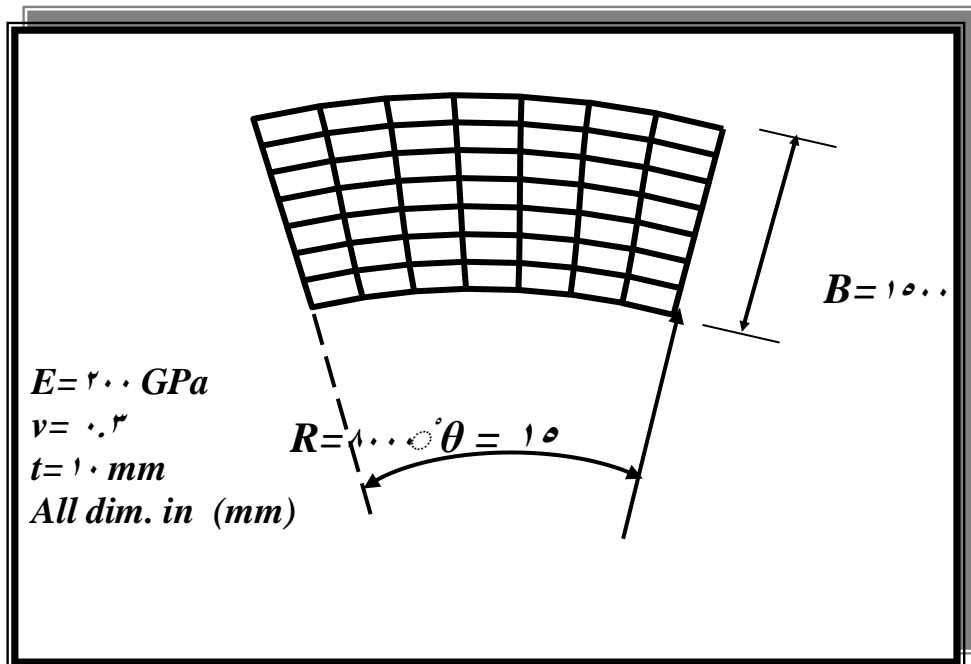


Figure (5-5) Mesh of a flange plate girder used to evaluate the buckling stress in NASTRAN program

could increase beyond the critical (or buckling) stress, provided the effective width of the plate is steadily decreased.

5.2.3.1 Effective Width Expression

The evaluation of the effective width of a buckled plate is the primary focus of the ultimate strength discussion⁽⁵⁶⁾. So, a reliable effective width is needed for stiffened plate elements in pure compression (like compression flange in grillage analogy). Different empirical formulas are available for the determination of the effective width. An important early method for calculating the effective width is attributed to *Von Karman et al.* (1932)⁽⁵⁸⁾. According to this method, the following expression was suggested:

$$b_e = b \left(\frac{\sigma_{cr}}{\sigma} \right)^{0.5} \tag{5.12}$$

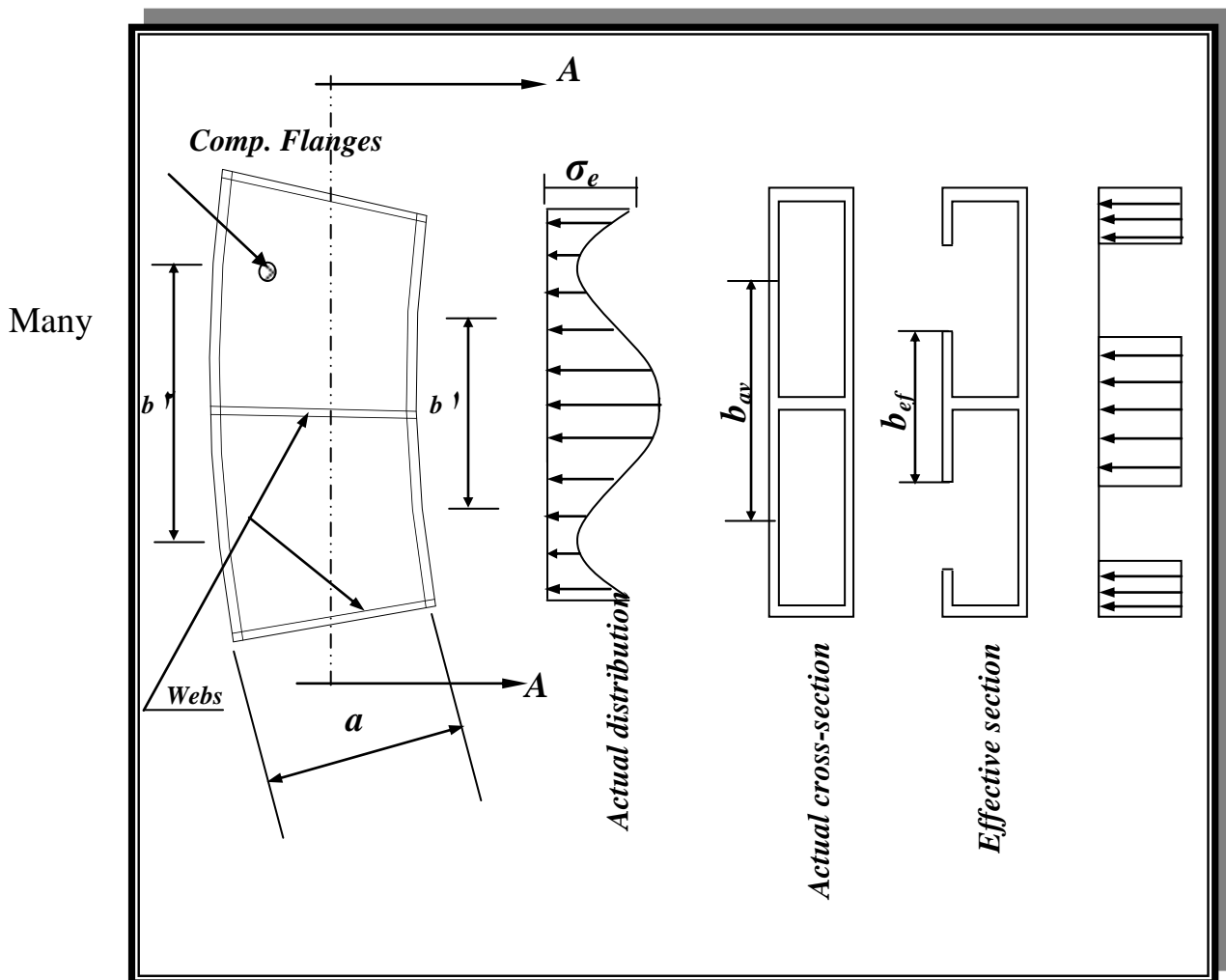
where:

b_e = the effective width of the plate.

b = the actual width of the plate.

σ_{cr} = the critical buckling stress.

σ = the applied compressive stress across the width of the plate ($\sigma > \sigma_{cr}$).



investigators have manifested somewhat more accurate results than Von Karman's equation. Marguerre^(v) gave the following expression for the effective width of a plate with simple boundary condition:

$$b_e = 0.5b \left(\frac{1 + \sigma_{cr}}{\sigma_m} \right) \quad (0-13)$$

where $\sigma_m = \frac{\sigma_1 + \sigma_2}{2}$ is the mean stress in the edge of the plate.

Winter (1947)⁽⁹¹⁾ proposed an empirical correction to *Von Karman* formula, and suggested the following expression to predict the effective width of a buckled plate:

$$b_e = b \left(\frac{\sigma_{cr}}{\sigma} \right)^{0.5} \left(1 - 0.25 \left(\frac{\sigma_{cr}}{\sigma} \right)^{0.5} \right) \quad (5.14)$$

Koiter (91) gave, for all edge conditions, the following approximation to evaluate the effective width:

$$b_e = b \left[1.2 - 0.65 \left(\frac{\sigma_{cr}}{\sigma_m} \right)^{\frac{2}{5}} + 0.45 \left(\frac{\sigma_{cr}}{\sigma_m} \right)^{\frac{4}{5}} \right] \left(\frac{\sigma_{cr}}{\sigma_m} \right)^{\frac{2}{5}} \quad (5.15)$$

Cox (91) suggested that for plates with clamped edges, the effective width can be represented by the approximate formula:

$$b_e = b \left[0.14 + 0.86 \left(\frac{\sigma_{cr}}{\sigma_m} \right)^{\frac{1}{2}} \right] \quad (5.16)$$

Faulkner (1977)⁽⁹²⁾ proposed the following empirical formula:

$$b_e = 1.05b \left(\frac{\sigma_{cr}}{\sigma} \right)^{0.5} \left(1 - 0.27 \left(\frac{\sigma_{cr}}{\sigma} \right)^{0.5} \right) \quad (5.17)$$

Shanmugam and *Evans* (1981)⁽⁹³⁾, *Evans* and *Shanmugam* (1984)⁽⁹⁴⁾ recommended using *Winter's* formula for the effective width of the compression flange panel. *Shanmugam* and *Evans* (1981)⁽⁹³⁾ clarified that the loss in effective width for the equivalent grillage member begins to become significant when a compression flange panel is subjected to a stress equal to 1.5 times its buckling stress. Also, they suggested that the reference stress for each grillage member be taken as the average of the calculated nodal stresses of the member. This suggestion is considered in the present study.

Several recent studies (*Kalyanaraman and Rao* (1991)^(εΛ), *Schafer and Peköz* (1991)^(ν1), *Marsh* (1991)^(εε) and *Ranby* (1991)^(ν0)) have shown that the expression suggested by *Von Karman* overrates the ultimate load resistance, while *Winter's* formula (which is used in *Eurocode 3 Part 1.2* (1991)^(νΛ) and *AISI* (1991)^(ε) in a slightly modified form) is sufficiently accurate and confidently recommended for use as follows:

$$\text{For } \left(\frac{\sigma_{cr}}{\sigma} \right)^{0.5} < 0.673$$

$$b_e = b \left(\frac{\sigma_{cr}}{\sigma} \right)^{0.5} \left(1 - 0.22 \left(\frac{\sigma_{cr}}{\sigma} \right)^{0.5} \right) \quad (5.18)$$

otherwise, $b_e = b$

Regarding the present work, Eq.(5.18) is used for evaluating the effective widths of compression flange panel at the start and the end of the grillage member.

5.2 Post-Buckling Behavior of Web Panel

5.2.1 Introduction

The primary functions of the web plate in a plate girder are to maintain the relative distance between the top and bottom flanges and to resist the introduced shearing force. In practical thin plate girders, the web plates carries (90%) or more of the applied transverse shear and that, although the flange resists most of the bending moment, the web may carry a considerable part. When the applied loads are increased the combination of stresses (shear and bending) acting on the web may initiate buckling, yielding, or both buckling and yielding. Then, as the applied loads are further increased the web must carry an even greater shearing force (because the flanges cannot carry considerable shearing force). In order to do this, the web must reduce its share of the bending moment. Thus, the flanges have to carry not only the increase in bending moment from the applied loads but also that which the web sheds off in order to carry the

increase in shearing force. This phenomenon is known as **Load Shedding** (5.8).

Web behavior in the post buckling range and at collapse has been studied by many investigators (5.3, 5.3, 6.8, 6.9...). The most well known approach is the so-called "**Rockey's approach**" which is the resultant of many studies carried out by professor **Rockey** and his colleagues in **Cardiff** (7.3, 7.4). Many researchers (5.5, 5.6) recommended to use this approach to predict the post buckling behavior of the web panels till collapse. In the present study, **Rockey's** method, with some modifications, is utilized in the grillage simulation of the nonlinear analysis of cellular plate structures curved in plan for predicting the post-buckling behavior for the web panels.

5.3.2 Evaluation of Elastic Critical Shearing Stress

Tests indicate that a stiffened web panel may still have a tendency to buckle even when vertical stiffeners are incorporated into the design. This is because the combination of diagonal tension and diagonal compression can cause closely spaced buckles to form across a diagonal (5.8).

In order to accurately calculate the elastic buckling strength of the web panel, the boundary conditions need to be properly determined. The elastic shear buckling stress of a rectangular web plate was given by **Timoshenko** and **Gere** (1961) (5.9) as follows:

$$\tau_{cr} = K \frac{\pi^2 \cdot E}{12(1 - \nu^2)} \left(\frac{t_w}{h} \right)^2 \quad (5.19)$$

where:

K = the shear buckling coefficient.

E = The modules of elasticity.

ν = Poisson's ratio.

h = the depth of web panel (clear distance between upper and lower flanges).

t_w = the thickness of the web panel.

The shear buckling coefficient (K) depends upon the boundary conditions and aspect ratio of the web panel (B/h), where (B) is the unstiffened length of the web panel (clear spacing between transverse stiffeners). Although the real boundary condition at the flange-web juncture is somewhere between simple and fixed, the boundary condition for a mathematical solution has been arbitrarily assumed, mainly due to the lack of means to evaluate it in a rational manner⁽⁶³⁾.

Basler and **Thürlimann** (1969)⁽¹²⁾, **Porter et al.** (1970)⁽¹³⁾ and **Rockey et al.** (1974)⁽¹⁴⁾ assumed that the web panel is simply supported at the flange-web juncture, while **Chern** and **Ostapenko** (1979)⁽¹⁵⁾ obtained the elastic buckling strength by assuming that the juncture behaves like a fixed supported.

Sharp and **Clark** (1971)⁽¹⁶⁾ assumed intuitively that the boundary condition lies halfway between the simply supported and fixed condition. **AISC** (1989)⁽⁷⁾ and **AASHTO** (1996)⁽¹⁾ specification followed **Basler's** procedure, in which the boundary condition of web panels at the juncture is conservatively assumed to be simple.

A study by **Let et al.** (1997)⁽¹⁷⁾ suggested simple design equations to determine shear buckling coefficients that represent various boundary condition. According to this study, the boundary condition at the flange-web juncture is closer to a fixed condition. They reported that the relative flange rigidity expressed in terms of the ratio of the flange thickness to the web thickness (t_f/t_w) affects the overall ultimate strength by influencing the elastic buckling strength. **Bradford** (1997)⁽¹⁸⁾ also pointed out that **AASHTO** assumption underestimated the shear buckling strength. He

developed a local buckling design chart for shear buckling coefficients for plate girders that represented more accurately the field condition. The local buckling chart by *Bradford* gives values of shear buckling coefficients very close to that suggested by *Lee et al.* (1997)⁽⁵⁷⁾.

Lee and Yoo (1998)⁽⁵⁸⁾ confirmed the validity of the design equations by *Lee et al.* (1997)⁽⁵⁷⁾ and recommended them for use in the investigation of the ultimate shearing strengths of web panels. They also concluded that the assumption of the boundary condition at the flange-web juncture being simply supported gives much too conservative shearing strength for many web panels. Using *NASTRAN* computer program, they conducted nonlinear analyses by three-dimensional finite element models on a transversely stiffened plate girder web panel subjected to pure shear. The results obtained from these analyses showed that the boundary condition at juncture is much closer to a fixed supported. Accordingly, they suggested that the shear buckling coefficient (*K*) could be calculated as follows:

Form *Timoshenko and Gere* (1971)⁽⁵⁹⁾ and *SSRC Guide* (1988)⁽⁶⁰⁾:

- 1- For plates simply supported at all edges;

$$K_{ss} = 4 + 5.34 \left(\frac{h}{B} \right)^2 \quad \text{for} \quad \frac{B}{h} < 1 \quad (5.20a)$$

$$K_{ss} = 5.34 + 4\left(\frac{h}{B}\right)^2 \quad \text{for } \frac{B}{h} \geq 1 \quad (5.20b)$$

γ- For plates where two opposite edges are simply supported and the others fixed;

$$K_{sf} = 5.34\left(\frac{h}{B}\right)^2 + 2.31\left(\frac{h}{B}\right) - 3.44 + 8.39\left(\frac{h}{B}\right) \quad \text{for } \frac{B}{h} < 1 \quad (5.21a)$$

$$K_{sf} = 8.98 + 5.61\left(\frac{h}{B}\right)^2 - 1.99\left(\frac{h}{B}\right)^3 \quad \text{for } \frac{B}{h} \geq 1 \quad (5.21b)$$

The shear buckling coefficient (K) of a web panel according to the previously mentioned study by *Lee et al.* (1997)⁽⁵⁷⁾ is;

$$K = K_{ss} + \frac{4}{5}(K_{sk} - K_{ss}) \left[1 - \frac{2}{3} \left(2 - \frac{t_f}{t_w} \right) \right] \quad \text{for } \frac{1}{2} < \frac{t_f}{t_w} < 2 \quad (5.22a)$$

$$K = K_{ss} + \frac{4}{5}(K_{sf} - K_{ss}) \quad \text{for } \frac{t_f}{t_w} \geq 2 \quad (5.22b)$$

$$K = K_{ss} \quad \text{for } \frac{t_f}{t_w} \leq 2 \quad (5.22c)$$

Regarding the present study, Eqs.(5.22a, 5.22b and 5.22c) are used to evaluate the shear buckling coefficients for straight web panels.

The critical shearing stress for a curved web plate panel is affected by the web curvature. *Batdorf, Stein* and *Shilderout*⁽⁵⁹⁾ analyzed this special case. They suggested that the critical shearing stress is affected by both the curvature parameter (Γ) and the shear buckling coefficient (Kc). The curvature parameter is:

$$\Gamma = \left(\frac{h}{R}\right) \left(\frac{h}{t_w}\right) \sqrt{(1 - \nu^2)} \quad (5.23)$$

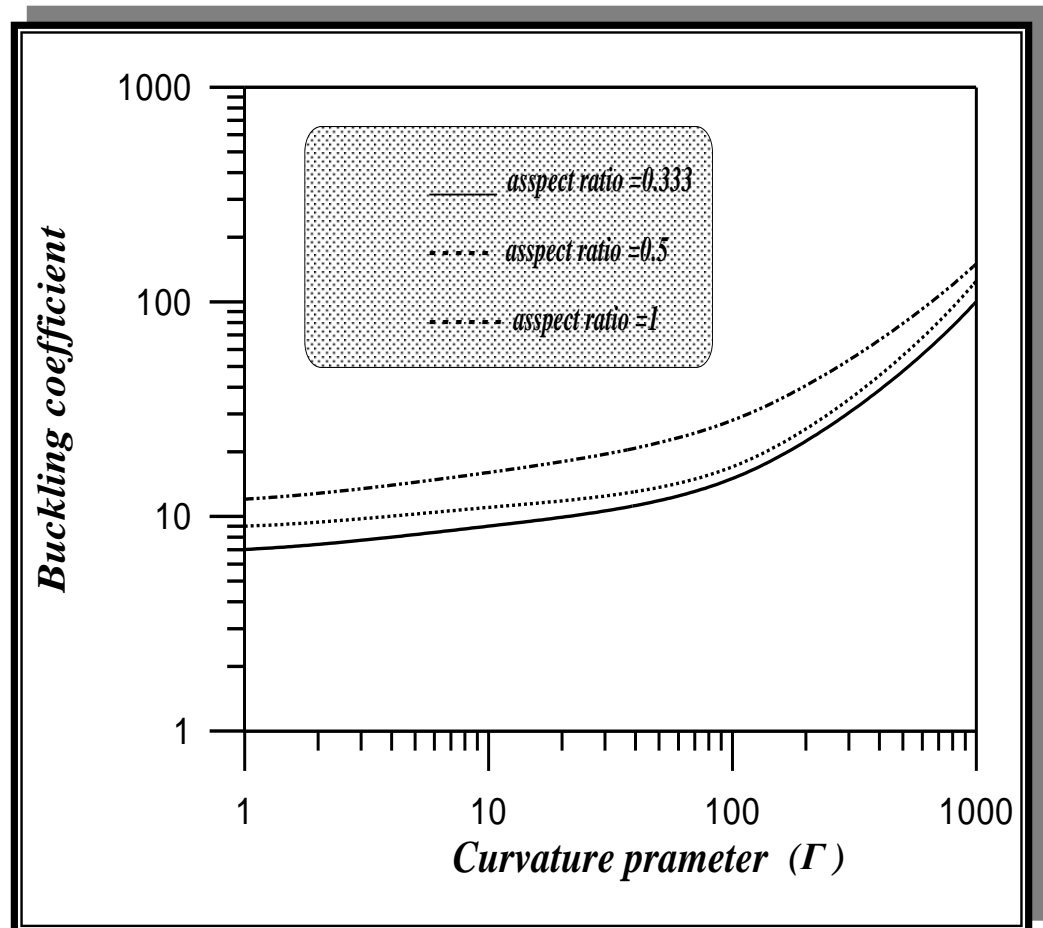
Fig.(5-6) shows the variation of the shear buckling coefficient (Kc) with the curvature parameter (Γ). Thus, the critical shearing stress is given by:

$$\tau_{cr} = K_c \frac{\pi^2 \cdot E}{12(1 - \nu^2)} \left(\frac{t_w}{h}\right)^2 \quad (5.24)$$

5.3.3 Review of Failure Theories for Web Panels

The various possible failure modes of a web are illustrated by *Murray* (1984)⁽⁶⁸⁾, as shown in Fig.(5-7). The following brief review of failure theories for web panels is presented depending on various modes of failure.

Basler and *Skalout* (1971)⁽⁶⁷⁾ assumed that since flange in practical plate girders under pure shear, do not possess sufficient flexural rigidity to resist the diagonal tension, the diagonal tension field does not develop near the web-flange juncture and the web collapses after development of the yield zone, as shown in Fig.(5-7a). *Rockey* and *Skalout* (1972)⁽⁶⁹⁾ found



Figure(5- 7) Variation of buckling coefficient with curvature parameter

that collapse mechanism involved plastic hinges in the flanges and that these flanges often had a strong influence upon the behavior of the web

panel. They assumed that for the case when the transverse shearing force acts alone (i.e., $M=0$) the plastic mechanism had the form shown in Fig.(5-1b), where it is seen that the tension field is assumed to be parallel to the diagonal of the web panel.

Porter et al. (1979)⁽¹⁴⁾ developed a failure theory for a web panel loaded in shear, based on the assumption that the flanges are able to anchor the diagonal tension field, as shown in Fig (5-1c). According to their theory, plastic hinges form after the development of the yield zone, and finally, the web panel fails in a sway mechanism.

Rockey et al. (1974)⁽¹⁵⁾ proposed a design method that allowed for combined loading of shearing force and bending moment. Their method can cater for all of the collapse modes illustrated in Fig.(5-1)⁽¹⁶⁾ with some modifications, and when it was compared with the test-measured collapse loads of eighty-eight girders reported by various investigators, it was found that the average value (predicted collapse load/measured collapse load) was (1.11). This method will be studied in details in the next section, and will be used in present study.

Lee and Yoo (1994)⁽¹⁷⁾ presented a parametric study to predict the ultimate shearing strengths of web panels subjected to pure shear by conducting nonlinear finite elements analysis using *NASTRAN* computer program. From this study, they concluded that when the plastic shearing force (V_{YW}) is greater than the elastic shear buckling (V_{CR}), the post – buckling strength (V_{PB}) is approximately equal to (40%) of the difference between (V_{YW}) and (V_{CR}). Accordingly, new design equations were proposed for the determination of the ultimate strengths of the web panels, as follows:

$$V_{PB} = 0.4(V_{yw} - V_{cr}) \quad (5.25)$$

where

$$V_{yw} = \frac{\sigma_{yw}}{\sqrt{3}} \cdot h \cdot t_w$$

in which

V_{yw} = the shearing force required to make the web fully plastic.

σ_{yw} = the yield stress of the web material.

$$V_{cr} = K \frac{\pi^2 \cdot I}{12(1 - \dots)}$$

(0.26)

The ultimate

shearing

strength (V_u)

is obtained by

adding (V_{pB})

to (V_{cr})

$$V_u = V_{cr} + V_{pB}$$

(0.27)

By

substituting

Eq. (0.20)

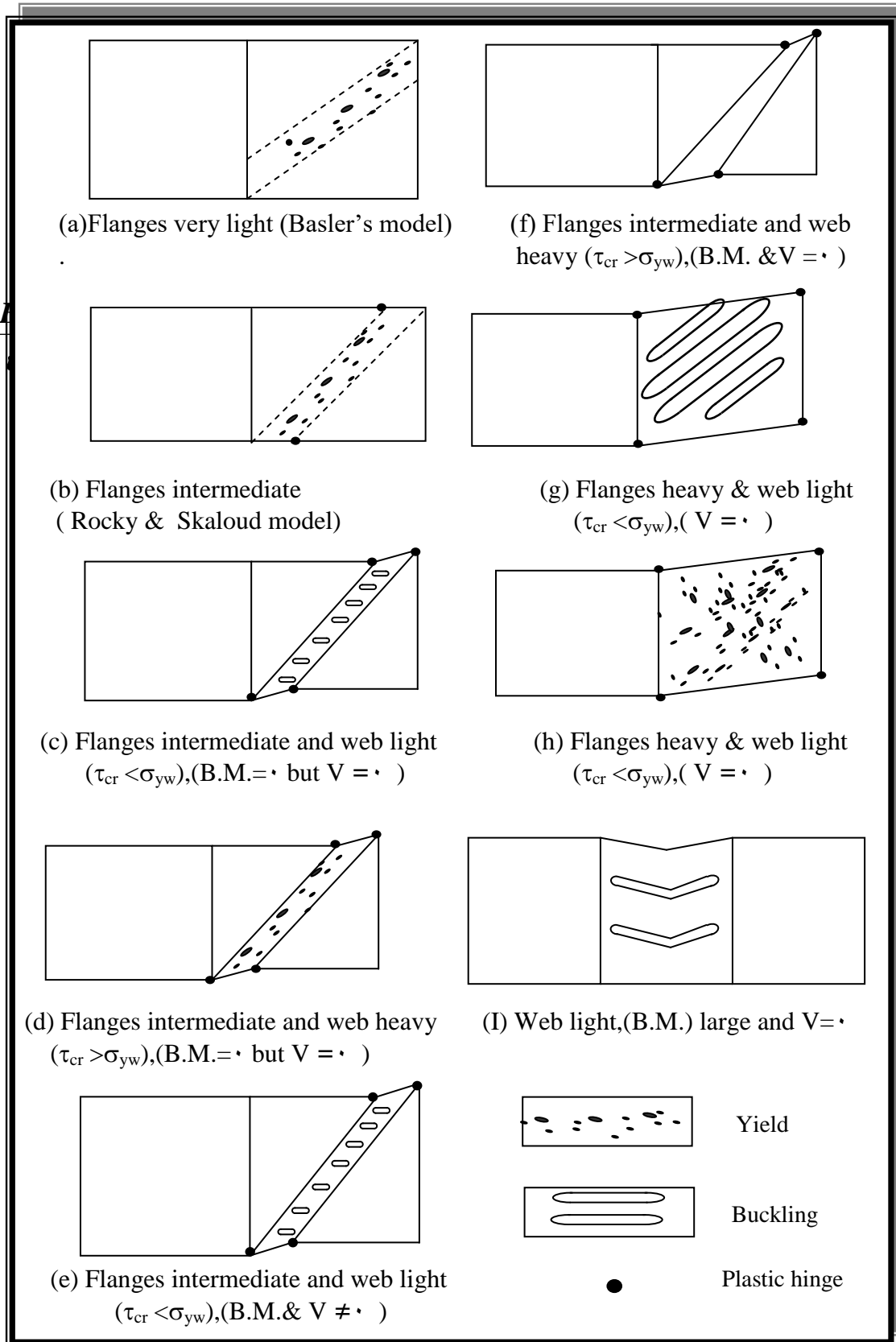


Figure (5.1) Modes of failure of plate girder (0.8)

into Eq (5.27):

$$V_u = \alpha V_{cr} + \beta V_{yw} \quad (5.28)$$

5.3.4 Proposed interaction diagram

The parametric studies carried out by *Evans, Porter and Rockey* (1977)⁽²⁷⁾ have established that the interaction between the transverse shear and the bending acting on a web panel can be quite accurately represented by the interaction diagram shown in Fig (5-8). In this diagram, the transverse shearing capacity of the web is plotted on the vertical axis and the bending moment capacity is plotted horizontally. Thus, any point on the interaction diagram shows the coexistent values of shearing force and bending moment that can be sustained by the section.

The interaction diagram has three main stages, for each there is a specified limit for the web ultimate shearing capacity (V_s , V_c , and V_b) acting with their associated limits of bending moments (M_s ; M_f , and M_{ult}), respectively. These notations will be explained in the next section. The three stages may be summarized as follows:

1- A straight line joins (S) and (S') which represents a constant value for the ultimate shearing capacity (V_s), which exists when the associated bending moment varies from zero (pure shear) to (M_s').

2- A parabola with its crown at (S') is fitted between (S') and (C), and this corresponds to a bending moment value between (M_s') and (M_f) with its associated ordinates (V_s) and (V_c), respectively.

3- A further reduction in the shearing capacity will exist when the bending moment exceeds (M_f). Then, the interaction diagram terminates at a shearing capacity of (V_b) associated with the ultimate bending capacity (M_{ult}). The curve (CBE) is also a parabola with its crown at point (E)^(5.8). According to the simplified design method presented by *Rockey et al.* (1974)⁽²⁷⁾, the points (S , S' , C , B and D) which construct the interaction diagram are located according to simple formulas and the curves

connecting these points are either straight lines or parabolas. This method will be discussed in detail in the following section.

0.3.0
Rockey's
Method
 As
 mentioned
 in Section
 (0.3.0),
Rockey,
Evans,
 and
Porter

(1971)

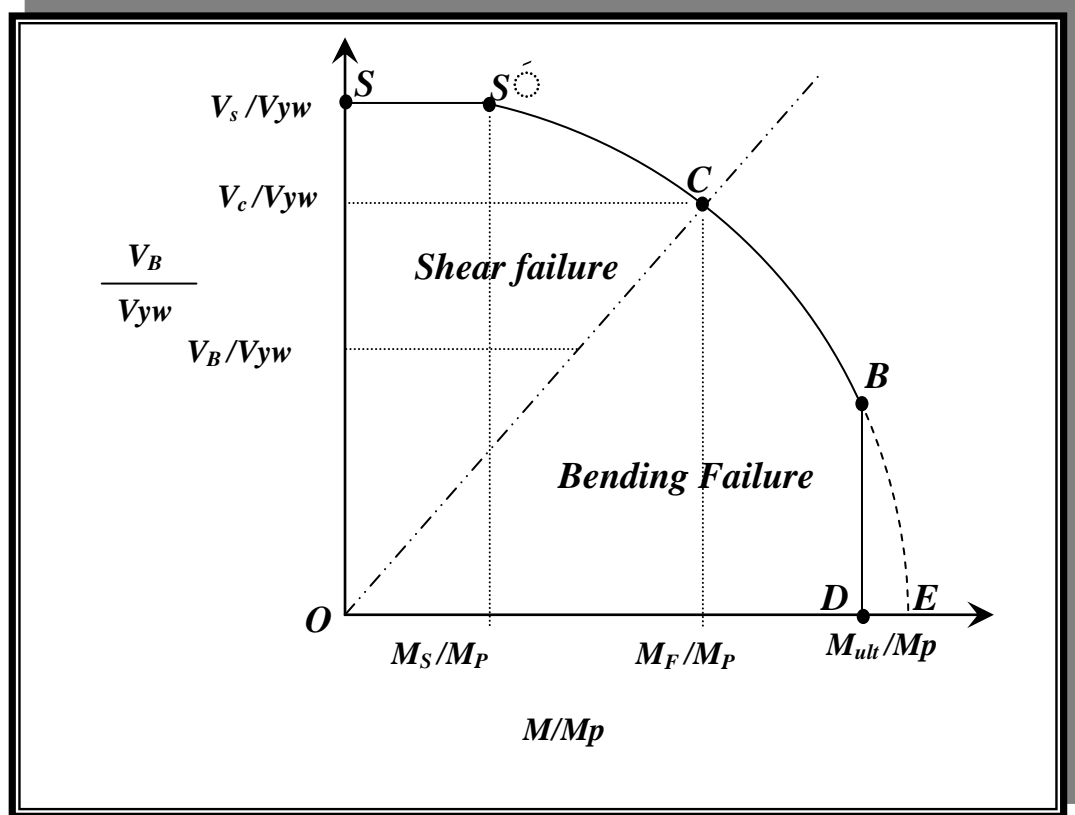
presented
 a simple

design method for predicting the collapse behavior of web panels subjected to combined action of transverse shearing force and bending moment. This method is considered to be the most general of the collapse mechanisms illustrated in Fig.(0-7), that is, as that shown in Fig.(0-7e), other cases can be treated as special cases of this mechanism (0.8).

According to **Rockey's** method, three stage of web behavior leading up to collapse are considerable, as follow:

1-Stage 1 (Unbuckled behavior)

When a web panel is subjected to a uniform shearing stress of magnitude (τ), equal tensile and compressive principal stresses of ($\sigma_t = \sigma_c$) of



Figure(0-7) Interaction diagram between shear and bending effect

magnitude equal to τ) will be developed prior to incipient buckling at (ϵ°) and (ν°) , as shown in Fig.(5-9a). The web plate remains perfectly flat until the applied shearing stress (τ) reaches the critical value (τ_{cr}) at which the panel will buckle (along the diagonal of the compressive stress). This critical value (τ_{cr}) is determined as mentioned in Section (5.3.2).

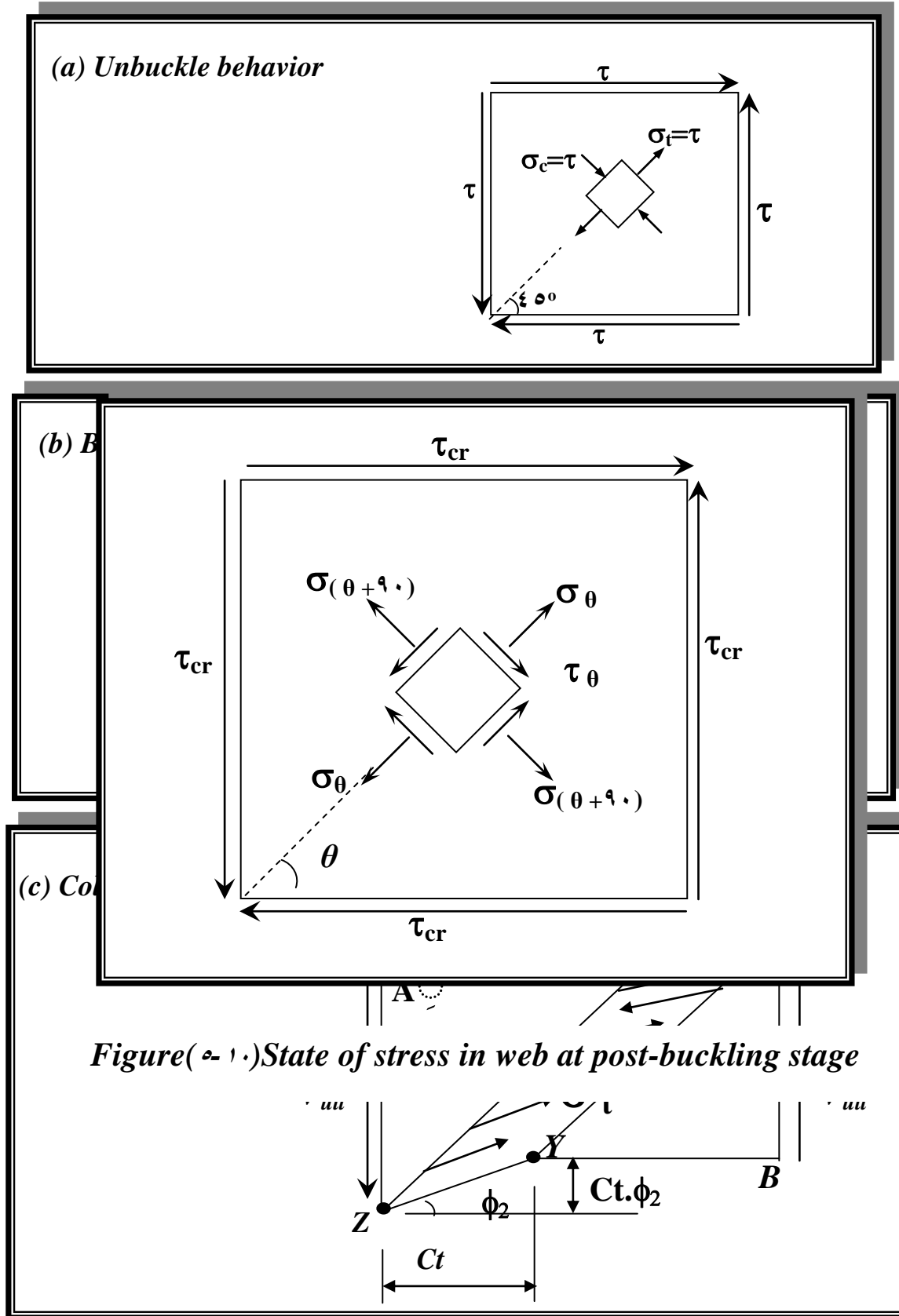
II- Stage 2 (Post-buckled behavior)

When the critical stress (τ_{cr}) is reached, the web panel starts to buckle and it cannot resist any increase in compressive stress. Any additional load, beyond the buckling load, has to be supported by tension field action (or tensile membrane field), which is anchored against the top and bottom flanges and against the adjacent transverse webs on either side of the longitudinal web panel, as shown in Fig (5-9b). In this field, the tensile membrane stresses (σ_t) are inclined at an angle (θ) to the horizontal. At the start of this stage, the stresses acting on the faces of a small rectangular element obtained by a rotation through angle (θ), as shown in Fig.(5-10), may be found using *Mohr's circle* ^(5.8), as follows:

$$\sigma_{\theta} = \tau_{cr} \sin(2\theta) \quad (5.29a)$$

$$\sigma_{\theta+\pi/2} = \tau_{cr} \sin(2\theta) \quad (5.29b)$$

$$\tau_{\theta} = \tau_{cr} \cos(2\theta) \quad (5.29c)$$



Accordingly, the total stress in web behavior up to collapse obtained by superimposing the tensile membrane stresses (σ_t) to the tensile

stresses (σ_θ) set up when the applied shearing stress reaches its critical value (τ_θ). So, Eq.(5.29a) becomes:

$$\sigma_{\theta PB} = \tau_{cr} \cdot \sin(2\theta) + \sigma_t \quad (5.30)$$

Since the flanges are of finite bending (or flexural) rigidity, they begin to bend inwards under the pull exerted by the diagonal tension field.

III-Stage r (*Ultimate load behavior*);

Upon further increase of the applied shear loading, the membrane tensile stress (σ_t) (developed in the web panel) increases and a greater pull is exerted upon the flange. Eventually, the membrane tensile stress reaches such a value that when combined with that from the critical shearing stress (τ_{cr}) as in Eq.(5.30), the resulting stress ($\sigma_{\theta PB}$) reaches the yield stress (σ_{YW}) for the web material. This value of the tensile membrane stress will be denoted as (σ_t^y) and it may be determined by applying *Von Mises-Hencky* yield criterion, which is common to use in plasticity problems, as follows:

$$\sigma_y^2 = \sigma_1^2 + \sigma_2^2 - \sigma_1 \cdot \sigma_2 + 3\tau^2 \quad (5.31)$$

where

σ_y = the yield stress

σ_1, σ_2 = the direct stresses acting on two orthogonal planes

τ = the shearing stress

Thus, for the web panel:

$$\sigma_{yw}^2 = (\sigma_\theta + \sigma_t^y)^2 + \sigma_{(\theta+\pi/2)}^2 - (\sigma_\theta + \sigma_t^y) \sigma_{(\theta+\pi/2)} + 3\tau_\theta^2 \quad (5.32)$$

By substituting Eqs.(5.29a, 5.29b, and 5.29c) in Eq. (5.32), the value of the tensile membrane stress to produce yield (σ_t^y) is obtained in terms of the critical shearing stress (τ_{cr}) and the inclination (θ) of the tension field, as follow:

$$\frac{\sigma_t^y}{\sigma_{yw}} = \left[1 + \left(\frac{\tau_{cr}}{\tau_{yw}} \right)^2 (0.75 \sin^2 2\theta - 1) \right]^{1/2} - \frac{\sqrt{3}}{2} \cdot \frac{\tau_{cr}}{\tau_{yw}} \sin 2\theta \quad (5.33)$$

where:

$$\tau_{yw} = \frac{\sigma_{yw}}{3} \quad (5.34)$$

When the material in the region (**WXYZ**) of the web panel in Fig.(5-9c) reaches the yield stress (σ_{yw}), the panel cannot sustain any further increase in load and the final sway failure of the web will occur due to the formation of the plastic hinges in the flange panels, as shown in the same Fig (5-9c). The failure load may be determined by applying a virtual sway displacement to the web panel in its collapse stage, Fig(5-9c). It is convenient to consider the yield region (**WXYZ**) of the web panel to be removed and to replace its action upon the adjacent flange and regions by the membrane tensile stresses (σ_t^y).

Murray (1944)^(5A) proposed the following equations to determine the reduced plastic moments of the flanges (due to the influence of the normal stresses acting on the compression and tension flanges):

For the compression flange:

$$M'_{Pfc} = M_{Pfc} \left[1 - \left(\frac{\sigma_{cf}}{\sigma_{yf}} \right)^2 \right] \quad (5.35)$$

For the tension flange:

$$M'_{Pft} = M_{Pft} \left[1 - \left(\frac{\sigma_{tf}}{\sigma_{yf}} \right)^2 \right] \quad (5.36)$$

where:

M_{pfc}, M_{pft} = are the plastic moment capacities of the compression and tension flanges, respectively which be determined later.

σ_{cf}, σ_{tf} = are the average normal stresses in the compression and tension flanges respectively.

σ_{yf} = is the yield stress of the flange material.

Now there is a need to determine the position of the plastic hinges (C_c, C_t) in the compression and tension flange, respectively. For this purpose, *Murray*⁽²⁴⁾ suggested that during the virtual displacement (ϕ_1) of the mechanism the compression flange, as shown in Fig (2-9c), the work done by the shearing force at (X) is equal to the energy absorbed by the plastic hinges at (X and W) and to the work done against the tension field stress (σ_t^y). It is convenient to take an average value for the membrane tensile stress, that is, (σ_t^y) at the midpoint of (WX)⁽²⁴⁾, as shown in Fig (2-11).

Thus:

$$V_X \cdot C_C \cdot \phi_1 = \sigma_t^y \cdot t_w \cdot \frac{C_C^2}{2} \cdot \sin^2 2\theta + 2M'_{PFC} \cdot \phi_1 \quad (2.27)$$

then:

$$V_x = \frac{C_c}{2} \cdot \sigma_t^y \cdot t_w \cdot \sin^2 2\theta + \frac{2M'_{PFC}}{C_c} \quad (e.38)$$

The minimum value of (V_x) is obtained by taking the derivative of (V_x) in Eq.(e.38) with respect to (C_c) and putting this derivative equal to zero. Thus:

These equations define the locations of the plastic hinges in the flanges, but there is a restriction that (Cc) and (Ct) must be less than (B) (unstiffened length of web) ^(e), from Eqs. (e.39) and (e.40):

$$M_{pfc} < \frac{t_w \cdot B^2 \cdot \sin^2 \theta}{4} \cdot \sigma_t^y \quad (e.41)$$

$$M_{pft} < \frac{t_w \cdot B^2 \cdot \sin^2 \theta}{4} \cdot \sigma_t^y$$

Flanges which satisfy the criteria of Eq. (e.41) are said to be light, while those which do not are said to be heavy ^(e). If these criteria are not satisfied then the plastic hinges would form at the four corners of the web panel, i.e., the points (A, X, B, Z) shown in Fig (e-9c), and the panel will fail like a *Vierendeel* girder. In this case, the tension field occupies the whole of the web panel and $(Cc=Ct=B)$, as shown in Fig.(e-9g)and (e-9h) ^(e).

In order to locate the ordinate (OS) in the interaction diagram Fig. (e-8), *Rockey et al.* (1978) ^[e] presented the following equation to determine the pure shearing load ratio (V_s/V_{yw}) for members with identical top and bottom flanges, i.e., the neutral axis is at the mid-depth of the section. Thus, $(C_c=C_t=C)$ and $(M_{pfc}=M_{pft}=M_{pf})$ Accordingly, the failure mechanism for this case will be as shown in Figs.(e-9c) and (e-9d):

$$\frac{V_s}{V_{yw}} = \frac{\tau_{cr}}{\tau_{yw}} + \sqrt{3} \sin^2 \theta \left(\cot \theta - \frac{B}{h} \right) \frac{\sigma_t^y}{\sigma_{yw}} + 4\sqrt{3} \sin \theta \sqrt{\frac{\sigma_t^y}{\sigma_{yw}} \cdot M_p^*} \quad (e.42)$$

where:

V_{yw} = the shearing force required to make the web panel fully plastic.

$$V_{yw} = \tau_{yw} \cdot t_w \cdot h = \frac{\sigma_{yw}}{\sqrt{3}} \cdot t_w \cdot h$$

$$M_p^* = \frac{M_{pf}}{t_w \cdot h^2 \cdot \sigma_{yw}} \quad \text{and} \quad M_{pf} = \frac{1}{4} \sigma_{yf} \cdot b_f \cdot t_f^2$$

It is be noted that ($b_f=b_c=b_t$) for identical top and bottom flanges.

Mashal (1991) suggested that when a compression flange panel of a cellular plate structure buckles and after adopting the effective width concept for post-buckling, the idealized grillage member is no more symmetrical (the neutral axis moves towards the tension flange). According to this concept, he suggested new derivations by modifying Eq.(5.27), for symmetrical plate girders, to be applicable to unsymmetrical plate girders. So, the following equations were presented:

$$V_S = \tau_{cr} \cdot h \cdot t_w + \sigma_t^y \cdot t_w \cdot \sin \theta (h \cdot \cot \theta - B - C_c) + \frac{2M_{pfc}}{C_c} + \frac{2M_{pft}}{C_t} \quad (5.28)$$

in which:

$$M_{pfc} = \frac{1}{4} \cdot b_{ey} \cdot t_f^2 \cdot \sigma_{yf} \quad (5.29)$$

$$M_{pft} = \frac{1}{4} \cdot b_{ey} \cdot t_f^2 \cdot \sigma_{yf}$$

and:

b_{ey} = the effective width of the compression flange at yield.

b_t = the width of the tension flange.

By substituting Eq.(5.29) and Eq.(5.30) into Eq.(5.28) and after dividing by (V_{yw}) the final expression is:

$$\frac{V_S}{V_{yw}} = \frac{\tau_{cr}}{\tau_{yw}} + \sqrt{3} \sin^2 \theta \left(\cot \theta - \frac{B}{h} \right) \frac{\sigma_t^y}{\sigma_{yw}} + \sqrt{3} \sin \theta \sqrt{\frac{\sigma_t^y}{\sigma_{yw}}} \cdot \left(3 \sqrt{M_{pc}^*} + \sqrt{M_{pt}^*} \right) \quad (5.30)$$

$$M_{pc}^* = \frac{M_{pfc}}{t_w \cdot h^2 \cdot \sigma_{yw}}$$

$$M_{pt}^* = \frac{M_{pft}}{t_w \cdot h^2 \cdot \sigma_{yw}} \quad (5.31)$$

M_{pc}^* and M_{pt}^* = are the non-dimensional flange strength parameters for the compression and tension flange, respectively.

Regarding the present study, Eq.(5.3) is used, with some modifications, to calculate (V_S) for cellular plate structures, as follows:

$$V_S = \tau_{cr} \cdot h \cdot t_w + \sigma_t^y \cdot t_w \cdot \sin \theta (h \cdot \cot \theta - B - C_C) + \frac{2M_{pfc}^*}{C_c} + \frac{2M_{pft}^*}{C_t} \quad (5.47)$$

where, (M_{pc}^* and M_{pt}^*) are determined from the previously mentioned equations (5.35) and (5.36). In these equations (M_{pfc}, M_{pft}) are:

$$M_{pfc} = \frac{1}{4} \cdot b_{ey(av)} \cdot t_f^2 \cdot \sigma_{yf} \quad (5.48)$$

$$M_{pft} = \frac{1}{4} \cdot b_{t(av)} \cdot t_f^2 \cdot \sigma_{yf}$$

in which

$$b_{ey(av)} = \frac{b_{ey1} + b_{ey2}}{2} \quad (5.49)$$

$$b_{t(av)} = \frac{b_{t1} + b_{t2}}{2}$$

and:

b_{ey1}, b_{ey2} = the effective width, at yield, of the compression flange at the start and end of grillage member, respectively.

b_{t1}, b_{t2} = the width of the tension flange at the start and end of the grillage member, respectively.

Concerning the evaluation of (θ), the parametric studies carried out by **Evans, Porter, and Rockey (1977)** (22) showed that (V_S / V_{yw}) has a stationary value when (θ) is approximately equal to two third of the inclination of the diagonal of the web panel, i.e.:

$$\theta = \frac{2}{3} \tan^{-1} \left(\frac{h}{B} \right) \quad (5.50)$$

The use of Eq.(5.5) will lead either to correct value or to underestimation of the collapse load (σ) . So this approximation is safe and it will be used in the present study.

The interaction diagram, Fig.(5-1) shows a constant ultimate shearing capacity (V_s) for an associated bending moment that varies from zero to ($M_{s'}$), where :

$$M_{s'} = V_s B \leq 0.5M_f \quad (5.6)$$

The bending moment may be of such a high value that it alters the mode of failure from a shear mode to a bending mode. Point (C) on the interaction diagram is the point at which this change occurs and the line (OC) is the dividing line between the two mode of failure. The parametric studies carried out by *Evans et al.* (1977)⁽¹⁷⁾ showed that the change in the failure modes occurs when the applied bending moment is equal to M_f , which represents the plastic moment of resistance of flanges alone (neglecting the contribution of the web) about neutral axis. Thus, the horizontal coordinate of point (C) for a symmetrical section is calculated as follows:

$$M_f = \sigma_{yf} b_f t_f d \quad (5.7)$$

where

d the distance between the centerline of the flange plates.

In the present study, the calculation of (M_f) for unsymmetrical grillage members (after applying the effective width concept for the compression flanges) is suggested, by taking the moments about the new position of the neutral axis, as follows:

$$M_f = \sigma_{yf} t_f (b_{ey} \lambda_y + b_t [d - \lambda_y]) \quad (5.8)$$

where

λ_y = the distance from the neutral axis to the centerline of the compression flange at yield, as shown in Fig.(5-12):

To evaluate the ultimate shearing capacity at point (C), the following empirical equation derived by the

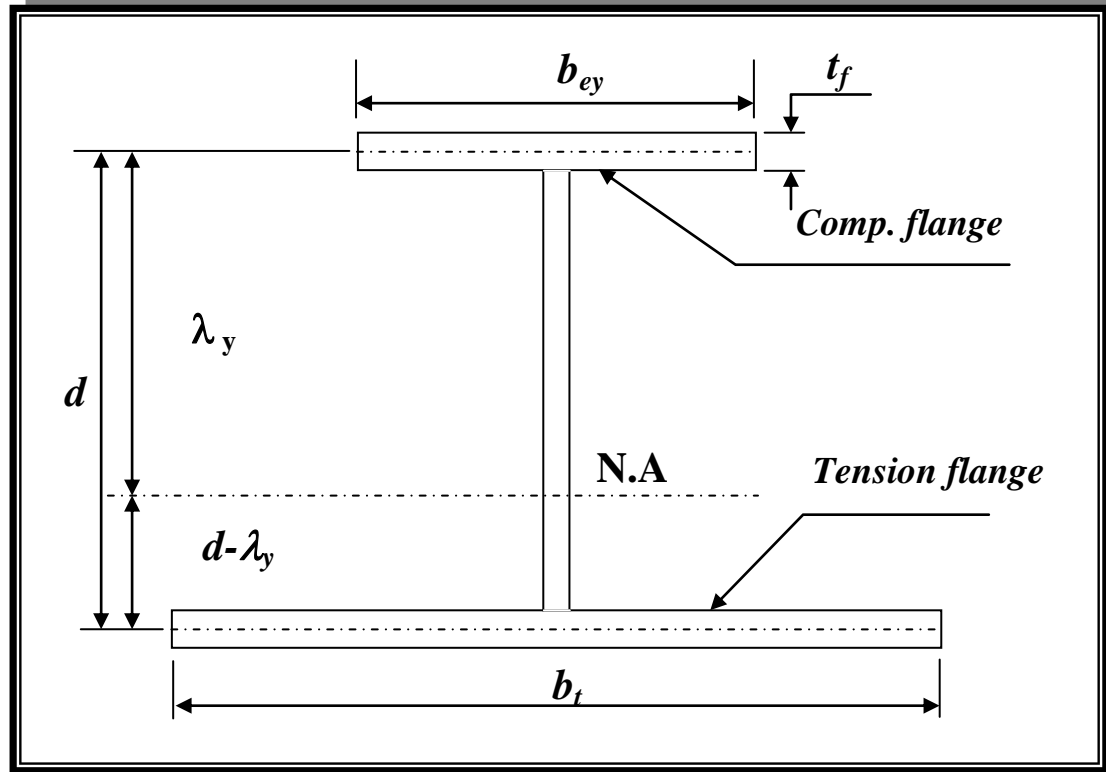


Figure (٥-١٧) Unsymmetrical section for the grillage member

previously mentioned

parametric studies are given:

$$\frac{V_c}{V_{yw}} = \frac{\tau_c}{\tau_{yw}} + \frac{\sigma_t^y}{\sigma_{yw}} \sin 2\theta \left(0.554 + 36.8 \frac{M_{pf}}{M_f} \right) \left(2 - \left[\frac{B}{h} \right]^{1/8} \right) \quad (٥-٥٤)$$

٥٤)

If $V_c > V_s$ then:

$$\frac{V_c}{V_{yw}} = \frac{V_s}{V_{yw}}$$

Regarding the present study it is suggested to take the parameter M_{pf} in Eq. (٥.٥٤) as $M_{pf)av.}$, where

$$M_{pf)av.} = \frac{M_{pfc} + M_{pft}}{2} \quad (٥-٥٥)$$

If a plate girder is subjected to a bending moment in excess of (M_f) then it will fail in a bending mode ^(٧٧). According to the load shedding

phenomenon that was described in Section (5.3.1), the web will shed off the bending stresses that it should carry to the flanges. Thus, the cross section will be unable to develop the full plastic moment of resistance of the full section (M_p), where (M_p) is used as the denominator to the nondimensionalized horizontal coordinate of the interaction diagram. Thus:

$$M_p = M_f + M_{pw} \quad (5-56)$$

where:

M_{pw} = the plastic moment of resistance of the web plate acting alone

$$M_{pw} = \frac{1}{4} \sigma_{yw} \cdot t_w \cdot h^2$$

The section will fail by inward collapse of the compression flanges. This type of flange failure will occur at an applied moment value (M_{ult}), which is approximately equal to the moment required to produce first yield in the extreme fiber of the compression flanges.

Schafer and *Peköz* (1994)⁽⁷⁾ suggested that since the web undergoes compressive stress, it is prone to buckling, and thus, its ultimate strength is governed by applying the effective width expressions, such as Eq.(5.17). They concluded that for most of the sections, the web is fully effective and the incorporation of its effective width due to buckling would have a little influence on the results.

In order to determine the ultimate moment capacity (M_{ult}), *Rockey et al.* (1974)⁽⁸⁾ suggested to use the following empirical formula due to *Cooper* (1970, 1971)^{(9), (10)}:

$$\frac{M_{ult}}{M_y} = 1 - 0.0005 \frac{A_w}{A_f} \left(\frac{h}{t_w} - 5.7 \sqrt{\frac{E}{\sigma_{yf}}} \right) \text{ for } M_{ult} \leq M_p \quad (5-57)$$

where

M_y = the bending moment required to produce the first yield in the extreme fiber of the compression flange, assuming a fully effective web (neglecting the effect of web buckling).

A_f, A_w = the cross sectional area of the web and each of the flanges, respectively.

In the present study the parameter will be approximately taken as $A_{f(av)}$:

$$A_{f(av)} = \frac{A_{fc} + A_{ft}}{2} \quad (5-58)$$

where

A_{fc}, A_{ft} = the cross sectional area of the compression and tension flanges, respectively.

When the applied bending moment reaches the value (M_{ult}) the corresponding bending stress in the web plate is below the yield. Consequently, the web plate can support a certain amount of coexistent shear loading. This load is defined by the ordinate (V_B) in the interaction diagram Fig.(5-8). In order to calculate the shearing force (V_B), which acts with the bending moment (M_{ult}), *Rockey et al.* (1974)⁽¹⁷⁾ recommended using the following equation:

$$V_B = V_C \left(\frac{M_p - M_{ult}}{M_{pw}} \right) \quad (5-59)$$

As mentioned before and according to the simple design method presented by *Rockey et al.* (1974), the curve (*CEB*) in the interaction diagram may be represented by a simple parabola. This curve will be terminated at point (**B**), as the applied bending moment reaches (M_{ult}), because the cross section cannot provide the full plastic moment of resistance (M_p) (as mentioned previously). Therefore, point (**B**) represents the terminating point of the interaction diagram. In this way the complete diagram is defined and drawn and can be programmed.

5.4 Computational Technique

In the present study, the nonlinear response of a thin walled cellular plate structure is investigated by the linear incremental approach. In this approach the load is applied as a series of small proportional increments (not necessarily equal in magnitude) and for each of these increments, the change in deformation is determined using a linear analysis, as shown in Fig.(5-13)

The magnitude of the load increment influences the accuracy of the solution. Accordingly, the load increment is chosen to be so small that a negligible difference in the estimated collapse load will occur (existence of convergence).

Also-called tangent stiffness matrix based on geometry and internal forces existing at the end of any step (beginning of load increment) is constructed. The total displacement and internal forces at the end of any step are obtained by summing the incremental changes in displacement and internal forces up to that load point.

At the end of the *n*-th increment, the total applied load is given by:

$$\{P\}_n = \sum_{i=1}^n \{\Delta P\}_i \quad (5.60)$$

where:

$\{P\}_n$ = The n-th applied accumulated incremental load vector.

$\{\Delta P\}_i$ = The i-th applied incremental load vector.

Similarly, the displacements at the end of the n-th incremental are:

$$\{X\}_n = \sum_{i=1}^n \{\Delta X\}_i \quad (5.61)$$

where:

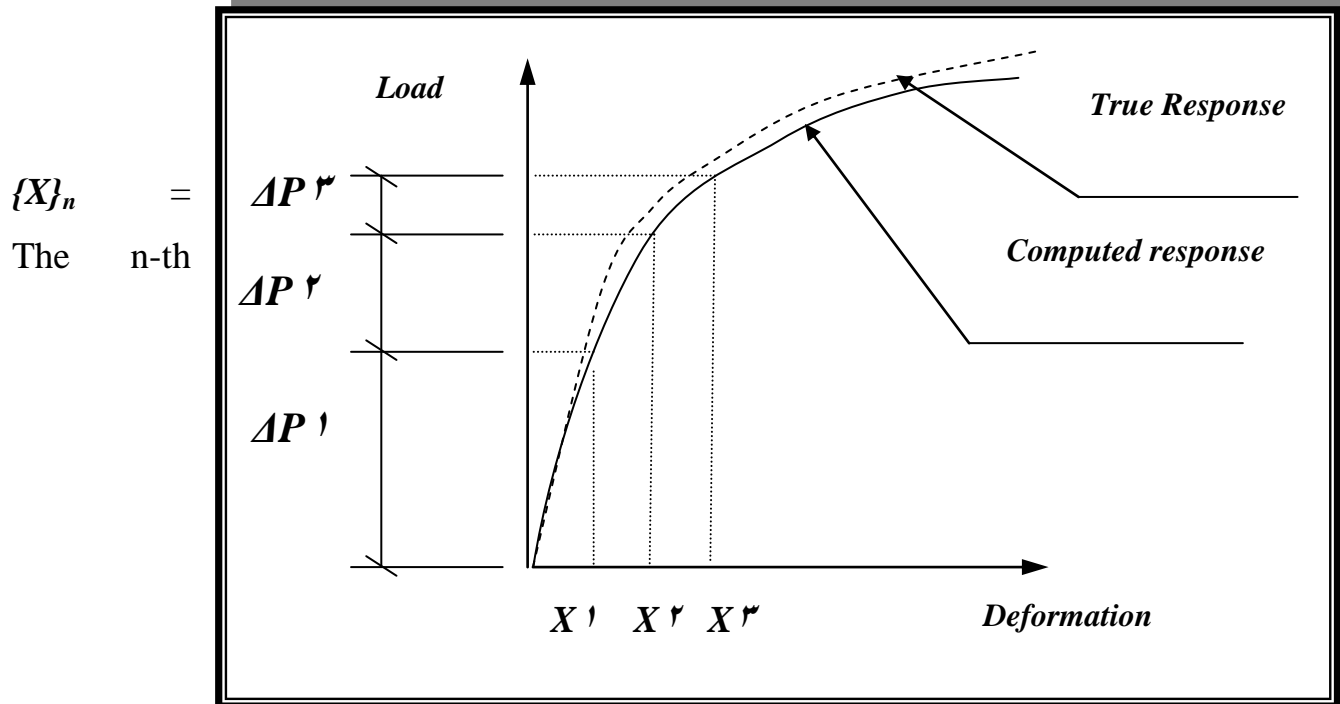


Figure (2.17) The nonlinear response of structure by incremental load approach.
 accumulated incremental displacement vector
 $\{X\}_i$ = The i-th incremental displacement vector

The tangent stiffness matrix for the i-th increment is formed for the conditions existing at the end of the previous [(i-1)-th] increment. Thus, the linearized simultaneous equations to be solved in each increment are given by:

$$[K]_{i-1} \cdot \{\Delta X\}_i = \{\Delta P\}_i \tag{0.62}$$

in which:

$$[K]_{i-1} = [K(\{P\}_{i-1}, \{X\}_{i-1})] \tag{0.63}$$

where:

$\{P\}_{i-1}$ = the vector of nodal forces at the end of the previous load increment.

$\{X\}_{i-1}$ = the vector of nodal displacement at the end of the previous load increment.

Accordingly, the stiffness matrix is nonlinear in terms of internal end forces and nodal displacements of members. The updated configuration of the structure are obtained depending on the internal forces reached by the

previous load increment from the updated internal forces, the effective widths in the pre-and post-buckling ranges and the development of plastic hinges will be determined

5.6 Interpretation of Output

According to the suggestion for considering the shear lag only in the tension flange and the effect of post-buckling in compression flanges only, the cross section of the grillage member will be unsymmetrical. Consequently, the neutral axis will not remain in the mid-depth of the section but moves towards the tension flanges as the applied loading increase. Thus, the second moment of area (I_y) for a certain section of a grillage member is calculated as follows:

$$I_y = \frac{1}{(1-\nu^2)} \left[t_f \cdot b_e \cdot \lambda^2 + t_f \cdot b_t (d - \lambda)^2 \right] + \frac{t_w \cdot h^3}{12} + t_w \cdot h \cdot \left(\lambda - \frac{d}{2} \right)^2 \quad (5-64)$$

where λ is the distance from the neutral axis to the centroid of the compression flange:

$$\lambda = \frac{0.5 \cdot t_w \cdot h + d \cdot b_t \cdot t_f}{(b_e + b_t) \cdot t_f + t_w \cdot h} \quad (5-65)$$

As mentioned in the previous section, the load will be applied as a series of small load increments. For each load increment (ΔP_i) the incremental (normal) stress (σ_{xi}) can be calculated from the grillage incremental bending and warping moments (M_{yi} and B_i) using the following formula :

$$\sigma_{xi} = \frac{M_{yi} \cdot Z}{I_{yi-1}} + \frac{B_i \cdot \omega}{I_w} \quad (5-66)$$

where:

Z = the distance from the neutral axis to the level at which the stress is desired.

I_{yi-1} = the second moment of area of a section at the end of the previous load increment.

ω = the sectorial area at the point where the normal stress is to be calculated

I_w = the warping moment of inertia for the whole section.

The total (accumulative) stress at the end of the load increment (i) is the sum of the previous incremental flexural stresses, as follows:

$$\sigma_x = \sum_{i=1,2,3,\dots} \sigma_{xi} \quad (5-17)$$

Regarding the compression flange, as the accumulative stress (σ_x) reaches the critical stress (σ_{cr}), the flange will buckle and the post-buckling behavior will be represented by applying the effective width concept, as mentioned previously. When (σ_x) in the compression or tension flange reaches the yield stress (σ_{yf}), the flange will fail and, accordingly, the cross section will be treated as (T-section) for further loading. At any end of the grillage member, if (σ_x) in both compression and tension flange reaches (σ_{yf}) then a plastic hinge will be inserted at this end.

5-7 Summary of The Present Study

In the present study, an attempt is made to predict the non-linear behavior of curved steel cellular plate structures and to investigate the collapse loading by applying the grillage analogy. So, the following guide lines are adopted:

- 1- An incremental loading procedure is used as discussed in sec (5-4).
- 2- The critical stress in the compression flange panel of a straight member is evaluated by Eq.(5-8).
- 3- **Von-Karman** approach (effective width concept) is adopted to represent the post-buckling behavior of the compression flange panel. The modified **Winter's** formula Eq.(5.18) is used to calculate the effective width of the compression flange panel in the nonlinear range.
- 4- During the incremental loading procedure, when the flexural stresses in the compression and tension flange reach the yield stress of the flange material (σ_{yf}) at an end of a grillage member, a hypothetical hinge

(plastic hinge) will form at that end. Finally when two plastic hinges exist (one at each end of the member), the member is assumed to have failed.

- **Rockey's** approach is adopted to represent the post-buckling tension field action of the web panel and its behavior at yield.
- ٦- The interaction diagram Fig.(٥-٨) is programmed to investigate the ultimate shearing capacity (V_{ult}) of the web panel, with the amount of bending moment acting on the section, as follows:

- a) When member end moment ($M \leq M_{s'}$), then:

$$V_{ult} = V_s \quad (\text{constant shear capacity})$$

- b) When ($M_{s'} < M \leq M_F$), then

$$V_{ult} = V_S - \frac{(V_S - V_c)}{(M_F - M_{S'})^2} \cdot (M - M_{S'})^2 \quad (٥-٦٨)$$

- c) When ($M_F < M \leq M_{ult}$), then:

$$V_{ult} = \left[V_c^2 - \frac{(V_c^2 - V_B^2)}{(M_{ult} - M_F)} \cdot (M - M_F) \right]^{\frac{1}{2}} \quad (٥-٦٩)$$

- ٧- As the shearing force reaches the ultimate capacity (V_{ult}), then the grillage member is assumed to have failed.

- ٨- When the determinant of the global stiffness matrix becomes equal to zero or the deflection due to load increments increase rapidly (sudden high deformation), the structure assumed to have collapsed and the corresponding load is the collapse load.

CHAPTER 6

APPLICATION AND DISCUSSION OF RESULTS

6.1 Introduction

The grillage analogy developed and described in chapter four is used to investigate the behavior of thin-walled cellular plate structures curved in plan in their nonlinear post-buckling range and at ultimate strength according to the nonlinear aspects discussed in the previous Chapter. In order to assess the efficiency and accuracy of the proposed grillage analogy, a number of steel cellular plate structures are analyzed in this chapter with different loading, support conditions and structural proportions. These structures are analyzed by the grillage analogy (using the computer program, *NLCRVGA* (*Non-Linear Curved Grillage Analysis*)). Then they are reanalyzed using the three-dimensional flat shell elements. In this method, the flanges and webs of the cellular plate structure are divided into a number of quadrilateral elements. Each element consists of four nodes and each nodes has six degrees of freedom (ζ -translations and ζ -rotations). The program used in performing the finite element analysis is the package program, *NASTRAN*⁽¹⁾. Consequently, the results of the vertical deflection and ultimate loads predicted by these two methods of analysis are compared. The computational analyses of the selected cellular plate structures by the two methods (the proposed simplified grillage method and the three – dimensional flat shell finite element method) have been performed with a *Pentium-III* (600MHz) personal computer.

6.1.1 Cellular Plate Structure Fixed at All Edges

When cellular structures used in the construction of ship's double bottoms, storage tanks or workshop floors, they are usually supported on all four sides. They then effectively span in two directions. The structures considered here are cellular plates fixed on all four edges.

The cellular structure curved in plan and shown in Fig.(6-1) is analyzed in the non-linear range and at collapse by using the grillage method. The dimensions, material properties and support conditions are illustrated in Fig.(6-1). As the accuracy of the proposed solution is dependent on the chosen magnitude of the loading increment, a load increment of 10 kN. was used in the present study. The interior web intersection nodes (7,8,9,12,13,14,17,18 and 19) were loaded with equal increments of loads. Each load increment is 10 kN. Fig.(6-2) shows the mesh used in the finite element analysis of the curved cellular plate structure.

For the cellular plate structure, the variation of central node deflection (node 13) with the applied nodal loads is shown in Fig (6-3). From comparison of the results predicted by the two methods of analysis, the following points concerning the accuracy of the proposed method, are noticed:

- 1-At near collapse load (equal to 1690 kN at interior nodes) the maximum vertical deflection (at center) obtained by the proposed grillage analogy is 20.8 mm. The corresponding deflection obtained for the same nodal (1690 kN) loads by the three-dimensional flat shell finite element method are 21.39 mm. The percentage difference with respect to the grillage value is about 10.7 %. This difference is not large as the structure is at the verge of collapse. Moreover, the central deflection (at node 13) obtained by the three dimensional finite element method at the ultimate load is 29.06 mm.
- 2-The substitute grillage structure has failed by a collapse mechanism at a nodal load of 1690 kN. This is compared well with the collapse load of 1810 kN from the finite element analysis. The percent difference is about 6.62%.

From the results of deflections and collapse loads, the grillage modeling gives less stiff structure than the finite element modeling. This is expected as the substitute (or equivalent) grillage is made up of beams in bending and torsion while the shell elements are usually stiffened by the assumed displacement fields.

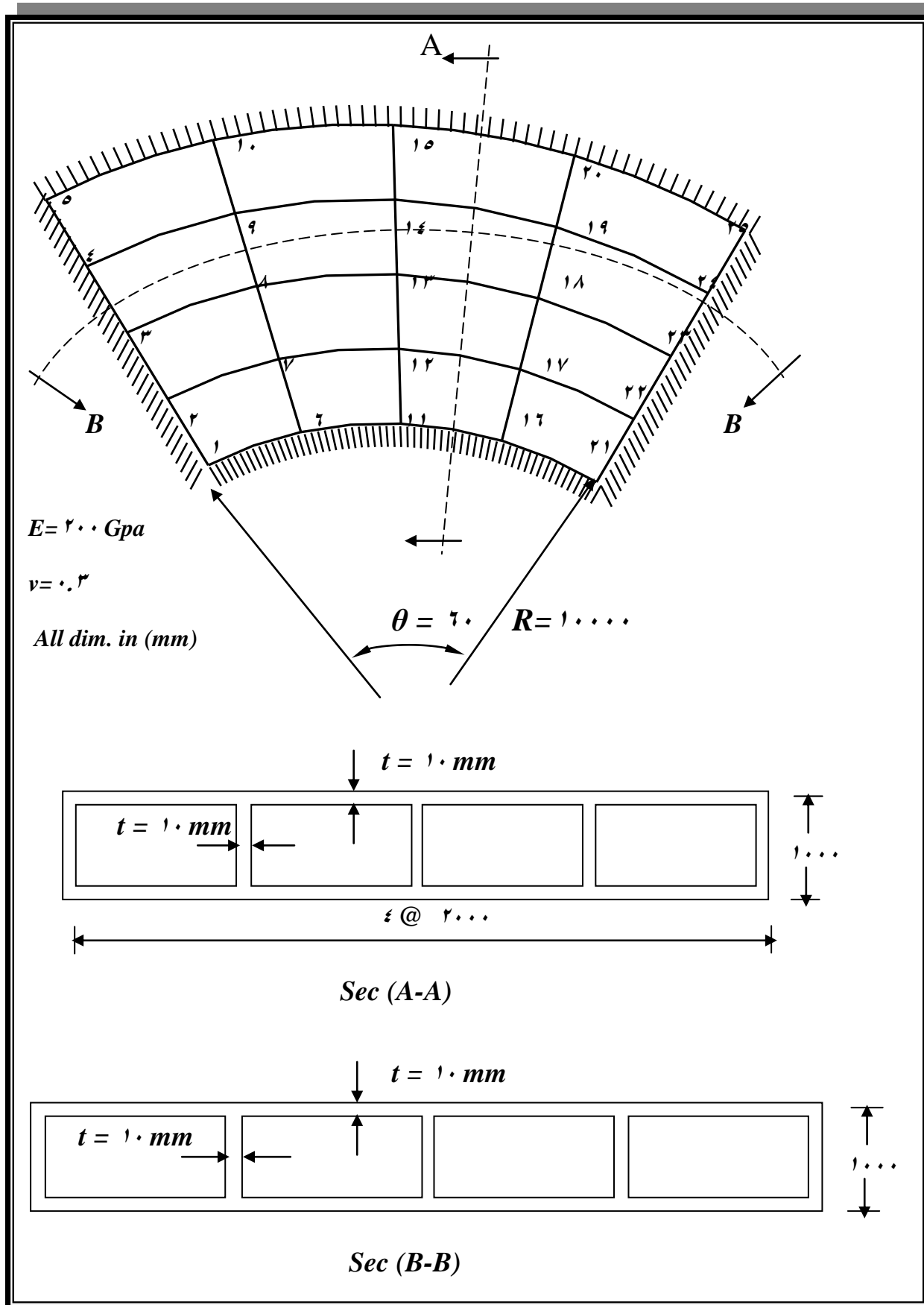
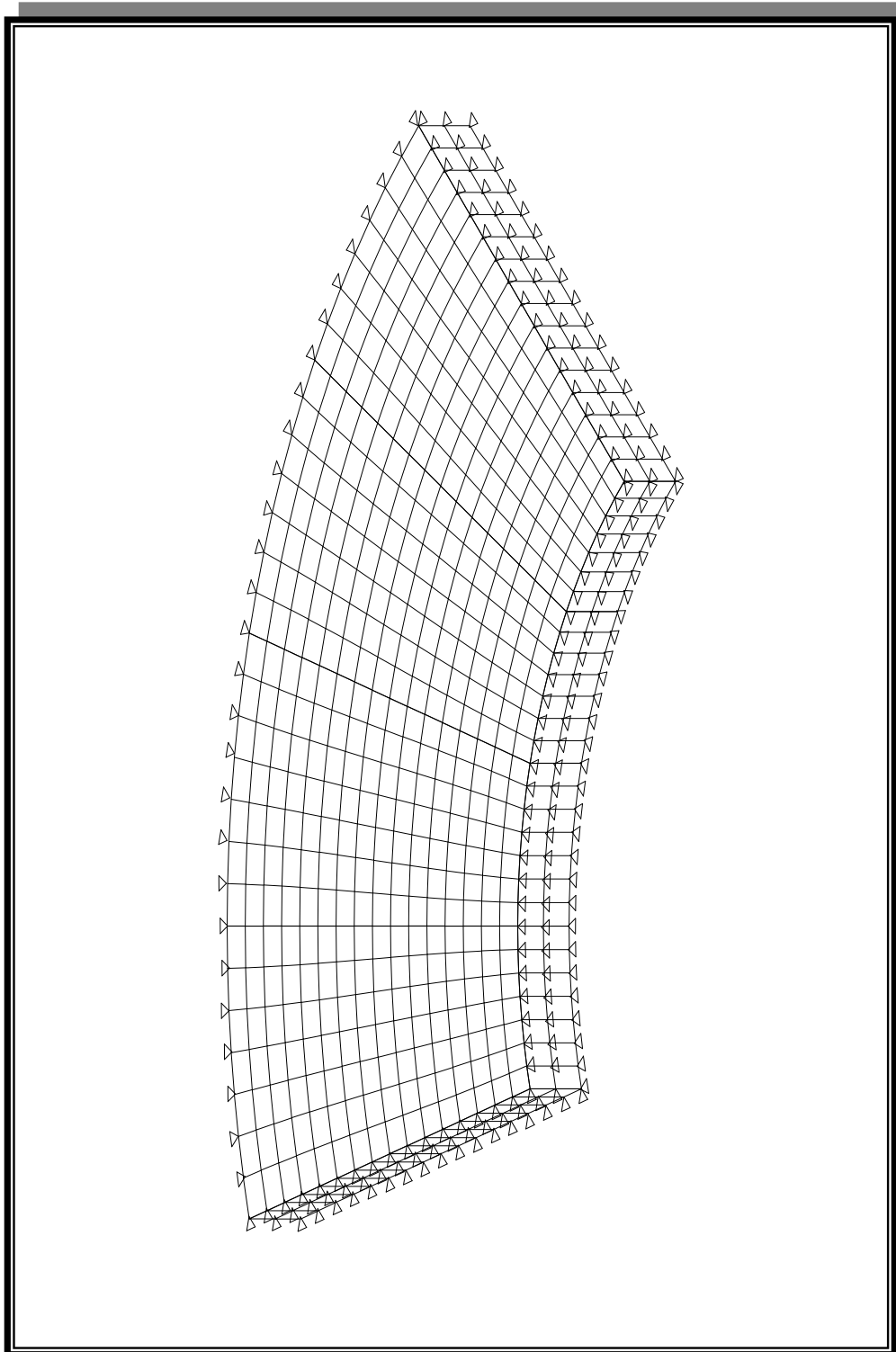


Figure (7-1) Detail of cellular structure fixed at all edges



Fig(7- 2)Finite element mesh used in the analysis of cellular plate structure fixed at all edges

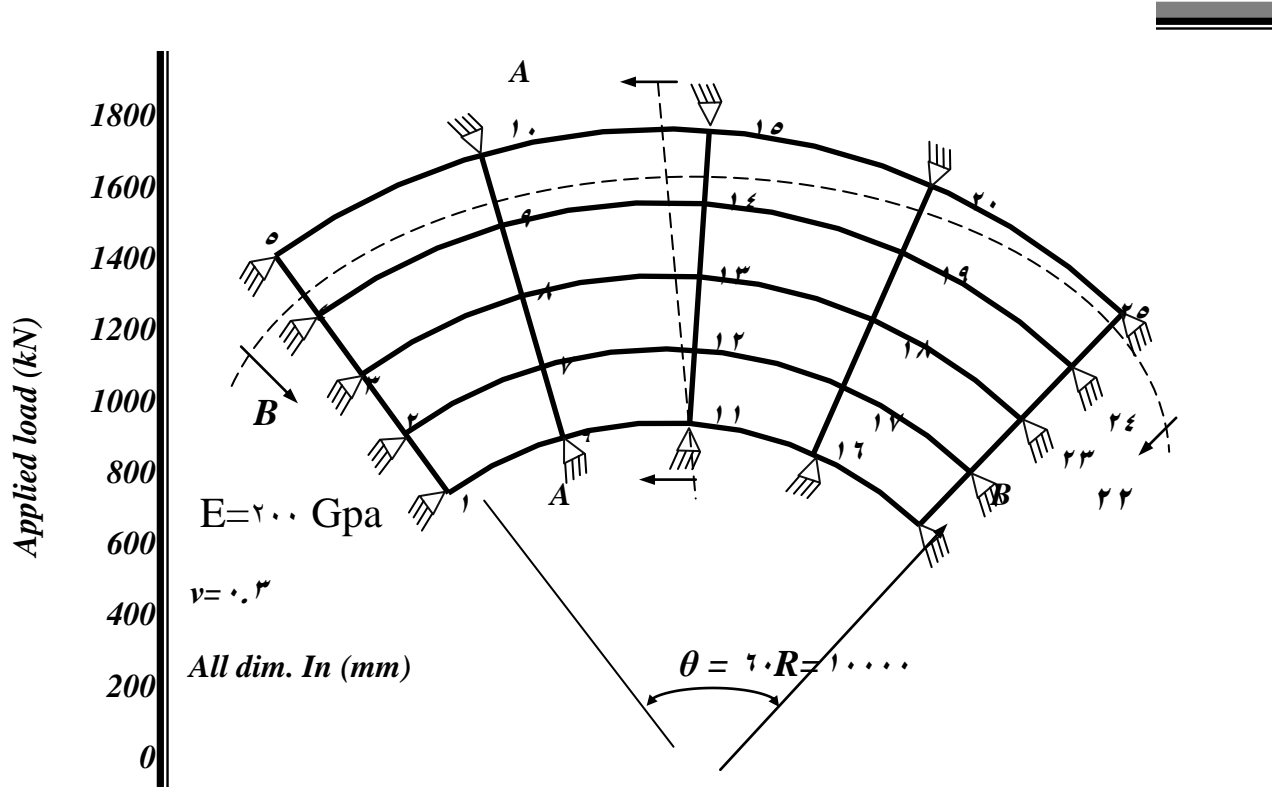
6.2 Cellular Plate Structure Simply Supported at All Edges

The structure considered here is a thin-walled cellular plate simply supported on all four edges. The cellular plate is curved in plan and shown in Fig. (6-5). It is analyzed in the nonlinear range and at collapse using grillage method. The dimensions, materials properties and support conditions are illustrated in Fig. (6-5). A load increment of 1 kN. was used in this example. The interior web intersection nodes (7, 8, 9, 12, 13, 14, 17, 18 and 19) were loaded with equal increments of load. Each load increment is 1 kN. per node. Fig.(6-6) shows the mesh used in the finite element analysis of the curved cellular plate structure.

For the cellular plate structure, the variation of the central deflection with the applied nodal load is shown in Fig (6-7). From comparison of the results predicted by the two methods of analysis, the following points concerning the accuracy of the proposed method, are noticed:

- 1- The maximum vertical deflection (at center) obtained by the proposed grillage analogy is 81.0 mm at a failure load of 166 kN per node. The corresponding deflection obtained for the same loads by the three-dimensional flat shell finite element method is 79.9 mm. The percentage difference with respect to the grillage value is about 1.3%. This difference is not large as the structure is at the verge of failure. Moreover, higher collapse loads are given by the finite elements and higher ultimate deflections are obtained.
- 2- The substitute grillage structure has failed by a collapse mechanism at a nodal load of 166 kN. This is compared well to the collapse load of 170 kN from the finite element analysis. The percent difference in collapse loads is about 0.2%. Also, from the results of deflections and collapse loads, the grillage modeling gives less stiff structure than the finite element modeling

Fig(7-7) Finite element mesh used in the analysis of cellular plate structure simply supported at all edges



Figure(7-8) load for a cell

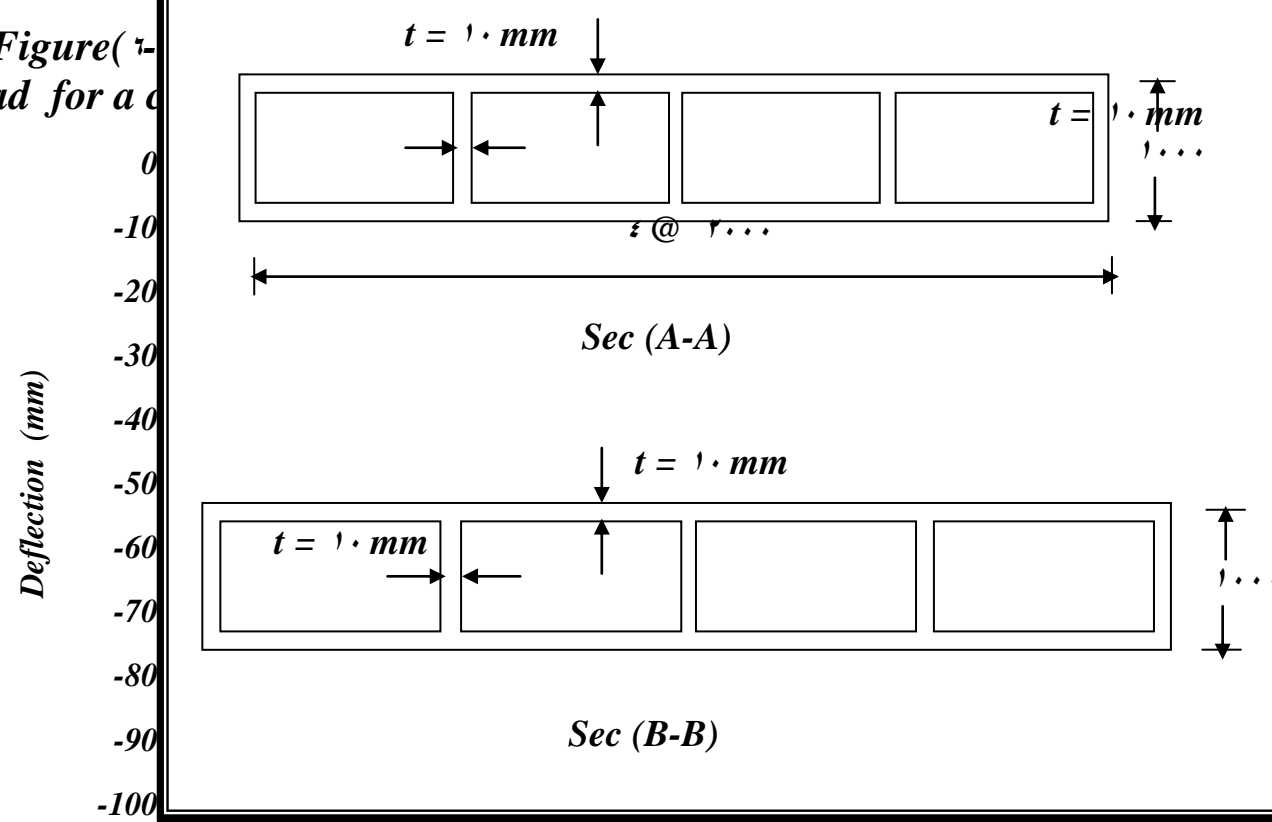


Figure (7-9) Detail of cellular structure simply supported at all edges

Figure(7-10) Vertical deflection finite element mesh used in the analysis of cellular plate structure simply supported at all edges

6.4 Cellular Plate Structure Fixed at Radial Edges

The structure considered here is fixed at the two radial side edges and free at the circumferential edges. This type of construction is used widely in highway interchanges. The dimensions and material properties for the cellular plate structure curved in plan are shown in Fig.(6-9). The load is applied only at node (12) with an increment of 10 kN. Fig.(6-10) shows the mesh used in the finite element analysis of the curved cellular plate structure. For the cellular plate structure, the variation of central deflection with the applied nodal load is shown in Fig. (6-11). From studying the results obtained by using the proposed grillage and the finite element method, the following points are noticed:

- 1- The maximum vertical deflection (at node 12) obtained by the proposed grillage analogy is 106.9 mm near the collapse load of 100 kN while the maximum deflections obtained by the flat shell finite element analysis is 160.2 mm. The percentage difference with respect to the grillage value is about 0% .
- 2- The substitute grillage structure has failed by a collapse mechanism when the applied load reaches 100 kN. The finite element method gives failure load of 111 kN. The percent deference in collapse load is about 0.4%. Also here, the grillage modeling gives less stiffness than the finite element modeling.

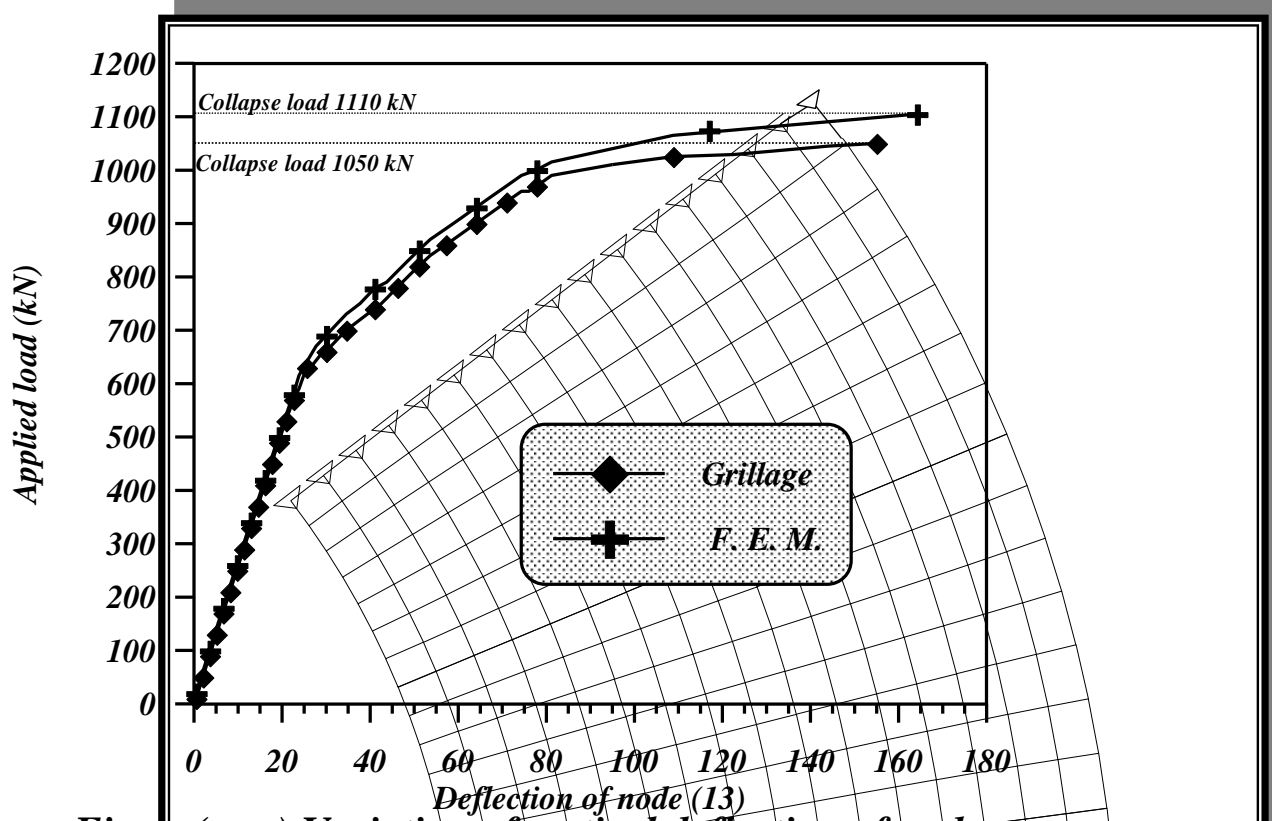


Figure (7-11) Variation of vertical deflection of node 13 with load for the cellular structure fixed at radial edges

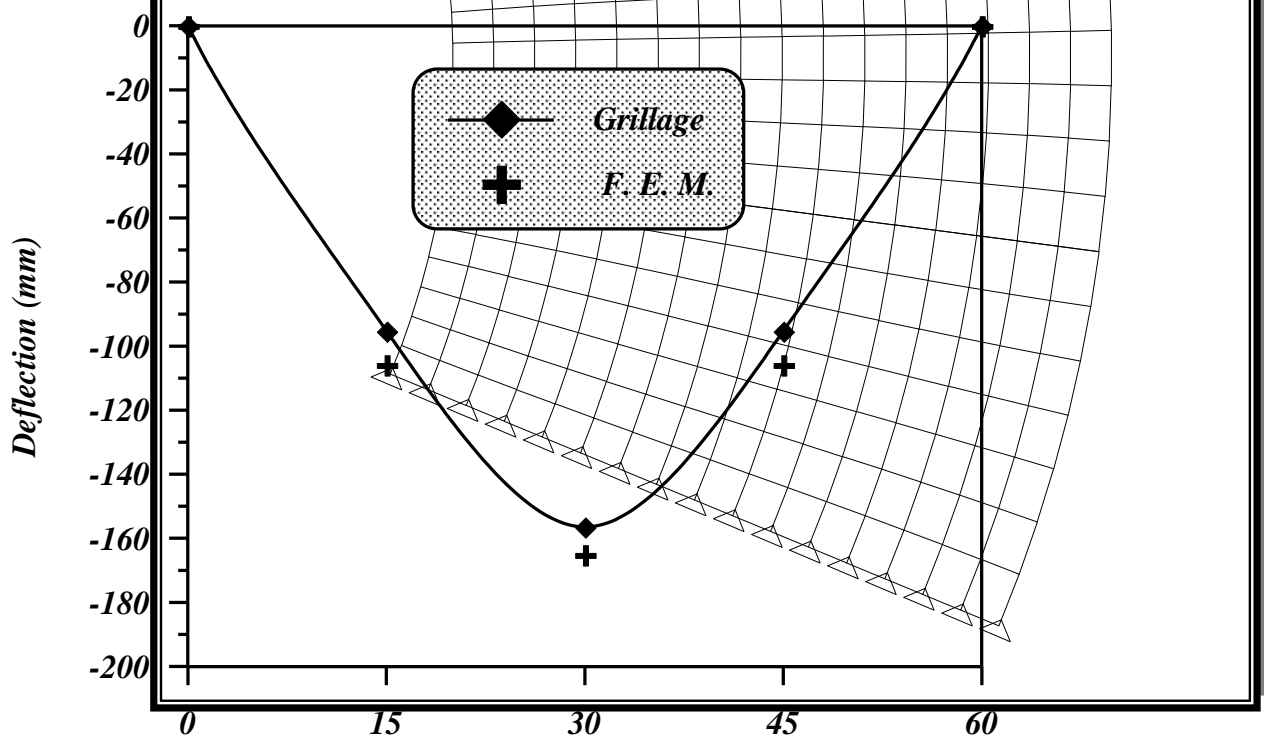


Figure (7-12) Finite element mesh used in the analysis of cellular

Figure (7-12) Vertical deflection of cellular structure fixed at radial edges

7.6 Cantilever Cellular Plate Structure

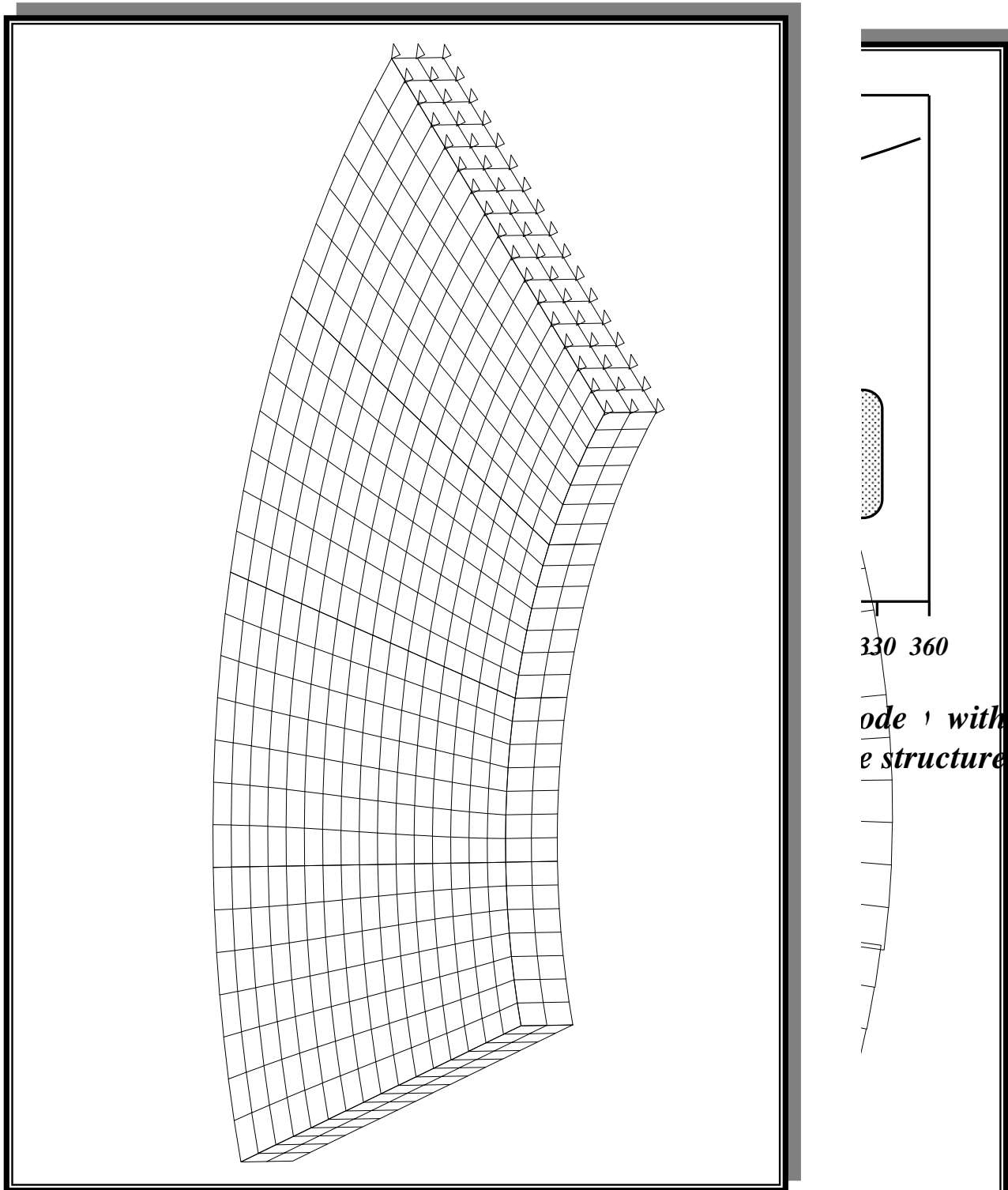
The structure considered here is fixed at one radial edge (side) and the other edges are free. The support conditions are representative of those encountered in aircraft wings. These applications are considered to assess the efficiency of the proposed grillage method for cellular plate structures having high twisting and bending moments. The dimensions and materials properties of this application are shown in Fig.(6-13). Fig.(6-14) shows the finite element mesh used for the cantilever cellular structure.

The loading condition considered in this application is a single load 10 kN increment at the corner of the outer free edge (node 6, Fig(6-13)). For the cellular plate structure, the variation of maximum deflection (corner of outer free edge) with the applied load are shown in Fig.(6-15).

From comparisons of results predicted from applying two methods of analysis, the following points are noticed:

- 1- The maximum vertical deflections (at the outer free edge at node 6) resulting from the proposed grillage method is 310 mm at a collapse load of 1100 kN, while the flat shell finite element analysis gives a maximum deflections of 300 mm. The percentage difference with respect to the grillage value is about 12.6%.
- 2- The collapse load of the substitute grillage structure is 1100 kn., while the flat shell finite element analysis gives a collapse load of 1280 kN. So, the percent deference in collapse load is 14.5%.

The deferences are not large and indicate the acceptable efficiency of the simplified grillage method.



Fig(7-14) Finite element mesh used in the analysis of the cantilever cellular plate structure

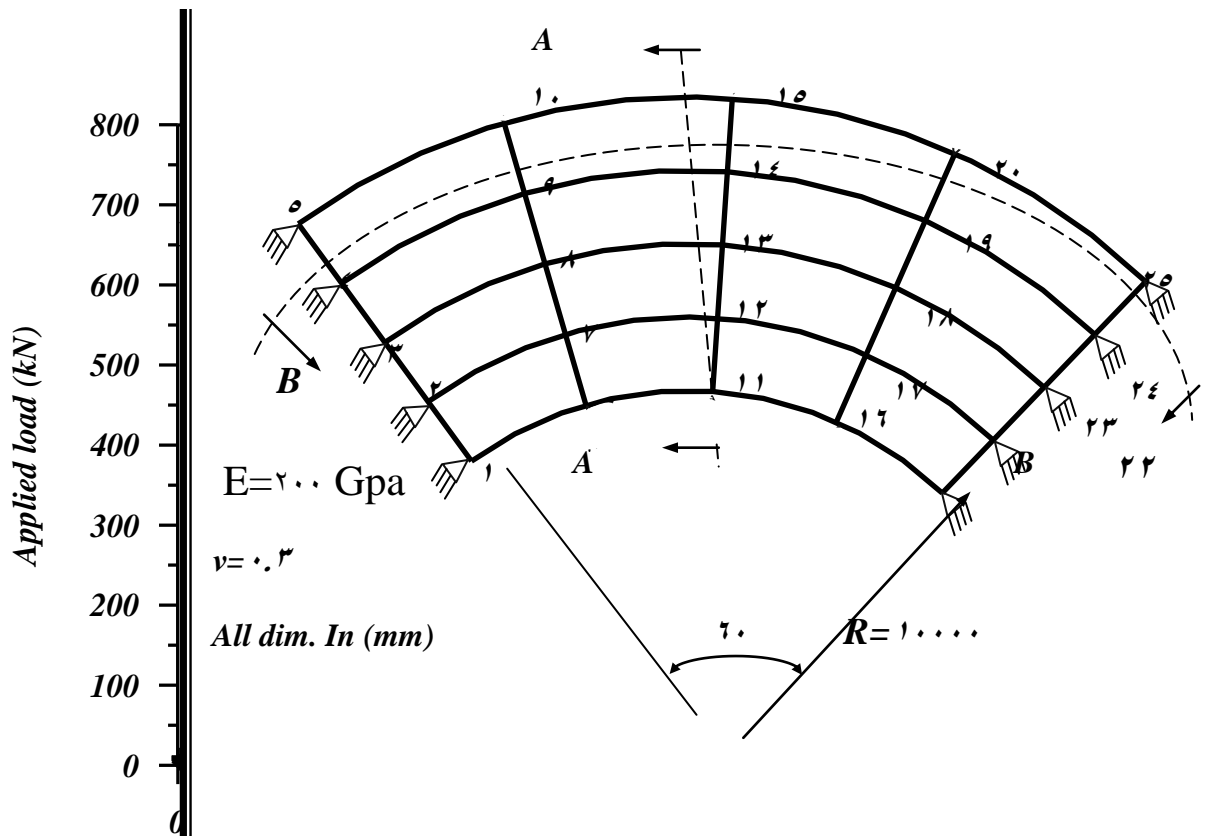
Figure(7-15) Vertical deflection ^{angle in degrees} along section (B-B) of the cantilever cellular plate structure

sis of

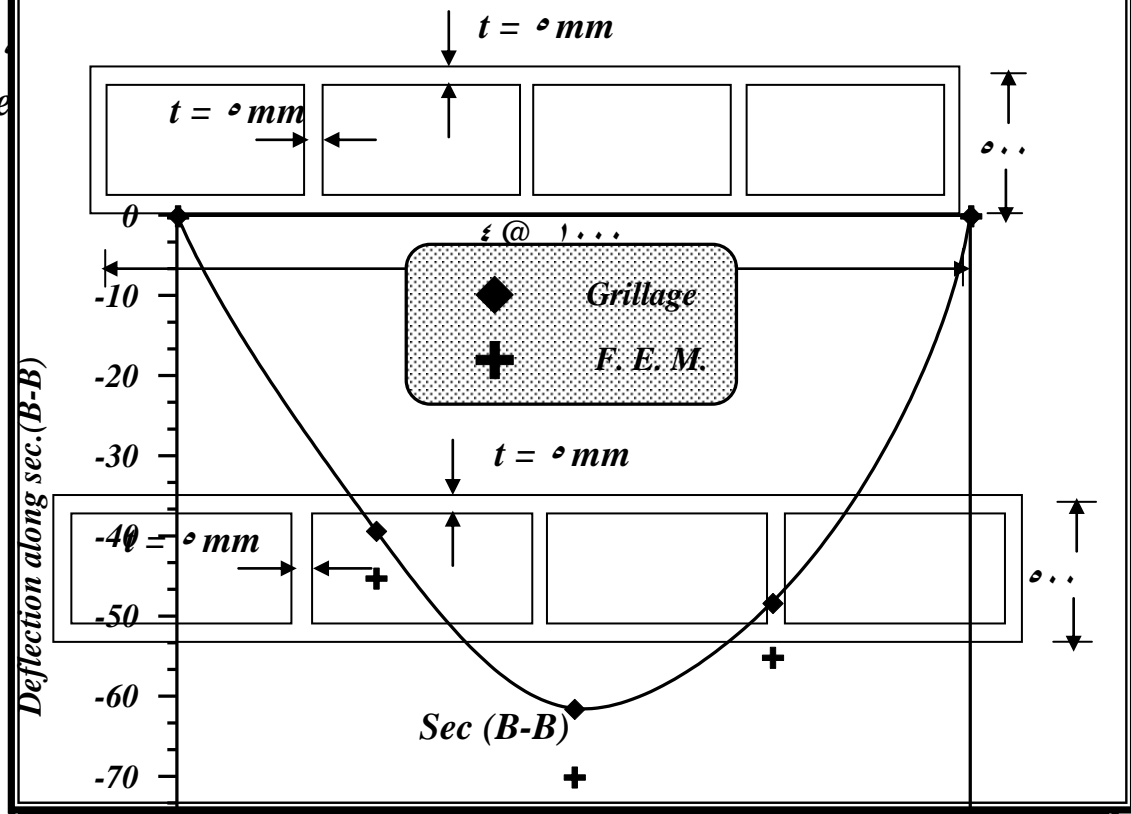
radial (side) edges. The dimensions and material properties for this cellular plate structures curved in plan are shown in Fig.(6-17). The load is applied only at node (13) with an increment of 10 kN. Fig.(6-18) shows the mesh used in the finite element analysis. For the cellular plate structure, the variation of the central deflection with the applied nodal load is shown in Fig. (6-19). From studying the results obtained by using the proposed grillage and the finite element method, the following points are noticed:

- 2- The maximum vertical deflection (at node 13) obtained by the proposed grillage analogy is 49.33 mm for a collapse load of 600 kN while the maximum deflections obtained by the finite element analysis is 50.1 mm for a collapse load of 680 kN. The percentage difference with respect to the grillage value is about 10.47% .
- 2- The substitute grillage structure has failed by a collapse mechanism when the applied load reaches 600 kn. The finite element method gives a failure load of 680 kN. The percent difference in collapse load is about 14.33%. Also here, the grillage modeling gives less stiffness than the finite element modeling.

Fig(7-7) Finite element mesh used in the analysis of cellular plate structure simply supported at all edges



Figure(7-1) for the ce



Figure(7-17) Detail of cellular structure simply supported at radial edges

Figure(7-20) Vertical deflection of cellular plate structure fixed at radial edges along sec. (B-B) at collapse

CHAPTER 7

CONCLUSION AND RECOMMENDATION

7.1 Conclusions

The applicability and accuracy of the proposed simplified grillage method have been examined by analyzing a number of cellular plate structures curved in plan in their nonlinear range and at ultimate load and under varieties of support and loading conditions. As no experimental work is available, the same structures are reanalyzed by adopting a more accurate method (three – dimensional flat shell finite elements) using the package program *NASTRAN*. From the comparisons of the results obtained by these two methods, the following main conclusions are summarized:

- 1- Extension of the grillage approach into the nonlinear post-buckling range and at ultimate load of cellular plate structures curved in plan is successfully attained by including the effects of warping deformations and both types of nonlinearities (geometric and material nonlinearly).
- 2- The approach grillage analogy is suitable at the design stage (especially in the nonlinear analysis) as it has the following advantages in comparison with the finite element analysis :
 - i- The analysis to be performed by this method is simple and takes a very short computer time .

- ii- The preparation of the input data requires considerably small time (as shown in Appendix B).
- iii- The output file obtained by the proposed method requires a small memory space .
- ϳ- The vertical deflection (at the ultimate load) calculated by the proposed method is compared with the more accurate finite element method and good agreement is observed. From these comparisons, the percentage differences are ranging between (ϳ% to 10.ϳ%) for the example considered. These differences are not large as the cellular plate structure is in a state of imminent failure.
- ϫ- The predicted values of the ultimate loads from the proposed grillage method are found to agree with those from the flat shell finite element method. The percentage differences of these values are ranging from (0.0 to 10.ϳ%). These differences are not large for the ultimate load prediction.
- 0- At the collapse load, the location and the sequence of formation of all plastic hinges can be easily indicated by the proposed grillage method. Moreover, this method can predict the failing members (due to flexure or shear) during the incremental loading procedure.

ϳ. ϳ Recommendations

For further work on the nonlinear post-buckling behavior of cellular plate structures, the proposed grillage method can be extended according to the following suggested recommendations:

- 1- Studying the behavior of cellular plate structure with variable depth in the nonlinear range and at collapse.

- ϒ- There is a need for further studies on the real representation of the boundary conditions of the compression flange plates in the evaluation of buckling coefficients of these plates.
- ϓ- Additional work is required to study the effect of initial imperfections and residual stresses (due to welding) in the component plates.
- ϔ- The present study can be developed by including the effects of openings in webs and or flanges on the behavior of cellular plate structures in their nonlinear range and at collapse.
- ο- The suggested method can be extended to allow for the dynamic analysis of cellular plate structures curved in plan.
- ϖ- The local bending and deflection behavior of the flanges directly under loads may be taken into consideration (by superimposing local effect to the general effect from the grillage analysis).

۲-۱	<i>Introduction</i>	
		۷
۲-۲	<i>Application of Grillage Analogy To Linear</i>	
	<i>Analysis of Plate Structure</i>	۷
۲-۳	<i>Application of Grillage Analogy To</i>	
	<i>Nonlinear Analysis of Plate Structures</i>	۱۱

۳-۱	<i>Introduction</i>	۱۴
۳-۱	<i>Evaluation of Elastic Rigidities</i>	
		۱۴
۳-۲-۱	<i>Flexural Rigidities</i>	
		۱۵
۳-۲-۲	<i>Torsional Rigidities</i>	
		۱۹
۳-۲-۳	<i>Shearing Rigidity</i>	
		۲۳
۳-۲-۳-۱	<i>Shear Correction Factor</i>	۲۴

۳-۲-۴ *Warping Moment of Inertia* ۲۴

۳-۲-۴-۱ *Straight Member*

۲۵

۳-۲-۴-۲ *Curved Members*

۲۵

۳-۳ *Programming of Section Properties* ۲۶

Chapter Four **GRILLAGE ANALOGIES**

۴-۱ *Introduction* ۳۵

۴-۲ *Inclusion of Warping Implicitly With*
۳۶

Torsional Stiffness

۴-۲-۱ *Member with One End Restrained*

۳۷

۴-۲-۲ *Member with Two Ends Restrained*

۳۸

۴-۳ *Grillage Analysis of Cellular Plate*

۳۹

Structure

ε-۳-۱	<i>Stiffness Matrix For Straight Member</i>	
۳۹		
ε-۳-۲	<i>Stiffness Matrix For Curve Member</i>	۴۳
ε-۵	<i>Application Examples</i>	۵۱
ε-۵-۱	<i>Example ۱</i>	۵۱
ε-۵-۲	<i>Example Two</i>	۵۲
ε-۵-۳	<i>Example Three</i>	۵۴

**Chapter Five NONLINEAR BEHAVIOR OF CELLULAR PLATE
STRUCTURES**

۵-۱	<i>Introduction</i>	۶۰
۵-۱-۱	<i>Material Nonlinearity</i>	۶۱
۵-۱-۲	<i>Geometric Nonlinearity</i>	۶۱
۵-۱-۳	<i>Necessary Assumptions</i>	۶۲
۵-۲	<i>Post-Buckling Behavior of Compression</i>	
	۶۳	
	<i>Flange Panel</i>	
۵-۲-۱	<i>Introduction</i>	۶۳
۵-۲-۲	<i>Evaluation of Elastic Critical Stress</i>	۶۴
۵-۲-۳	<i>Post-Buckling Behavior</i>	۶۹
۵-۲-۳-۱	<i>Effective Width Expression</i>	۷۱
۵-۳	<i>Post-Buckling Behavior of Web Panel</i>	۷۱
۵-۳-۱	<i>Introduction</i>	۷۱
۵-۳-۲	<i>Evaluation of Elastic Critical Shearing Stress</i>	۷۴

٥.٣.٣	<i>Review of Failure Theories for Web Panels</i>	٧٧
٥.٣.٤	<i>Proposed interaction diagram</i>	٨٠
٥.٣.٥	<i>Rockey's Method</i>	٨٢
٥.٤	<i>Computational Technique</i>	٩٦
٥.٥	<i>Interpretation of Output</i>	٩٨
٥-٦	<i>Summary of The Present Study</i>	٩٩

Chapter Six APPLICATION AND DISCUSSION OF RESULTS

٦-١	<i>Introduction</i>	١٠١
٦-٢	<i>Plated Structures Fixed at Radial Edges</i>	١٠٢
٦-٣	<i>Plated Structures Simply Supported at All Edges</i>	١٠٦
٦-٤	<i>Plated Structures Fixed at Radial Edges</i>	١١٠
٦-٥	<i>Cantilever Plated Structure</i>	١١٤
٦-٤	<i>Plated Structures simply supported at Radial Edges</i>	١١٨

Chapter Seven CONCLUSION AND RECOMMANDATION

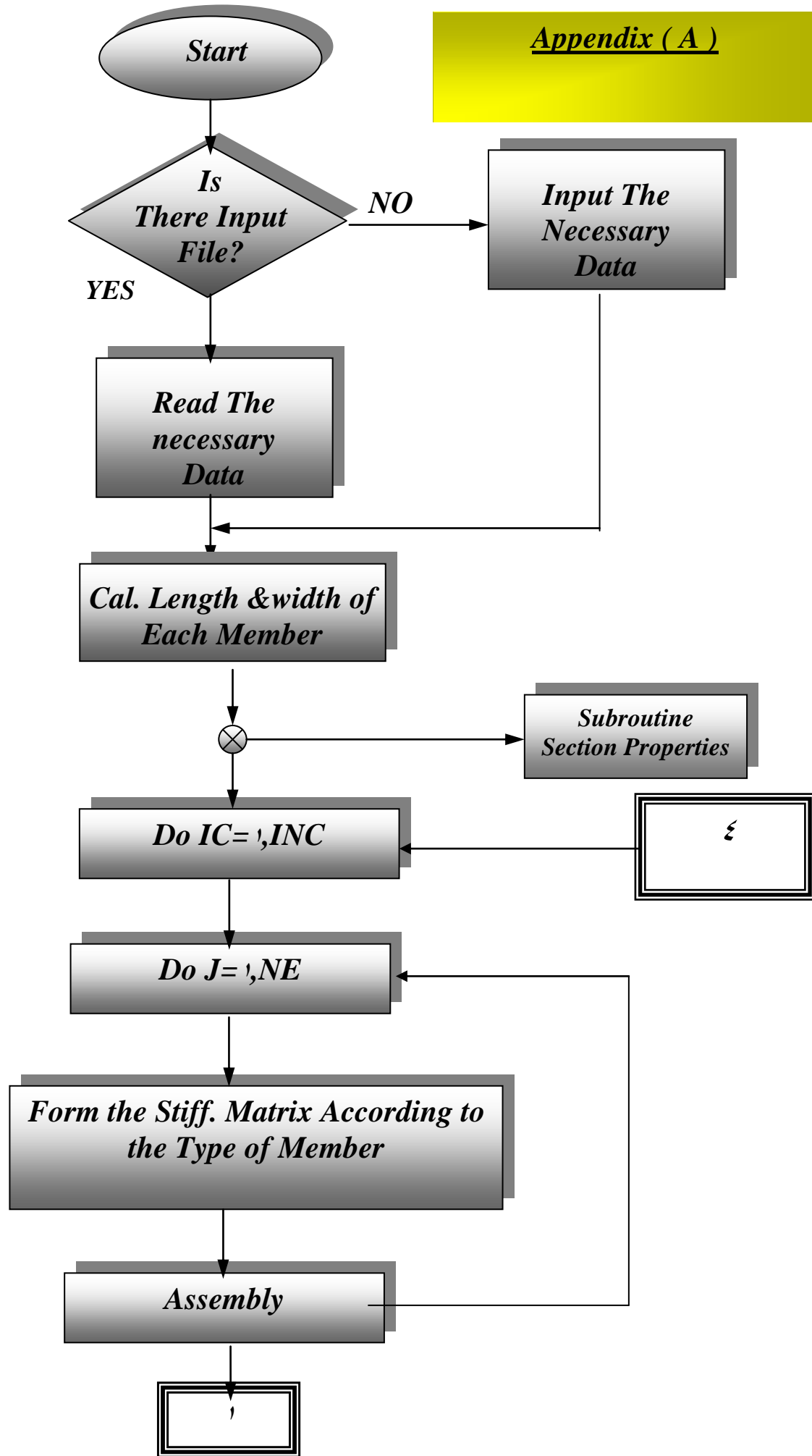
٧.١	<i>Conclusions</i>	١١٩
٧.٢	<i>Recommendations</i>	١٢٣
	References	١٢٤

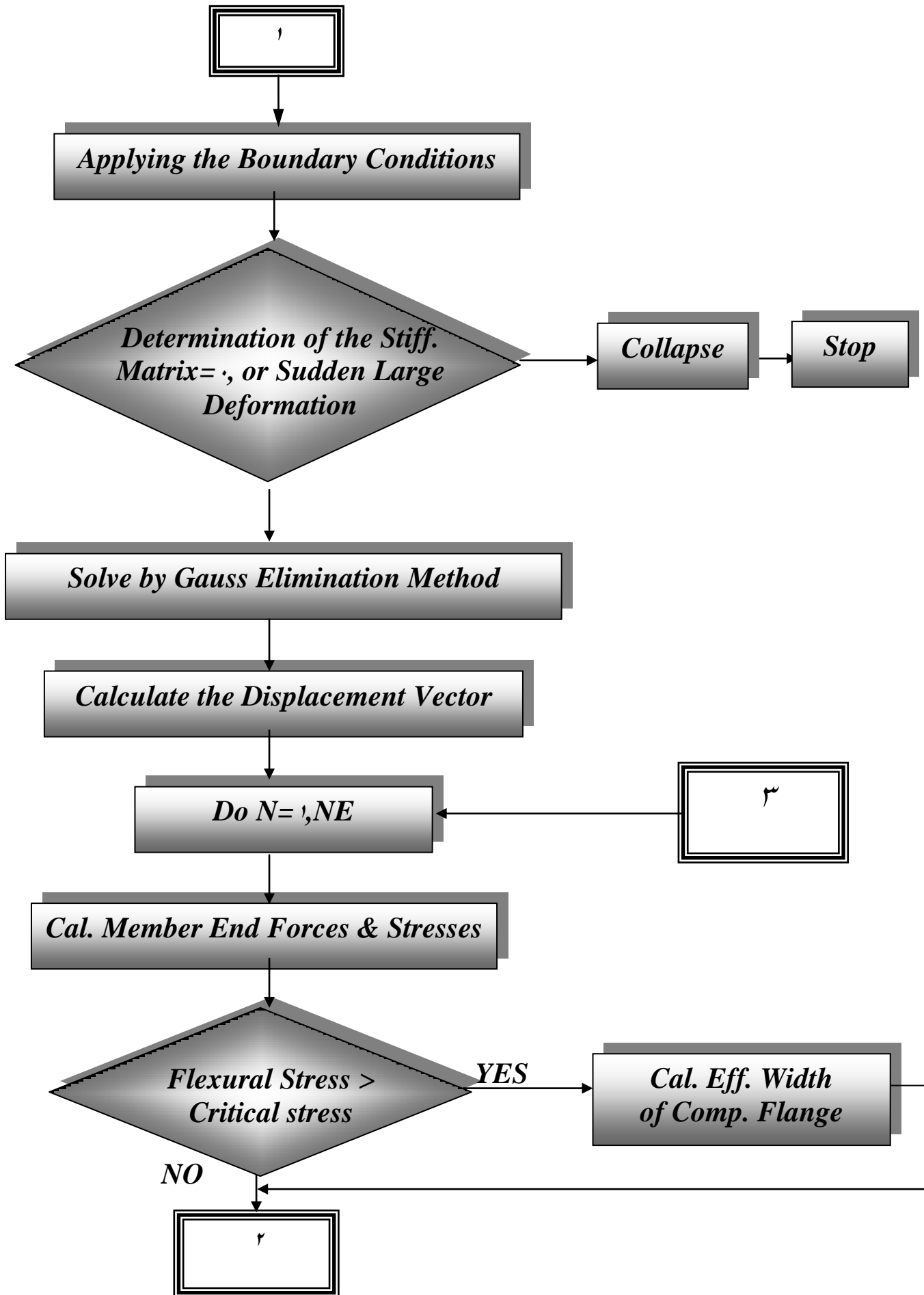
Appendix A

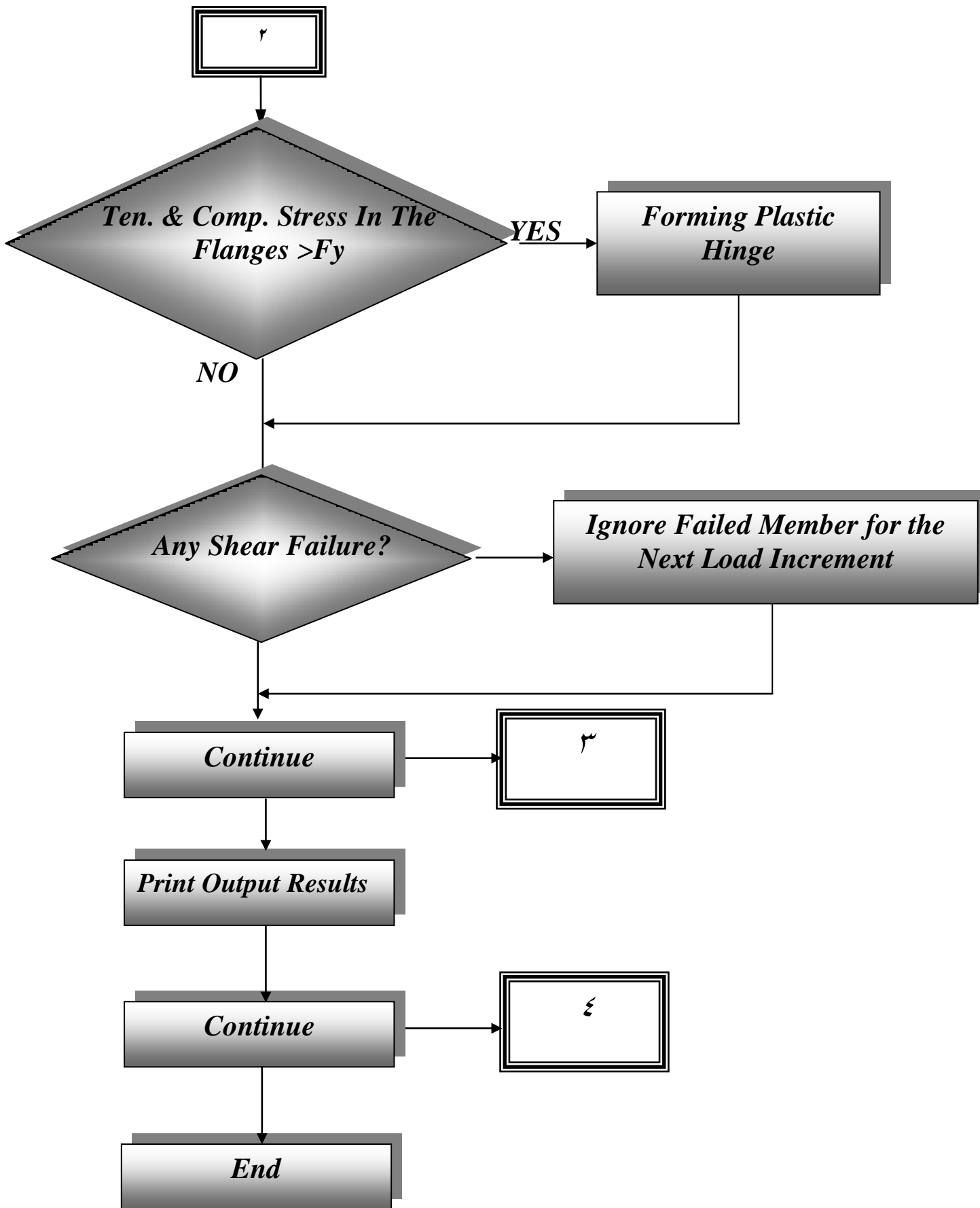
130

Appendix B

131







NOTATION

γ_a	Total length of a cellular plate structure.
γ_b	Total width of cellular plate structure.
a	Length of plate element.
A_f	Cross sectional area of flange.
A_{FC}, A_{FT}	Cross sectional areas of compression and tension flanges, respectively.
A_j	Area enclosed by the median line of the entire cross section of cell j.
A_{mn}	Amplitude of deflection of a plate.
A_v	Effective shear area of grillage beam element.
A_w	Cross sectional area of the web.
B	unstiffened length of the web.
B_s, B_e	Width at the start and end of the grillage member respectively.
b_s, b_e	Width at the start and end of plate element, respectively.
B_e	Effective width of a cell due to shear lag effect.
b_e	Effective width of compression flange due post-buckling behavior.
b_{ey}	Effective width of compression flange(at yield).
C_c	Position of plastic hinge at the compression flange.
C_t	Position of plastic hinge at the tension flange.
d	Depth of a cellular plate structure (distance between Centerline of the flange).
D_x, D_y	Flexural rigidities in x and y directions, respectively.

D_{xy}, D_{yx}	Torsional rigidities in x and y directions, respectively.
E	Modulus of elasticity.
$\{F'\}$	Force vector in local coordinate.
G	Total depth of cellular structure.
h	Clear distance between upper and lower flanges.
I	Second moment of area of a grillage beam element
J	Torsional constant of a grillage beam element
K	Coefficient of buckling.
$[K], [K']$	Stiffness matrix in global and local coordinates.
L	Length of a grillage beam element.
M_f	Plastic moment of resistance provided by flange alone.
M_{pfc}	Plastic moment capacity of the compression flange.
M_{pft}	Plastic moment capacity of the tension flange.
M'_{pfc}	Reduced plastic moment capacity of the compression flange.
M'_{pft}	Reduced plastic moment capacity of the tension flange.
M^*_{pc}	Non-dimensional strength parameter compression flange.
M^*_{pt}	Non-dimensional strength parameter of the tension flange.
M_{pw}	Plastic moment of resistance of the web plate acting alone.
M_{ult}	Ultimate moment capacity
N_x, N_y	Membrane normal forces (per unit width) in the x and y Direction, respectively.
N_{xy}, N_{yx}	Membrane shearing forces (per unit width) in the x and y Direction, respectively.

$\{P\}$	Applied accumulated incremental load vector.
$\{\Delta P\}$	Applied incremental load vector.
$[T]$	Transformation matrix.
t_{fc}	Thickness of compression flange.
t_{ft}	Thickness of tension flange.
t_w	Thickness of the exterior webs in x and y directions.
t_{wx}	Thickness of the interior webs in x directions.
t_{wy}	Thickness of the interior webs in y directions.
U	Total strain energy.
U_b	Strain energy due to bending.
U_s	Strain energy due to transverse shear.
U_s	Strain energy due to transverse shear.
U_w	Strain energy due to warping.
V	Shearing force.
V_c	Shearing capacity of the web corresponding to the plastic Moment of resistance provided by flange (M_F).
V_s	Shearing capacity of the web associated with applied Moment up to (M'_s).
V_{ult}	Ultimate shearing capacity of the web.
V_{yw}	Shearing force required to make the web fully plastic.
W	Transverse deflection of plate.
$\{X\}$	Accumulated incremental displacement vector.
λ	Distance from the neutral axis to the centerline of the compression flange.
$\{\Delta X\}$	Incremental displacement vector.
$\{\Delta'\}$	Displacement vector in local coordinate.
θ	Rate of twist.

ν	Poisson's ratio.
σ, σ	Direct (normal) stresses acting on two orthogonal planes
σ_{cf}, σ_{tf}	Average normal stresses in the compression and tension flanges, respectively.
σ_x	Normal stress in the x direction.
$\sigma_{x(cr)}$	Critical buckling stress of the compression flange.
σ_t	Membrane tensile stress.
σ_t^y	Membrane tensile stress that cause yielding in the web.
σ_{yf}	Yield stress of the flange material.
σ_{yw}	Yield stress of the web material.
τ	Shearing stress.
τ_{cr}	Critical shearing stress.
ϕ	Angle of inclination between the local and global axes of a grillage beam.
Φ, Φ_r	Inclination of the compression and tension flanges, respectively, when applying a virtual displacement.

Note: Other notations (not listed here) are defined as they appear in the text.

ABBREVIATIONS

AASHTO	American Association of Steel Highway and transportation Official.
AISC	American Institute Of Steel Construction.
AISI	American Iron and Steel Institute.
ASCE	American Society Of Civil Engineers
ASME	American Society Of Mechanical Engineers.
LRFD	Load and Resistance Factor Design.
SSRC	Structure Stability Research Council

References

1-

AASHT

O (1 9 9 7)

“ Standard Specifications for Highway Bridges: American Association of State Highway and Transportation Officials, 16th Edition, Washington D.C., Cited in (٥٣).

٢- **Abdel Rahman , H,H,and Hinton , E. (1 9 8 7)**

“ Nonlinear Finite Element Analysis of Reinforced Concrete Stiffened and Cellular Slabs. “ Computers and Structures”, Vol. ٢٢, No, ٣, Pp.٣٣٣-٣٥٠.

٣- **AISC (1 9 8 9)**

“Specification for Structural Steel Buildings, Allowable Stress Design and Plastic Design “ American Institute of Steel Construction, 9th Edition Chicago, I)) Cited in (٥٣).

٤- **AISI (1 9 9 1)**

“ Specification for Design of Cold –Formed Steel Structural Members “. American Iron Steel Institute, NW, Washington, D.C. Cited in (٥٣).

٥- **Al-Azawi , R. K. Sh. , (٢ ٠ ٠ ٠)**

“Linear and Non Linear Response of Thin – Walled Cellular and Ribbed Decks Curved in Plan “, Thesis Presented for the Doctor of Philosophy, Department of Civil Engineering University of Baghdad, Iraq.

٦- **Al-Daami,H,H. (٢ ٠ ٠ 1)**

“Linear and Non- Linear Static and Free Vibration Analysis of Thin-Walled Cellular and Ribbed Spherical Domes by Spherical Grillage Analogy ” Thesis Presented For the Degree of Doctor of Philosophy, Dept. of Civil Eng., University of Baghdad, Iraq.

٧- **Al-Dosari , M.J.I. (٢ ٠ ٠ 1)**

Elastic Analysis of Cellular Plate Structures With Nonparallel Webs and Diaphragms With Inclusion of Warping “ Thesis Presented for the Degree of Master of Science, Department of Civil Engineering, University of Baghdad, Iraq.

٨- **Al-Dulaimy R.A. (٢ ٠ ٠ 1)**

Static and Free Vibration Analysis of Cellular Plate and Cellular – Hyperbolic Paraboloid Shell by Grillage Analogy “ Thesis Presented for the Degree of Doctor of Philosophy, Department of Civil Engineering, University of Baghdad, Iraq.

٩- **Al-Musawi,A,M.I. (٢ ٠ ٠ ٠)**

“Analysis and Optimum Design of Large Diameter Domes ” Thesis Presented For the Degree of Doctor of Philosophy, Dept. of Civil Eng., University of Baghdad, Iraq.

1٠- **Al – Sherrawi , M.H.M. (1 9 9 ٥)**

“ Elastic Analysis of Steel Cellular Plate Structures with Nonparallel Webs and Diaphragms “. Thesis Presented for the Degree of Master of Science, Department of Civil Engineering, University of Baghdad, Iraq.

- 11- **Bakht B. Jaeger L.G. , Cheung ,M.S. and Mufti A.A. (1981)**
 “ The State of the Art in the Analysis of Cellular and Voided Slab Bridges “
 Canadian Journal of Civil Engineering, Vol.8, No. 3, Pp 376-391.
- 12- **Basler , K. and Thurlimann , B. (1969)**
 “ Plate Girder Research “ Proceedings of the National Engineering Conference,
 AISC, American Institute of Steel Construction, New York, N.Y., Cited in (53).
- 13- **Basler , K. (1971)**
 “ Strength of Plate Girders in Shear “ Journal of Structural Engineering, ASCE,
 Vol. 87 No. St8, Pp.101-110.
- 14- **Basu , A. K. and Dawson , J.M. (1970)**
 Orthotropic Sandwich plates “. Supplement to Proceedings of the Institution of
 Civil Engineers, Pp.87-110,Cited in (11).
- 15- **Brookhant, G.C. (1976)**
 “Circular Arc I-Type Girders”, Journal of Structural Division, ASCE Vol. 93,
 Pp.133-109.
- 16- **Bradford, M.A. (1997)**
 Improved Shear strength of Webs Designed in Accordance With LRFD
 Specifications “ ASIC Engrg, J. Vol.33, No. 3, Pp.90-100, Cited in (53).
- 17- **Brush,D.O. and Al- Mroth,B.O. (1975)**
 “ Buckling of Bars, Plates and Shells ”, Mc Graw Hill Company New York
- 18- **Chern , C. and Ostapenko , A . (1979)**
 “ Ultimate Strength of Plate Girders Under Shear “ Fritz Engineering Laboratory
 Report No. 328.7, Lehigh University, Bethlehem, Pa, Cited in (53).
- 19- **Chilver , A.H. (1977)**
 “ Thin Walled Structures “ A Collection of Papers On the Stability and Strength
 of Thin Walled Structural Members and Frames, Chatto and Windus, London.
- 20- **Chu,K.H. and Pinjavor,S.G. (1971)**
 “ Analysis of Horizontal Curved Box Girders and Bridges “, ASCE Structural
 Division, Vol. 97,No.St. 10,Pp. 2481-2500.
- 21- **Cooper, P.B. (1975)**
 “ Bending and Shear Strength of Longitudinally Stiffened Plate Girders “ Fritz
 Engineering Laboratory, Report No. 304.6, Lehigh University Cited (53).
- 22- **Cooper, P.B. (1971)**
 The Ultimate Bending Moment for Plate Girders “ Proceedings of the
 International Association of Bridge and Structural Engineers (IABSE) Vol.30,
 Pp. 113-148. Cited in (58).
- 23- **Crisfield , M. A. , and Twemlow R.P. (1971)**
 “ The Equivalent Plate Approach for the Analysis of Cellular Structures “ Civil
 Engineering and Public Works Review, Pp. 209-263.
- 24- **Cusens A. R., and Pama , R.P. (1975)**
 “ Bridge Deck Analysis “ John Wiley and Sons, London.
- 25- **Day, S.S. (1980)**
 “Finite Element Strip Method for Analysis of Orthotropic Curved Bridge,
 Decks”, Proc. Instn. Civil Eng., Part two, vol. 69, June, Pp 011-019.

٢٦- **Dabrowski, R.** (١٩٨٨)

“Curved Thin Walled Girders Theory and Analysis ”, Cement and Concrete Association, London Translation No. ١٤٤.

٢٧- **Dezi , L. and Mentrasti , L.** (١٩٨٥) .

Nonuniform Bending-Stress Distribution (Shear Lag) “ J. of Structural Engineering, ASCE, Vol. ١١١, No. ١٢, Pp. ٢٦٧٥-٢٦٩٠.

٢٨- **Eurocode ٣, Part ١.٣** (١٩٩٠)

“ Cold – Formed Thin Gauge Members and Sheeting “ Cited in (٤٨).

٢٩- **Evans, H. R., and Shanmugam , N.E.** (١٩٧٩)

“ An Approximate Grillage Approach to the Analysis of Cellular Structures “ Proceedings of the Institution of Civil Engineers, Part ٢, Vol. ٦٧, Pp. ١٢٣-١٥٤.

٣٠- **Evans, H. R., and Shanmugam , N.E.** (١٩٧٩)

“The Elastic Analysis of Cellular Structures Containing Web Openings “ Proceedings of the Institution of Civil Engineers, Part ٢, Vol. ٦٧, Pp. ١٠٣٥-١٠٦٣, Cited in (٣١).

٣١- **Evans, H. R., and Shanmugam, N.E.** (١٩٨٤)

“ Simplified Analysis for Cellular Structure “ Journal of Structural Engineering, ASCE Vol. ١١٠, No. ٣, Pp. ٥٣١-٥٤٣.

٣٢- **Evans, H. R., Pesksa, D. O. and Taherian A.R.** (١٩٨٥)

The Analysis of the Nonlinear and Ultimate Load Behavior of Plated Structures By the Finite Element Method “ Eng. Comput., Vol. ٢, Pp. ٢٧١-٢٨٤ , Cited in (٥).

٣٣- **Evans, H. R., Porter, D.M. and Rockey K.C.** (١٩٧٦)

“ A Parametric Study of the Collapse Behavior of Plate Girders “ University College, Cardiff, Report, Cited in (٧٢).

٣٤- **Fairooz , A. A.** (١٩٩٧)

“ Elastic Analysis of Steel Cellular Plate Structure Curved in Plan. “ Thesis Presented for the Degree of Master of Science, Department of Civil Engineering, University of Baghdad, Iraq.

٣٥- **Faulkner, D.** (١٩٧٣)

“ A Review of Effective Plating to Be in the Analysis of Stiffened Plating in Bending and Compression “ Massachusetts Institute of Technology, Cambridge, Mitsg ٧٣١١, Noaa ٧٣٠٧٢٣٠١.

٣٦- **Fujita, Y. and Yoshido, K.** (١٩٧٧)

“On Ultimate Collapse of Ships Structures-Researches in Japan”, Proc. Institutional Conference, Crosby Lockwood Staple, London.

٣٧- **Ghali , A. , Neville , A. M. and Cheung , Y. K.** (١٩٧٧)

“ Structural Analysis – A Unified Classical and Matrix Approach “. ٢nd Edition, John Wiley and Sons, New York.

٣٨- **Hambly , E.C. , and Pennels . E.** (١٩٧٥)

“ Grillage Analysis Applied to Cellular Bridge Decks “. The Structural Engineering, Vol. ٥٣, No. ٧, Pp. ٢٦٧-٢٧٤.

٣٩- **Harding, J. E.** (١٩٩٥)

“ Non – Linear Analysis of Components of Steel Plated Structures “ Proceedings of the ١st European Conference On Steel Structures, Athens Greece, ١٨-٢٠ May.

٤٠- **Harding, J. E., Hindi, W. and Rahal, K. (١٩٩٠)**

“ The Analysis and Design of Stiffened Plate Bridge Components “ SSRC (Structural Stability Research Council), Annual Technical Session St. Louis, USA., Pp. ٢٦٧-٢٧٦ .

٤١- **Hassan, A. F. (١٩٩٨)**

“Static and Dynamic Analysis of Spherical Domes By Method of Space Grillage“, Thesis Presented for the Doctor of Philosophy, Department of Civil Engineering, University of Baghdad, Iraq.

٤٢- **Hayashikawa, T. Watanabe, N. and Ohshima, H. (١٩٨٠)**

“ On Limit Analysis of Grillage Girders “ Journal of Civil Eng. Design, Vol.٢, No.٤, Pp.٣٧٩-٣٩٠.

٤٣- **Hsu, T.T.C, (١٩٨٨)**

“ Softening Truss Model Theory for Shear and Torsion ”, ACI Journal, Vol. ٨٠, No. ٦, Nov.-Dec., Pp. ٦٢٤-٦٣٠.

٤٤- **Husain, H.M. (١٩٦٤)**

“ Analysis of Rectangular Plates and Cellular Structures “. Thesis Presented for the Degree of Doctor of Philosophy, Department of Civil Eng. University of Leeds, England.

٤٥- **Husain, H.M., Al-Ausi, M.A.A. and Al-Azawi, R. K. (١٩٩٩)**

“Torsional Stiffness of Straight and Curved Thin Walled Member with Warping Restraint” The Scientific Journal of Tekreet University, Eng. Science Section, Vol. ٦, No. ٤, Pp ١-٣٠ .

٤٦- **Jaeger , L. G. and Bakht , B. (١٩٨٢)**

“ The Grillage Analogy in Bridge Analysis “ Canadian Journal of Civil Eng. , Vol.١٢ , No.١ , Pp. ٢٢٤-٢٣٠ .

٤٧- **Just, D.J (١٩٩٢)**

“ Circularly Curved Beam Under Plane Loads “ Journal of Structural Division, ASCE, Vol.١٠٨, No. St.٨ Aug., Pp. ١٨٠٨-١٨٧٣.

٤٨- **Kalyanaraman , V. and Rao , K. S. (١٩٩٨)**

“ Torsional – Flexural Buckling of Singly Symmetric Cold – Formed Steel Beam Columns “ Journal of Constructional Steel Research Vol.٤٦, No.١-٣, Paper No.٣٢٨, ISSN: ٠١٤٣-٩٧٤x.

٤٩- **Kuzmanovic , B.O. and Graham , H.J. (١٩٨١)**

“ Shear Lag in Box Girders “ Journal of the Structural Division, ASCE, Vol.١٠٧, No.St٩, Pp.١٧٠١-١٧١٢.

٥٠- **Koniki, I. and Komatsu, S. (١٩٦٥)**

“ Three Dimensional Analysis of Curved Girders With Thin- Walled Cross Section ”, Publication International Association for Bridges and Structural Engineers”, Vol.٢٥, Pp. ١٤٣-٢٠٣.

٥١- **Lamas, A.R.G., and Dowling, P. J. (١٩٧٩)**

“ Effect of Shear Lag on the Inelastic Buckling Behavior of Thin – Walled Structures “. Thin – Walled Structures, Vol. ٦, Pp.١٠٠-١٢١.

٥٢- **Lee, S.C. Davidson , J.S. , and Yoo, C.H. (١٩٩٦)**

“ Coefficients of Plate Girder Web Panels “ Computers and Structures, Vol.٥٩, No.٥, Pp. ٧٨٩-٧٩٥, Cited in (٥٣).

- ٥٣- *Lee, S.C., and Yoo, C.H. (١٩٩٨)*
 “ Strength of Plate Girder Web Panels Under Pure Shear “ Journal of Structural Engineering ASCE, Vol. ١٢٤, No. ٢, Pp. ١٨٤-١٩٤.
- ٥٤- *Marsh, C. (١٩٩٨)*
 “ Design Method for Buckling Failure of Plate Elements “ Journal of Structural Engineering ASCE, Vol. ١٢٤, No. ٧, Pp. ٨٥٠-٨٥٣.
- ٥٥- *Mashal, Y.T. (١٩٩٧)*
 “ Non-Linear and Ultimate Load Investigation of Steel Cellular Plate Structures by Grillage Analogy. Thesis Presented for the Degree of Master of Science Department of Civil Engineering, University of Baghdad, Iraq.
- ٥٦- *Mofatt, K.R. and Dowling, P.J. (١٩٧٥)*
 “ Shear Lag in Steel Box Girder Bridges. The Structural Engineering, Vol. ٥٣, and No. ١٠ Pp. ٧٤٩-٤٤٨.
- ٥٧- *Mohammed, H.K. (١٩٩٤)*
 “ Elastic Analysis of Steel Cellular Plate Structure Composite of Double Parallel Plates with Webs and Diaphragms “. Thesis Presented for the Degree of Master of Science Department, Civil Engineering, University of Baghdad, Iraq
- ٥٨- *Murray, N.W. (١٩٨٤)*
 “ Introduction to the Theory of Thin – Walled Structures “ Clarendon Press, Oxford.
- ٥٩- *Nakai, H. and Yoo, C.N. (١٩٨٨)*
 “ Analysis and Design of Curved Steel Bridges ”, McGraW Hill Book Company.
- ٦٠- *Nastran (١٩٩٤)*
 “ Msc/Nastran for Windows Ver ٢ “ The Macneal – Schwendler Corporation (Msc), Enterprise Software Products, Inc., Los Angles, California.
- ٦١- *Oden, J. T. (١٩٦٧)*
 “ Mechanics of Elastic Structures “, Mc GraW Hill Book Company.
- ٦٢- *Ova Lagerqvist (١٩٩٤)*
 “ Patch Loading Resistance of Steel Girders Subjected to Concentrated Forces “, Thesis Presented for the Doctor of Philosophy, Department of Civil Engineering Luleå University of Technology.
- ٦٣- *Pavlovic, M.N., Tahan, N., and Kostovos M.D. (١٩٩٨)*
 “ Shear Lag Effective Breadth in Rectangular Plates with Material Orthotropy “ Part ١: Analytical Formulation, Thin –Walled Structures, Vol. ٣٠, and Nos. ١-٤, Pp. ١٩٩-٢١٣.
- ٦٤- *Porter, D.M., Rockey, K.C. and Evans, H.R. (١٩٧٥)*
 “ The Collapse Behavior of Plate Girders Loaded in Shear “ The Structural Engineer, Vol. ٥٣, No. ٨, Pp. ٣١٣-٣٢٥, Cited in (٥٣).
- ٦٥- *Razaqpur, A.G. and Li, H.G. (١٩٩٧)*
 “ Analysis of Curved Multi-Cell Box Girder Assemblages ”, Journal of Structural Engineering and Mechanics, Vol. ٥, No. ١, Jan. Pp. ٣٣-٤٩.
- ٦٦- *Razaqpur, A.G. and Li, H.G. (١٩٩٤)*
 “Curved Thin-Walled Multi-Cell Box Girder Finite Element ”, Journal of computers and structures, Vol. ٥٣, No. ١, Pp. ١٣١-١٤٢.

٦٧- Reilly, R.J. (١٩٧٢)

“ Stiffness Analysis of Grids Including Warping ”, Proc. American Society of Civil Engineers, St.٧, Pp. ١٥١١-١٥٢٣.

٦٨- Rahal , K.N. and Harding , J.E. (١٩٩٠)

“ Transversely Stiffened Girder Webs Subjected to Shear Loading “ Proceedings of the Institution of Civil Engineers, Part ٢, Vol.٨٩, Pp.٦٧-٨٧.

٦٩- Rahal , K.N. and Harding , J. E. (١٩٩١)

“Transversely Stiffened Girder Webs Subjected to Combined In-Plane Loading “ Proceedings of the Institution of Civil Engineering. Part ٢, Vol.٩١, Pp.٢٣٧-٢٥٨.

٧٠- Ranby , A. (١٩٩٨)

“ Structural Fire Design of Thin Walled Steel Sections “ Journal of Constructional Steel Research, Vol. ٤٦, No.١-٣, Paper No. ١٧٦ and ISSN: ٠١٤٣-٩٧٤x.

٧١- Reissner , E. (١٩٤١)

“ Least Work Solutions of Shear Lag Problems. “ Presented At the Structures Session, ٩tyh Annual Meeting, i.e., New York, Journal of the Aeronautical Sciences, Pp.٢٨٤-٢٩١.

٧٢- Rockey, K.C., Evans. H. R. and Porter, D.M. (١٩٧٨)

“ A Design Method for Predicting the Collapse of Plate Girders “ Proceedings of the Institution of Civil Engineers, Part ٢, Vol.٦٥, Pp. ٨٥-١١٢.

٧٣- Rockey, K.C. and Skaloud , M.(١٩٧٢)

“ The Ultimate Load Behavior of Plate Girders Loaded in Shear.” The Structural Engineers,” Vol.٥٠, No.١, Pp. ٢٩-٤٧.

٧٤- Sawko , F. and Willcock , B.K. (١٩٦٧)

“ Computer Analysis of Bridges Having Varying Section Properties “ The Structural Engineering, Vol.٤٥, No.١١, Pp.٣٩٥-٣٩٩.

٧٥- Sawko, F. and Cope, R.G. (١٩٦٩)

“ Analysis of Multicell Bridges Without Transverse Diaphragms – A finite Element Approach. “ The Structural Engineers”, Vol.٤٧, No. ١١, Pp.٤٥٥-٤٦٠.

٧٦- Schafer , B.W, and Pekos , T. (١٩٩٨)

“Cold-Formed Steel Members With Multiple Longitudinal Intermediate Stiffeners “ Journal of Structural Engineering, ASCE, Vol. ١٢٤, No.١٠, Pp.١١٧٥-١١٨١.

٧٧- Shanmugam, N.E. and Evans, H.R. (١٩٧٩)

“ An Experimental and Theoretical Study of the Effects of Web Openings Upon the Elastic Behavior of Cellular Structures. “ Proceedings of the Institution of Civil Engineers,” Part ٢, Vol.٦٧, Pp.٦٥٣-٦٧٦, Cited in (٣١).

٧٨- Shanmugam, N.E. and Evans, H.R. (١٩٨١)

“ A Grillage Analysis of the Non- Linear and Ultimate Load Behavior of Cellular Plate Structures Under Bending Loads “Proceedings of the Institution of Civil Engineers, Part ٢, Vol.٧١, Pp.٧٠٥-٧١٩.

٧٩- Sharp, M.L. and Clark, J.W. (١٩٧١)

“ Thin Aluminum Shear Web “ Journal of Structural Division, ASCE, Vol. 97, No. 5, Pp. 1021-1038, Cited in (93).

10- *Smyth, W.J.R. and Sinavasan , S. (1971)*

“ The Analysis of Multicellular Box Structure “ Proceedings of the Conference On Development of Bridge Design and Construction, Cardiff, Crosby Lockwood and Sons, London, Pp. 441-453.

11- *Song, Q., and Scordelis , A.C. (1990)*

“ Formulas For Shear Lag Effect of T-, I- and Box Beams “ Journal of Structural Engineering, ASCE, Vol. 116, No. 6, Pp. 1306-1318.

12- *Song, Q., and Scordelis , A.C. (1990)*

“ Shear Lag Analysis of T- and I- and Box Beams “ Journal of Structural Engineering, ASCE, Vol. 116, No. 6, Pp. 1290-1300.

13- *Structural Stability Research Council (SSRC) (1988)*

“ Guide to Stability Design Criteria for Metal Structures “ 4th Edition, T.Galambos , Ed. , John Wiley and Sons , New York , N.Y. , Cited in (93).

14- *Szillard,R. (1974)*

“ Theory and Analysis of Plates (Classical and Numerical Method) ”, Prentice Hall. Inc., N. Journal.

15- *Timoshenko, S.P. and Gere , J.M. (1961)*

“ Theory of Elastic Stability “ 2nd Edition, McGraw – Hill Book Company, New York.

16- *Timoshenko, S.P. and Goodier , J.N. (1951)*

“ Theory of Elasticity “ 2nd Edition, McGraw-Hill Book, New York.

17- *Timoshenko, S.P (1980)*

“ Strength of Material “ Part 2 Advance Theory and Problem, Van Nostrand Rienhold Company, 3rd Edition.

18- *Von Karman, T., Schler , E.E and Donnell , L.H. (1932)*

“ The Strength of Thin Plates in Compression “ Trans ASME (American Society of Mechanical Engineers.) Vol. 54, Pp. 53-58, Cited in (96).

19- *Waldron, p. (1980)*

“ Elastic Analysis of Curved Thin-Walled Girders Including the effect of Warping Restraints “ Engineering Structure, Vol. 7, Apr., Pp. 93-104.

20- *Wang, C.K. (1973)*

“ General Computer for Limit Analysis “ Journal of the Structural Division, ASCE, Vol. 99, No. St 7, Pp. 101-117, Cited in (97).

21- *Winter, G. (1947)*

“ Strength of Thin Steel Compression Flanges “ Transaction, ASCE, Vol. 112, Pp. 1-10.

22- *Yang, Daily and Chang (1997)*

“ Torsional Analysis for Multi Box Cells Using Softening Truss Model “, Journal of Structural Engineering and Mechanics, Vol. 6, No. 1, Jan. Pp. 21-32.

23- *Younis, M. H. (2001)*

“ Non Linear Analysis and Ultimate Strength Investigation of Cellular Plate Structure with Non-Parallel Webs”, Thesis Presented for the Degree of Master of Science, Department of Civil Engineering, University of Baghdad, Iraq.

